

Oncogenic analysis of TRF2 in the murine hematopoietic system

Von der Naturwissenschaftlichen Fakultät der Gottfried Wilhelm Leibniz
Universität Hannover

zur Erlangung des Grades eines

**Doktors der Naturwissenschaften
Dr. rer. nat.**

genehmigte Dissertation

von

Dipl.-Biol. Sebastian Begemann
geboren am 11.04.1977 in Lemgo, Deutschland

2007

Referent: Prof. Dr. Walter Mueller

Korreferent: Prof. Dr. Bernd Otto

Korreferent: Prof. Dr. Jan Karlseder

Tag der Promotion: 21. Mai 2007

Danksagung

An dieser Stelle möchte ich mich bei den zahlreichen Menschen bedanken, die mir im Rahmen meiner Doktorarbeit in vieler Weise geholfen haben.

Bei Dr. Jan Karlseder bedanke ich mich für seine optimale Betreuung am Salk Institute. Er hat es mir ermöglicht, an diesem aussergewöhnlichen Institut unter exzellenten Bedingungen zu arbeiten. Mein ganz besonderer Dank gilt Prof. Dr. Walter Müller für die externe Betreuung meiner Arbeit. Ohne seine Hilfe wäre meine Doktorarbeit in den USA nicht möglich gewesen. Bei Prof. Dr. Bernd Otto möchte ich mich bedanken für seine Bereitschaft als Prüfer der Disputation beizusitzen.

Bei meinen Kollegen im Karlseder Lab möchte ich mich für ihre Unterstützung bedanken. Mein Dank gilt hier besonders Colleen Naeger für das Korrekturlesen meiner Doktorarbeit. Bei Laure Crabbe, Hugo Maruyama und Pepper Stockton möchte ich mich für all die belanglosen, aber lustigen Konversationen und Momente bedanken, die das Laborleben erst richtig interessant machen. Mein Dank gilt auch Candy Haggblom, Nicole Schick, Ramiro Verdun und Roddy O'Sullivan für ihre Hilfe und Unterstützung während des Laboralltags.

Das Verma Lab, ohne das die erfolgreiche Durchführung meiner Arbeit nicht möglich gewesen wäre, möchte ich ebenfalls hervorheben. Mein spezieller Dank gilt hier zunächst Francesco Galimi für seine hervorragende Unterstützung bei der Etablierung des Mausmodels. Bei Nien Hoong und Nina Tonnu möchte ich mich für ihre Hilfe bei den p24 ELISAs und für die "kleinen Tricks" bei der Lentivirus Produktion bedanken. Niels-Bjarne Woods und Thomas Sternsdorf (Evans Lab) danke ich für die hilfreichen Kommentare und Ratschläge bei der Auswertung des Mausmodels.

Ganz ausdrücklich danke ich den unzähligen Leuten der Animal Facility: Lili Vera, Craig Palmer, Laurie Gerken, Hector, Maria, und den vielen anderen, die mich 7/24 über den Gesundheitszustand meiner Mäuse genaustens informierten. Ohne ihre hervorragende Organisation wäre dieses komplexe Projekt ebenfalls unmöglich gewesen.

And here are the special acknowledgements for Briardo, Buddy, Chris, Daniela, Dave, Fernando, Jose, Matthias, and Mike from the Emerson Lab. Without you this time would have been way less fun. Thanks for teaching me all the stereotypes about Germans. Finally, I love David Hasselhoff and Wienerschnitzel. I will always remember our Foosball nights and tournaments we had, though I'm somehow concerned who will bring the magic to the table once I have left?

Schliesslich möchte ich all diejenigen nennen, die ich immer und irgendwie mit meiner Doktorarbeit verbinden werde: Matt Penfield, Wild Bill & Ernie, Café 42 Mike, Ling Qi, und Dirk Nowitzki.

Zu guter Letzt, und doch eigentlich an erster Stelle, möchte ich aber meinen Eltern danken. Ihr habt mir während meines Studiums immer geholfen und habt dies alles erst ermöglicht.

Table of Content

| | |
|--|----|
| 1. Abstract | 9 |
| 2. Zusammenfassung | 10 |
| 3. Introduction | 12 |
| 3.1. Telomeric DNA sequences | 14 |
| 3.2. Telomerase | 16 |
| 3.3. Telomerase-associated proteins | 17 |
| 3.3.1. hTERT-associated proteins | 18 |
| 3.3.2. hTR-associated proteins | 19 |
| 3.4. Alternative ways of telomere lengthening | 19 |
| 3.5. The telomere terminus | 20 |
| 3.6. The T-loop | 21 |
| 3.7. Shelterin | 22 |
| 3.7.1. TRF1 | 25 |
| 3.7.2. TRF2 | 26 |
| 3.7.3. TIN2 | 26 |
| 3.7.4. Rap1 | 27 |
| 3.7.5. TPP1 | 27 |
| 3.7.6. POT1 | 28 |
| 3.8. Non-shelterin telomeric proteins | 29 |
| 3.9. Repression of the telomere-damage response by shelterin | 30 |
| 3.10. The response to telomere attrition | 31 |
| 3.10.1. NHEJ | 32 |
| 3.10.2. HR | 33 |
| 3.11. The role of TRF2 in telomere protection and ATM inhibition | 36 |
| 4. Methods and Material | 39 |
| 4.1. Cell culture | 39 |
| 4.2. Lentiviral vectors | 39 |
| 4.3. Lentiviral plasmid isolation | 40 |

| | |
|--|----|
| 4.4. Transfection of primary cells _____ | 41 |
| 4.5. Lentivirus production _____ | 41 |
| 4.6. Mice _____ | 43 |
| 4.7. Isolation of bone marrow _____ | 43 |
| 4.8. Infection of bone marrow _____ | 44 |
| 4.9. Transplantation of bone marrow _____ | 44 |
| 4.10. Genotyping of primary and secondary recipient mice _____ | 44 |
| 4.11. Protein isolation _____ | 46 |
| 4.12. <i>Western</i> analysis _____ | 46 |
| 4.13. Immunofluorescence on cultured cells, bone marrow and spleen ____ | 47 |
| 4.14. Immunofluorescence on microtome sections _____ | 48 |
| 4.15. Flow cytometry _____ | 48 |
| 4.16. Cell sorting for colony forming assay (CFA) and liquid assay ____ | 49 |
| 4.17. Annexin V apoptosis assay _____ | 50 |
| 4.18. Pathological observations _____ | 50 |
| 4.19. Peptide nucleic acid (PNA) fluorescence in-situ hybridization (FISH) on metaphase spreads _____ | 50 |
| 5. Results _____ | 53 |
| 5.1. Experimental overview of the over-expression of recombinant mTRF2 in C57BL/6J mice _____ | 53 |
| 5.2. Functional over-expression of recombinant mTRF2 and GFP-mTRF2 in vitro _____ | 55 |
| 5.3. Production and quantitative verification of lentivirus batches _____ | 57 |
| 5.4. Transduction and transplantation of bone marrow into primary C57BL/6J recipient mice _____ | 58 |
| 5.5. Functional over-expression of the mTRF2 transgene in CD45.1 donor ____ bone marrow _____ | 60 |
| 5.6. Detection of virus integration into the hematopoietic system of C57BL/6J primary recipient mice by nested PCR and <i>Southern</i> analysis _____ | 61 |
| 5.7. Transplantation of bone marrow from primary recipients into secondary_ C57BL/6J recipient mice _____ | 63 |

| | |
|--|-----|
| 5.8. Functional over-expression of transgenic mTRF2 in the hematopoietic system of C57BL/6J mice | 65 |
| 5.9. Tumor occurrence in TRF2 over-expressing C57BL/6J recipient mice | 66 |
| 5.10. Mouse Colony-Forming cell assay | 69 |
| 5.10.1. CFC Assay in MethoCult Media | 70 |
| 5.10.2. Liquid-based CFC Assay in M5300 Media | 70 |
| 5.11. Induction of apoptosis in mice over-expressing TRF2 | 72 |
| 5.11.1. Detection of irradiation induced apoptosis by Annexin V | 73 |
| 5.11.2. Detection of irradiation-induced apoptosis in individual cells over-expressing TRF2 by confocal microscopy | 74 |
| 5.12. <i>Western</i> analysis of tumorigenic tissue for transgenic TRF2 | 76 |
| 5.13. Genotyping for transgenic TRF2 integration in tumorigenic tissue samples | 77 |
| 5.14. Pathological observations on potential TRF2 related tumor tissue | 80 |
| 5.15. Characterization of T-cell lymphoma by flow cytometry | 82 |
| 5.16. Analysis of pathological samples and metaphase spreads for genome instability | 83 |
| 6. Discussion | 85 |
| 7. References | 100 |

List of Figures

| | | |
|--------------|--|----|
| Figure I - 1 | Schematic of replication at the very end of a chromosome _____ | 13 |
| Figure I - 2 | Telomere structure _____ | 21 |
| Figure I - 3 | Shelterin _____ | 23 |
| Figure I - 4 | How shelterin may shape telomeres _____ | 24 |
| Figure I - 5 | Proposed role for shelterin in protecting telomeres from NHEJ and overhang loss _____ | 33 |
| Figure I - 6 | Control of T-loop HR by shelterin _____ | 35 |
| Figure I - 7 | TRF2 over-expression in mouse hematopoietic stem cells might cause genome instability and tumor development _____ | 37 |
| Figure 1 | Experimental setup for the over-expression of recombinant mTRF2 in the hematopoietic system of C57BL/6J mice _____ | 54 |
| Figure 2 | Recombinant mTRF2 and GFP-mTRF2 was over-expressed in 3T3 cells by transfection _____ | 55 |
| Figure 3 | Functional expression of transgenic mTRF2 in 3T3 cells displayed by immunofluorescence _____ | 56 |
| Figure 4 | Generation of primary recipient mice by lentiviral transduction of transgenic TRF2 into GFP and CD45.1 donor bone marrow _____ | 59 |
| Figure 5 | Over-expression of recombinant (GFP-)mTRF2 in bone marrow cells isolated from CD45.1 donor mice _____ | 60 |
| Figure 6 | Functional expression of recombinant GFP-mTRF2 in CD45.1 donor bone marrow cells _____ | 61 |
| Figure 7 | Schematic of primer binding in the nested PCR _____ | 62 |
| Figure 8 | Genotyping of primary recipient mice transduced with transgenic (GFP-) mTRF2 and GFP by nested PCR and subsequent <i>Southern</i> analysis _____ | 62 |
| Figure 9 | Transplantation of bone marrow from primary recipient mice into secondary recipient mice _____ | 64 |

- Figure 10 Transgenic GFP-mTRF2 is functionally expressed in the _____ hematopoietic system of recipient C57BL/6J mice _____ 65
- Figure 11 Applied criteria for the definition of TRF2 related tumor development _____ 67
- Figure 12 Differentiation analysis on sorted bone marrow cells with respect to their over-expression of GFP-mTRF2 _____ 71
- Figure 13 Irradiation induced apoptosis in mice over-expressing mTRF2 and GFP-mTRF2 measured by the percentage of Annexin V positive thymocytes using flow cytometry _____ 74
- Figure 14 Irradiation induced ATM activation in spleen from mice over-expressing GFP or GFP-mTRF2 _____ 75
- Figure 15 *Western* analysis of spleen from a secondary recipient mouse, which expressed GFP-mTRF2 and died from a CD4/CD8-double-positive T-cell lymphoma _____ 77
- Figure 16 Genotyping for the integration of transgenic TRF2 in tissue samples from mice transduced with GFP, GFP-mTRF2 or mTRF2 _____ 78
- Figure 17 H&E - staining of tumor tissue _____ 81
- Figure 18 Flow cytometric analysis of thymoma material _____ 82
- Figure 19 Anaphase bridges in H&E - stained liver and spleen sections from a secondary recipient mouse carrying a CD4/CD8-double-positive T-cell lymphoma _____ 83
- Figure 20 Genome instability was observed in metaphase spreads (MPS) prepared from splenocytes of a secondary recipient mouse carrying a CD4/CD8-double-positive T-cell lymphoma _____ 84

List of Tables

| | | |
|-------------|---|----|
| Table I - 1 | Sequences of telomeric DNA in selected species _____ | 15 |
| Table I - 2 | Human telomerase-associated proteins _____ | 18 |
| Table I - 3 | Examples of non-shelterin proteins at human telomeres _____ | 29 |
| Table M - 1 | PCR-mixture and -program for genotyping _____ | 45 |
| Table 1 | Summary of potential TRF2 related tumors _____ | 68 |
| Table 2 | Origin of the genomic DNA used in genotyping assay in Figure 16 _ | 79 |

List of Abbreviations

| | |
|--------------------|--|
| A-T | ataxia telangiectasia |
| ATM | ataxia telangiectasia mutated |
| ATR | ATM and Rad-3 related |
| BM | bone marrow |
| bp | base pairs |
| DABCO | 1, 4 diazabicyclo (2.2.2) octane |
| DAPI | 4', 6'-diamidino-2-phenylindole |
| ddH ₂ O | double-distilled H ₂ O |
| D-loop | displacement loop |
| DMEM | Dulbecco's Modified Eagle's Medium |
| DNA, cDNA | deoxyribonucleic acid, complementary DNA |
| DNA-PK | DNA-dependent protein kinase |
| dNTP | deoxyribonucleotide triphosphate |
| DSB | double-stranded breaks |
| EDTA | ethylene diamine tetraacetic acid |
| ELISA | enzyme-linked immunosorbent assay |
| FACS | fluorescence activated cell sorter |
| FBS | fetal bovine serum |
| FCS | fetal calf serum |
| FITC | fluorescein isothiocyanate |
| GFP | green fluorescent protein |
| HBSS | Hank's Balanced Salt Solution |
| HEPES | 4-(2-Hydroxyethyl)-1-piperazine-ethanesulphonic acid |
| HJ | homologous junction |
| HR | homologous recombination |
| IF | immunofluorescence |
| IR | irradiation |
| kbp (kb) | (kilo) base pairs |
| kDa | kilo Dalton |

| | |
|--------|---|
| LB | Luria-Bertani |
| MRN | Mre11-Rad50-NBS1 |
| NER | nucleotide excision repair |
| NHEJ | non-homologous end joining |
| PARP | poly (ADP-ribose) polymerase |
| PBS | phosphate-buffered saline |
| PCR | polymerase chain reaction |
| Pen | Penicillin |
| PNA | peptide nucleic acid |
| PS | phosphatidylserine |
| PVA | polyvinyl alcohol |
| rpm | rounds per minute |
| SDS | sodium dodecyl sulphate |
| Strep | Streptomycin |
| TE | TRIS-EDTA |
| T-loop | telomere loop |
| TRF | telomere repeat binding factor |
| Tris | 2-Amino-2-hydroxymethylpropane-1,3-diol |
| TRITC | tetramethyl rhodamine isothiocyanate |
| T-SCE | telomere sister chromatid exchange |
| U | unit |
| UV | ultraviolet |
| v/v | volume per volume |
| w/v | weight per volume |

1. Abstract

The telomere repeat binding factor, TRF2, is a key component of the shelterin complex, which plays an important role in the maintenance of telomeres and the protection of the telomeric DNA from uncontrolled processing by the DNA damage machinery. Telomeres resemble double-stranded breaks (DSBs) and the shelterin complex hides the telomeres in a loop structure, called T-loop. Recent studies have suggested that TRF2 is able to bind and inhibit ATM, which scans the genomic DNA for DSBs. Therefore, TRF2 might be the key regulator of ATM at the telomeres. While TRF2 is abundant at the telomeres, it is possible that over-expression of TRF2 expands its ATM-inhibiting potential throughout the nucleus and therefore jeopardizes the DNA surveillance machinery elsewhere in the genome, which could give TRF2 oncogenic potential *in vivo*. To investigate this, it was the goal of my thesis to over-express TRF2 in the mouse hematopoietic system. I delivered two variants of TRF2, transgenic mTRF2 and GFP-mTRF2, into mouse hematopoietic stem cells using lentiviral technology. The transduced cells were transplanted into C57BL/6J recipient mice and the successful integration of transgenic TRF2 was confirmed by genotyping. Functional over-expression of transgenic TRF2 in the hematopoietic system was verified by *Western* analysis and fluorescence microscopy. Pathological data and FACS analysis showed the development of CD4/CD8-double-positive T-cell lymphomas in a subset of TRF2 over-expressing mice but not in GFP-control mice. Surprisingly, over-expression of the TRF2 transgene was not detectable in tumor cells and a genomic screen did not show the presence of the TRF2 transgene. I considered that TRF2 had oncogenic potential only in early stages of tumorigenesis and genome instability, which was detected by FISH analysis and the presence of anaphase bridges, explained the loss of the transgene in later stages of tumor development. However, the results of my thesis studies suggest that TRF2 does not act as a dominant oncogene in the mouse hematopoietic system.

2. Zusammenfassung

Das Telomerprotein TRF2 ist ein Hauptbestandteil des Shelterin-Komplexes, welcher die Funktionsfähigkeit der Telomere und deren Schutz vor einem unkontrollierten nucleolytischen Angriffs des DNA Reparaturmechanismus der Zelle sicherstellt. Telomere ähneln in ihrer Form Doppelstrang-Brüchen (DSBs), und der Shelterin-Komplex schützt die Telomere durch die Formation einer sogenannten T-loop Struktur. Neue Studien zeigen, dass TRF2 in der Lage ist ATM zu binden und dessen Funktion, nämlich die Suche nach DSBs innerhalb des Genoms, zu unterdrücken. Daher könnte TRF2 eine Schlüsselrolle in der Regulation von ATM an den Telomeren zukommen. Unter normalen Umständen ist TRF2 lediglich an den Telomeren in hoher Konzentration zu finden, jedoch könnte dessen Überproduktion die Unterdrückung von ATM auch andernorts der Telomere zur Folge haben. Somit würde der gesamte ATM-abhängige DNA Reparaturmechanismus in seiner Funktionalität beeinträchtigen. Im Zuge dessen würde TRF2 *in vivo* ein onkogenes Potential zu Teil. Um diese Hypothese zu untersuchen, war es das Ziel meiner Arbeit, TRF2 im murinen hematopoietischen System zu überproduzieren. Dazu habe ich zwei Varianten von TRF2, mTRF2 und GFP-mTRF2, mittels lentiviraler Transduktion in murine hematopoietische Stammzellen eingeschleust. Die infizierten Zellen wurden in C57BL/6J Empfängermäuse transplantiert und die erfolgreiche Integration des Transgens wurde mittels Genotypisierung überprüft. Die funktionale Überproduktion von transgenem TRF2 im hematopoietischen System wurde mit Hilfe einer *Western* Analyse und Fluoreszenz Mikroskopie sichergestellt. Pathologische Befunde und FACS Analyse zeigten die Entstehung von CD4/CD8-doppel-positiven T-cell Lymphomen in einem Teil der TRF2 überproduzierenden Mäuse, nicht aber in den GFP-Kontrollmäusen. Überraschend war dabei, dass weder die Überproduktion von transgenem TRF2 in den Tumorzellen, noch die Präsenz des Transgens innerhalb des Genoms nachweisbar war. Daher zog ich es in Betracht, dass TRF2 sein onkogenes Potential nur in den frühen Stufen der Tumorbildung zeigt, und das genomische Instabilität, wie sie nachweisbar war

durch FISH Analyse und durch die Präsenz von Chromatid-Brücken in Anaphasen, zum Verlust des TRF2 Transgens in späteren Phasen der Tumorentwicklung führte. Die Ergebnisse meiner Arbeit lassen jedoch die Schlussfolgerung zu, dass TRF2 nicht als dominantes Onkogen im murinen hematopoietischen System wirkt.

Keywords:

TRF2, hematopoietic, oncogenic

Schlagworte:

TRF2, hematopoietisch, Onkogen

3. Introduction

Circular genomes, as found in prokaryotes, can be fully replicated by conventional polymerases, while the presence of linear chromosomes, in mammals and other eukaryotes, presents a tremendous challenge to the replication process. Because cells divide and their genome needs to be replicated during each cell division, inevitably DNA is lost at the tip of the chromosomes due to the inability of conventional polymerases to replicate the linear ends of the chromosomes. This phenomenon has been characterized by Watson and Olovnikov as the so called “end replication problem” [1, 2], which results from the enzymatic activity of DNA polymerases that use a short RNA primer to initiate polymerization in the 5'-3' direction. The DNA strands at the end of linear chromosomes are replicated in a different mode (Figure I - 1). For the replication of the one strand, termed the leading strand, a single primer can be continuously extended, presumably resulting in a blunt-ended molecule. The replication of the other strand, termed the lagging strand, requires a different mechanism of replication. Multiple short RNA primers are extended and the resulting Okazaki fragments are joined together after the removal of the RNA primers. While the internal gaps, which result from the removal of the RNA primers, can be filled in by polymerases, the gap at the very end of the replicated strand remains. It cannot be processed by any conventional polymerase and the replication of the lagging strand appears incomplete. With regard to the length of a RNA primer, each replication theoretically leads to a loss of 3 to 6 bp of DNA per end. But the actual loss is much larger in most organisms bearing linear chromosomes, as evidenced by the presence of single-stranded 3' extensions of the G strand. Depending on the organism, overhang size can range from 12-16 nucleotides in ciliates [3-5], around 30 nucleotides during S phase in *S. cerevisiae* [6, 7], and as long as 300 nucleotides in human cells [8]. Surprisingly, this overhang has been detected on both chromosome ends. Not only both termini of human chromosomes [8], but also those in *Trypanosoma brucei* [9], and Tetrahymena [10], end in an overhang estimated to be up to a few hundred

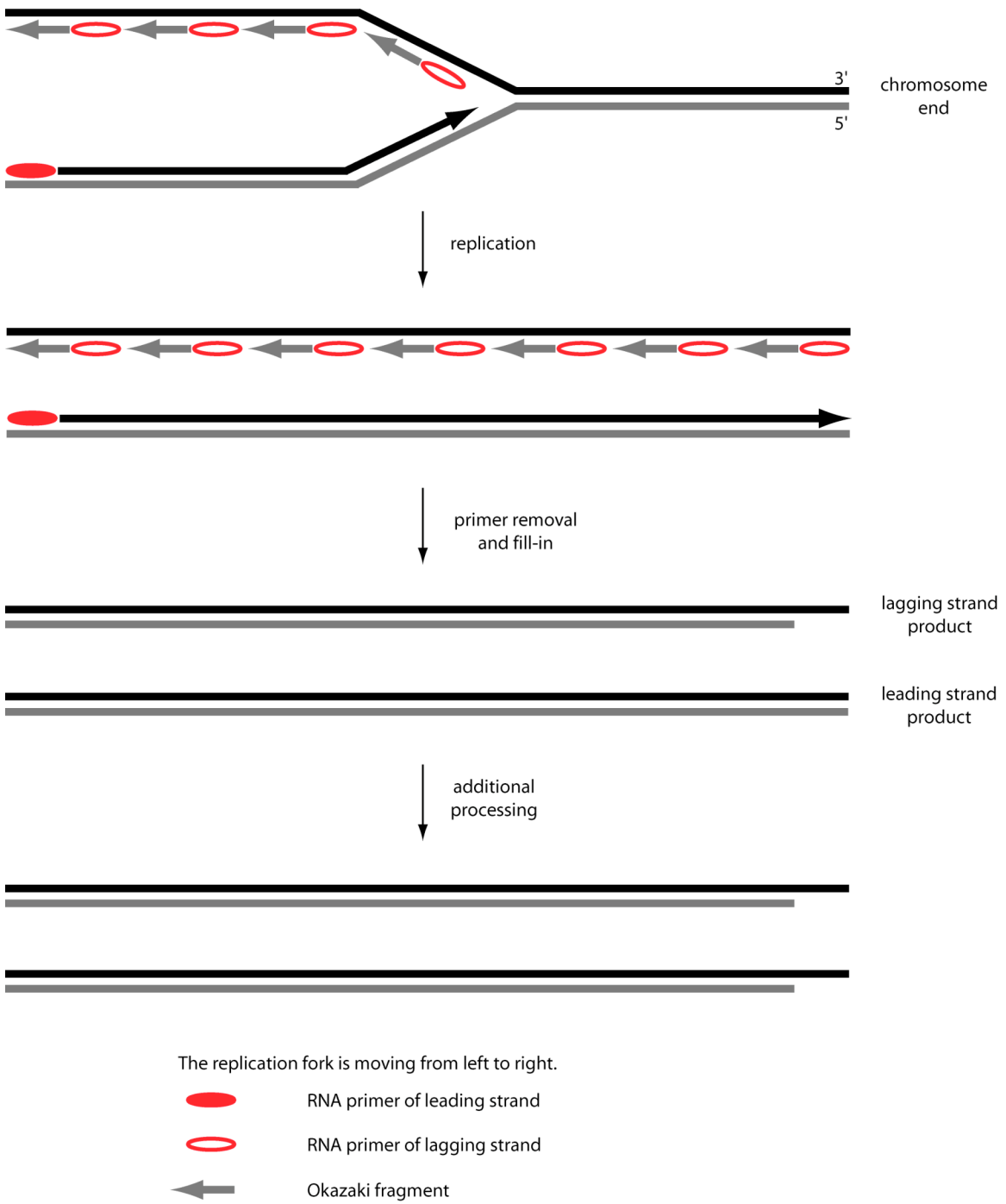


Figure I - 1 Schematic of replication at the very end of a chromosome

nucleotides in length. While for the lagging strand this can be explained assuming that the RNA primer binds not at the very terminus of the actual chromosome tip, replication of the leading strand should theoretically result in a blunt end. However, this is not the case. The presence of an overhang suggests a nucleolytic process, which creates a single-stranded overhang in the case of the leading strand or extends the single-stranded overhang, in the case of the lagging strand. It is mandatory that generation of an overhang is counteracted to avoid the permanent loss of DNA with each cell division.

In addition to preventing loss of the chromosome ends, organisms with linear chromosomes have to overcome the cellular response to DNA ends. Unprotected DNA ends resemble double-stranded breaks [11, 12], which are recognized and processed by the DNA damage machinery. It is necessary for the cell to eliminate chromosomal breaks that result from environmental stress, internal metabolism, DNA replication, and physiological breaks acquired during development. The solution is a mechanism that allows the cellular machinery to distinguish between common DNA breaks and the ends of linear chromosomes. Throughout evolution cells have developed a sophisticated complex, called the telomere, which allows higher organisms to overcome the loss of important DNA information during replication and to protect chromosomal ends from the cellular machinery. First defined as “free ends” that are unable to fuse with broken DNA [13], telomeres are complexes of repetitive DNA and associated proteins that can be found at all ends of linear chromosomes.

3.1. *Telomeric DNA sequences*

Telomeres were first characterized as long stretches of highly repetitive DNA in the ciliated protozoan *Tetrahymena thermophila*. In this organism the ends of the linear DNA minichromosomes that comprise the amplified RNA genes (rDNAs) consist of approximately 50 tandem repeats of the hexanucleotide unit CCCCAA/GGGGTT, with the G-rich strand bearing the 3'-OH end of each end of the linear DNA [14]. The knowledge of telomere sequences in other organisms

expanded soon thereafter (Table I - 1), sharing an extremely simple, tandemly repeated DNA sequence containing a cluster of C residues [15]. Exceptions to these very conserved structures were discovered in *K. lactis* [16], where the telomeric repeats were expanded, and in *S. cerevisiae* and *S. pombe* with their irregular telomere repeats [17, 18]. In *Drosophila melanogaster*, these telomeres consist of repetitive sequences, which are actually retrotransposons of the non-LTR type [19-21]. Although dipteran telomere structure and maintenance is unlike in any other organism, the telomeric functions are conserved.

Table I - 1 Sequences of telomeric DNA in selected species. ¹These are non-canonical since they are not maintained by telomerase.

| Telomeric sequence | Species | Reference |
|--|---|-----------|
| TTGGGG | Tetrahymena | [14] |
| TTTTGGGG | Oxytricha, Euplotes | [3] |
| TTAGGG | <i>Trypanosoma brucei</i> | [22, 23] |
| T(G) ₂₋₃ (TG) ₁₋₆ | <i>Saccharomyces cerevisiae</i> | [17] |
| GGTTACA | <i>Schizosaccharomyces pombe</i> | [18, 24] |
| ACGGATTTGATTAGGTATGTGGTGT | <i>Kluyveromyces lactis</i> | [16] |
| TTAGGC | <i>Caenorhabditis elegans</i> | [25] |
| Het-A and TART retrotransposons ¹ | <i>Drosophila melanogaster</i> | [19-21] |
| TTAGG | <i>Bombyx mori</i> (silkworm) | [26] |
| TTTAGGG | <i>Arabidopsis thaliana</i> | [27] |
| TTAGGG | <i>Homo sapiens</i> and other vertebrates | [28] |

Telomere length is highly variable among organisms. While in Tetrahymena and yeasts telomeric tracts are approximately 300 bp in length [14, 17], the TTAGGG repeats in human cells range from 2 kbp to 25 kbp [28-30]. Telomeres of up to 50 kbp are found in some mouse species including the laboratory *Mus musculus* [31]. During each replication process part of the terminal tip of each chromosome gets lost so telomeres can act as a buffer to prevent the cell from losing important genomic information, which is located in the more proximal area of the centromeres. Telomeres, however, only delay the end-replication problem and

for a single cell to overcome this problem and become immortal, it needs an active mechanism to maintain the length of the telomeric DNA over generations.

3.2. *Telomerase*

A cell can overcome extensive telomere shortening by the effective maintenance of the telomere length, which is accomplished by a widely employed mechanism, performed by the ribonucleoprotein telomerase. This protein contains two essential components, a **telomerase reverse transcriptase catalytic subunit** (TERT) [32] and a functional telomerase RNA (TR). While the RNA component serves as a template to align with the telomeric 3'-overhang, TERT synthesizes one repeat as specified by the RNA [33, 34]. Telomerase can then relocate to the newly synthesized telomeric end and repeat the process, or it continues the process at another DNA substrate. In general telomerase synthesizes the G strand first, followed by the C strand [35], with the result of a double-stranded repeat array. One possibility for the generation of the G strand overhang as it is found at chromosome ends could be by the abrogation of the process after the last G strand synthesis. This idea, however, is controversial since cells that lack telomerase activity can contain G-overhangs [8, 36-38]. A nucleolytic process is therefore a more likely explanation for the generation of the 3'-overhang.

The G-overhang plays an important role in the maintenance of telomeric DNA. *In vitro* assays have shown that telomerase needs a single-stranded overhang to extend a DNA fragment, while blunt-ended DNA cannot be extended [39, 40]. Surprisingly, telomerase has a limited selectivity on the overhang. As shown, telomerase can elongate non-telomeric sequences both *in vitro* [39, 41-45] and *in vivo* [41, 46, 47]. This *de novo* addition of telomeric DNA is thought to be important for the "healing" function of telomerase, through which broken ends can be capped [48].

In unicellular organisms telomerase has a housekeeping function and its two essential subunits are always expressed. This expression level, however, can fluctuate and expression of telomerase RNA can increase at a specific

development stage, for example during macronuclear development in *Tetrahymena* [49]. Telomerase activity is detectable in most mouse tissue [50], due to expression of both subunits of the enzyme [51-53]. The catalytic subunit of the mouse telomerase, in contrast to the RNA subunit, is haplo-insufficient so that cells heterozygous for mTERT gradually shorten their telomeres [54].

In most normal human tissue telomerase activity is repressed [55]. Activity is detectable only in ovaries and testis [56], and in highly proliferative tissues including hematopoietic cells [57, 58]. While the RNA subunit, hTR, is present in many telomerase negative cells, the regulation of telomerase appears to be at the level of hTERT expression. Telomerase activity is found in most of the primary tumors and tumor cell lines, showing the presence of mRNA of hTERT [59-61]. That hTERT regulates telomerase activity is further supported by the fact that the expression of hTERT alone in primary fibroblasts can establish telomerase activity [62, 63]. The fine balance between the suppression and the activation of telomerase activity needs to be further elucidated. To date, little is known about what leads to the suppression of telomerase in human somatic tissue and what causes its activation in 90% of human tumors [64].

3.3. Telomerase-associated proteins

Telomerase activity cannot be constituted by the sole expression of the two subunits, hTR and hTERT. Biochemical and genetic studies suggest the existence of additional protein subunits of telomerase that may be involved in the assembly or biogenesis of active telomerase. These proteins may mediate or regulate the access of telomerase to its substrate, the telomeres (Table I - 2).

Table 1 - 2 Human telomerase-associated proteins. aa - amino acids; nt - nucleotides [65].

| Protein | Interacting region | Function |
|-------------------------|--------------------|-------------------------------------|
| <i>hTERT associated</i> | | |
| TEP1 | aa 1-350, 601-927 | Unknown |
| P23/p90 | aa 1-195 | Assembly/conformation |
| 14-3-3 | aa 1004-1132 | Nuclear localization |
| <i>hTR associated</i> | | |
| TEP1 | nt 1-871 | Unknown |
| hGAR1 | hTR H/ACA domain | Stability, maturation, localization |
| Dyskerin/NAP57 | hTR H/ACA domain | Stability, maturation, localization |
| hNOP10 | hTR H/ACA domain | Unknown |
| hNHP2 | hTR H/ACA domain | Stability, maturation, localization |
| C1/C2 | nt 33-147 | Stability, maturation, localization |
| La | nt 1-205, 250-451 | Accessibility to telomeres? |
| A1/UP1 | nt 1-208 | Unknown |
| hStau | nt 64-222 | Accessibility to telomeres? |
| L22 | nt 64-222 | hTR processing, localization? |

3.3.1. hTERT-associated proteins

In previous studies in *Tetrahymena thermophila* [66-68], the first protein to be found associated with telomerase activity is TEP1 (telomerase-associated protein 1), which was subsequently identified in humans, mice, and rats [69, 70]. However, although association of TEP1 with the RNA and the catalytic subunit of telomerase had been shown [69, 71], the exact role of TEP1 in the context of telomerase has not been explained so far. Other proteins found to interact with telomeres are the chaperones p23 and p90 [72]. Both appear to be important for the functional assembly of the two basic subunits of telomerase since recent studies have shown stable association of both chaperones with the human telomerase [73]. The same studies suggest a role of p23 and p90 in the

translocation process during telomere extension. Other proteins found to interact with hTERT are the 14-3-3 proteins [74]. While they are not required for the activity *in vitro* or in intact cells, the results suggest that 14-3-3 proteins promote the nuclear localization of hTERT.

3.3.2. hTR-associated proteins

A number of proteins such as hGAR1, dyskerin/NAP57, hNOP10, and hNHP2 [75-78] are found to interact with mammalian telomerase RNA by binding to the 3'-terminal extension of the RNA subunit, which structurally resembles H/ACA snoRNAs [79, 80]. Small nucleolar ribonucleoprotein complexes (snoRNPs) [80] and some heterogeneous nuclear ribonucleoproteins (hnRNPs) [81-83] are also found to interact with hTR. SnoRNPs and hnRNPs appear to play a role in telomerase localization and also in telomerase accessibility to telomeres [83, 84]. Specifically, the La antigen interacts with hTR and telomerase and influences telomere length *in vivo* [85]. Finally, hStau and L22 interact with hTR and may play a role in hTR processing, localization and telomerase assembly [86]. The proteins mentioned above constitute a small portion of all that interact with hTR. The list of known telomerase-associated proteins is still growing, but their specific roles need to be further elucidated.

3.4. *Alternative ways of telomere lengthening*

While telomere length maintenance in most tumor cells is regulated by telomerase, another way of length control is termed “**A**lternative **L**engthening of **T**elomeres”, or ALT [87]. The exact mechanism of ALT is not yet understood, but it is believed that a DNA strand from one telomere of an ALT cell anneals with the complementary strand of another telomere, thereby priming synthesis of new telomeric DNA using the complementary strand as a copy template [88]. The ALT pathway appears to be more dominant in cell lines and tumors of mesenchymal

origin than in those of epithelial origin [89]. Unlike cells where telomerase activity drives telomere maintenance and telomere length is very homogenous, ALT cells are characterized by the presence of a highly heterogeneous telomere pattern (i.e. the telomere lengths range from very short to extremely long). Other data have shown that the coexistence of normal telomerase activity and the ALT mechanism in an individual tumor cell is a possibility [90-93]. It seems very likely that the cancerous and the normal cell lines that utilize ALT are subverting a normal mechanism, which is not discovered yet. Alternatively, other data suggest a dominance of telomerase over ALT, most likely because TERT may affect cellular functions in addition to telomere length and, although telomerase and ALT appear to be equivalent in their ability to immortalization, their contributions to tumor growth and survival *in vivo* may differ [94]. Finally, since inhibition of telomerase results in apoptosis or senescence [95-99], repression of the ALT mechanism also results in cell death or senescence [100, 101].

3.5. *The telomere terminus*

As described previously, mammalian telomeres end with a 3'-overhang, composed of a several hundred nucleotide long stretch of the TTAGGG repeat. The overhang seems to play an important role in T-loop formation, a secondary structure of the telomeres I will describe later. Of all the possibilities that may explain the presence of the 3'-overhang, a 5' to 3' exonuclease or a combination of an endonuclease and a helicase are most likely needed to process telomere termini [8]. It has been further recognized that the 3' nucleotide of the telomeres can represent each position within the TTAGGG repeat [102]. However, in the presence of telomerase, a prevalence of TAG-3' ends was observed. In contrast, the 5' end of a telomere is nearly always ATC-5' [102].

3.6. The T-loop

Electron microscopic studies on purified human and mouse telomeres have revealed a secondary structure, termed the telomeric loop, or T-loop (Figure I - 2) [103]. The large duplex T-loop structures are formed by the invasion of the 3'-overhang into the double-stranded part of the telomere. It is believed that T-loops hide the ends of the telomeres from the DNA damage machinery. The formation of the T-loop structure appears to be heavily dependent on the presence of telomere proteins, such as TRF1 and TRF2, because the T-loop resolves when it gets isolated and purified from proteins.

Mammalian Telomeres

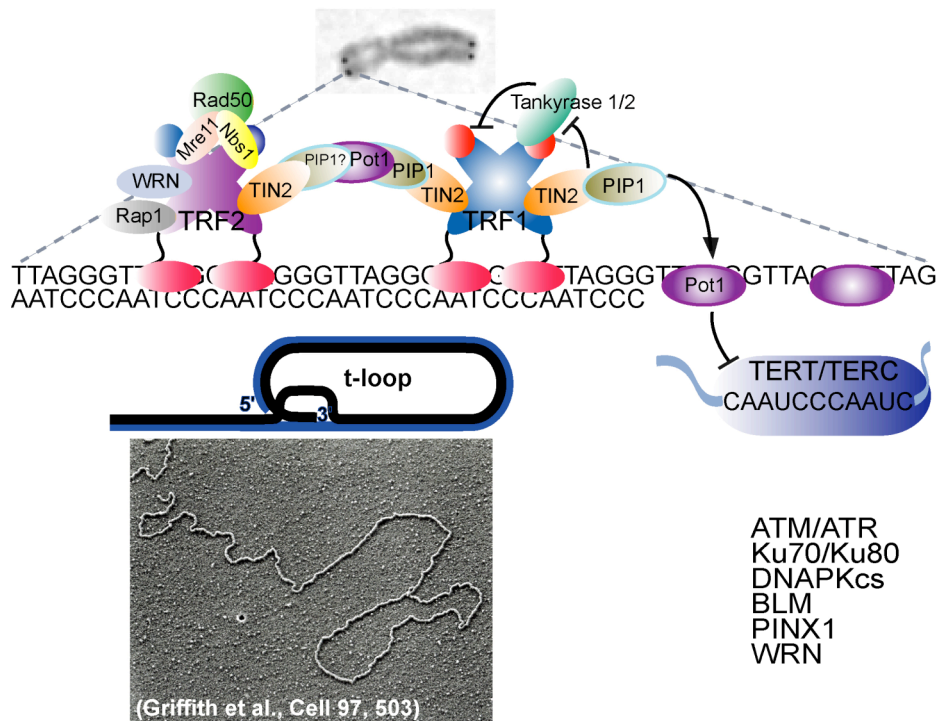


Figure I - 2 Telomere structure. Schematic of human telomeres in the "open" and T-loop states and (bottom left) electron microscopic micrograph of human telomeric DNA in the T-loop configuration in naked isolated DNA.

3.7. Shelterin

In general three types of factors associate with telomeric DNA: nucleosomes, which obviously play a role in the chromatin structure of telomeres, some other chromosome transaction factors that also function elsewhere, and a six protein telomere core complex, recently termed shelterin [104]. To date little is known about the nucleosomes and chromosome transaction factors in the context of telomeres, although their role at the telomeres might be significant and will require further investigation. The role of the shelterin complex (Figure I - 3), however, appears to be essential for the functionality of telomeres. The shelterin complex is characterized by its high abundance at the telomeres throughout the cell cycle, but does not accumulate elsewhere since its function is limited to the telomeres.

The first shelterin protein to be discovered was the mammalian telomere repeat binding factor, TRF1 [105, 106]. TRF1 showed *in vitro* binding specificity for double-stranded TTAGGG repeats. TRF2 was identified as a TRF1 paralog in genome databases [107, 108] and TIN2 and Rap1 were found in two-hybrid screens with TRF1 and TRF2, respectively [109, 110]. TPP1 [111-113] recently emerged from searches for TIN2-interacting proteins. POT1 appears to be the most conserved component of shelterin and was identified based on sequence homology to telomere end-binding factors in unicellular eukaryotes [114].

The cornerstone within the shelterin complex appears to be TIN2, which tethers TPP1/POT1 to TRF1 and TRF2. TIN2 also connects TRF1 to TRF2 and this link contributes to the stabilization of TRF2 on telomeres [112, 115]. Although subcomplexes of shelterin have been found [116], little about the number of shelterin units bound per telomere, the stoichiometry of the shelterin subunits, is known. The shelterin complex affects the structure of telomeric DNA (Figure I - 4).

It determines the structure of the telomere terminus, it is implicated in the generation of the T-loop, and it controls the synthesis of telomeric DNA by telomerase. As described in a later section, the shelterin complex appears to protect the telomeres from the DNA damage machinery. The following sections describe the characteristics of the six known shelterin subunits in more detail.

3.7.1. TRF1

TRF1 is a 439 amino-acid protein with three domains: an amino terminal acidic region, a dimerization domain, and a carboxy-terminal DNA-binding domain. The DNA-binding domain is an approximately 50 amino-acid region of the SANT/Myb-type that is also structurally related to the homeodomain. The DNA-binding of TRF1 predominantly happens after dimerization of TRF1 [118, 119]. This dimerization is mediated by the TRF homology (TRFH) domain, a hallmark of the TRF family, which includes TRF2, *S. pombe* Taz1, and TRF from trypanosomes [108, 110, 119-121]. The linker region between the Myb domain and the TRFH domain appears to be flexible and diverges rapidly in mammalian evolution [120]. It has also been found that as a result of alternative splicing, hTRF1 molecules are expressed as two closely migrating proteins [122, 123], but they appear to be functionally identical. TRF1 can be found at the sites of telomeres throughout the cell cycle, including all stages of mitosis and meiosis [106, 108, 123-125]. The binding of TRF1 to the telomere sequence is highly specific and it has been shown that 5'-AGGGT-3' is the core sequence required for TRF1 DNA-binding [126]. *In vivo*, where TRF1 is dimerized, the presence of two Myb domains increases the binding of TRF1 by tenfold. It is believed that the extreme spatial flexibility of dimerized TRF1 *in vivo* is due to the unstructured linker region in between the TRFH and Myb domain.

TRF1 can act as a negative regulator of telomere length in telomerase-positive cells and, although diminished TRF1 loading on telomeres leads to telomere elongation, no telomere deprotection phenotype has been observed. However,

TRF1 is essential in the mouse, suggesting that TRF1 contributes to the protection of telomeres [127].

3.7.2. TRF2

TRF2 is a 500 amino-acid protein containing a TRFH domain and a short basic amino-terminal domain [108]. Although the structures of TRFH domains of TRF1 and TRF2 are very similar, a steric clash prevents heterodimerization between both of them. TRF2 shows strong parallels to the TRF1 DNA-binding features. However, although this is true for sequence specificity and spatial flexibility, TRF2 has a greater tendency to form higher order oligomers and does not have telomeric DNA pairing activity [128]. In mice, TRF2 deficiency leads to early death during the embryogenesis [129]. The deletion of TRF2 results in p53-dependent senescence, genome-wide chromosome end fusions, and a DNA damage response [129].

Since my thesis was based on certain abilities of TRF2 in the context of DNA damage response, I will describe further characteristics of TRF2 in more detail later in the introduction.

3.7.3. TIN2

TIN2 is a small 354 amino-acid protein that binds the TRFH domain of TRF1 with its central region. This protein shows interaction with most shelterin subunits, including TRF1, TRF2, and TPP1, making it the cornerstone of the complex. TIN2 has also been shown to interact with POT1 through TPP1. Binding of TIN2 to the telomeres is mediated by TRF1 and TRF2 [115, 130]. It has been suggested that the interaction of TRF1 and TRF2 through TIN2 enhances the binding affinity of both TRFs to telomeres. Disruption of the TRF1-TIN2-TRF2 connection by a mutant version of TIN2 shows a telomere deprotection

phenotype [130]. It has also been shown that TIN2 acts to stabilize shelterin by protecting TRF1 from tankyrase 1 [131].

3.7.4. Rap1

Human Rap1 is a 399 amino-acid protein with three domains: a BRCT domain, a single Myb domain, coiled region, and the Rap1 carboxy-terminal (RCT) domain. The RCT mediates the interaction with TRF2 as well as homotypic interactions. The Rap1 carboxyl terminus also contains a putative nuclear localization signal (NLS). Unlike Rap1 in budding yeast, which has diverged from human Rap1, the mammalian variant has only one Myb domain, which lacks the overall positive charges necessary to directly bind DNA [110]. The role of Rap1 within the shelterin complex is likely limited to the mediation of protein-protein interaction. It has also been shown that Rap1 levels at telomeres decrease in the absence of TRF2, similar to the Rap1 ortholog in *S. pombe*, which also localizes to the telomeres through a TRF2-like protein, Taz1p [132, 133]. Rap1 plays a role in telomere length regulation and affects telomere length heterogeneity [110, 134]. Furthermore, it was shown that mice lacking Rap1 are not viable, suggesting an important role of Rap1 in the protective activity of shelterin.

3.7.5. TPP1

TPP1 has been found as a component of shelterin by independent studies [111-113]. The carboxy-terminal 60 amino-acids of TPP1 bind to the amino-terminal half of TIN2, and a central 100 amino-acid region in TPP1 binds to the carboxy-terminus of POT1. Other than a serine-rich region separating these two interaction domains, the TPP1 sequence does not contain notable features. TPP1 appears to play a role in the recruitment of POT1 to telomeres and the inhibition of TPP1 consistently leads to inappropriate telomere elongation, a phenotype associated with diminished POT1 loading [112, 113]. Very recently

TPP1 has been demonstrated to be a putative mammalian homologue of TEBP-beta in *Oxytricha nova* [135, 136].

3.7.6. POT1

POT1 binds single-stranded DNA with two oligonucleotide/oligosaccharide-binding (OB) folds [137]. It shows a high specificity for the sequence 5'-(T)TAGGGTTAG-3', which it can bind at the 3' end or within a longer single-stranded region [137, 138]. Studies suggest that POT1 can bind to the 3'-overhang of telomeres over the full length of the single strand, but it prefers the most proximal and also the most terminal sequence of the 3'-overhang. The carboxy-terminal half of POT1, which binds to TPP1, is important for the localization of POT1 to telomeres, whereas the DNA-binding domain of POT1 is not. Recently it has been shown that two forms of POT1 emerge from alternative splicing: one full-length form and a shorter form that lacks the first of the two OB folds required for the single-stranded DNA-binding [138, 139]. The presence of the shorter POT1 variant is diminished and its function is not explored so far. Inhibition of human POT1 in primary cells leads to growth defects [140]. In addition, the mouse genome contains two variants of POT1, termed POT1a and POT1b. Although they are very similar in sequence and they both bind to telomeres, mice lacking POT1a die early in embryogenesis, indicating that these two versions of POT1 are not functionally redundant. In summary, POT1 plays a crucial role in telomere length control, acting as the terminal transducer. It also contributes to the protection of chromosome ends, since partial knock-down of POT1 results in a DNA damage response at telomeres, reduction in the single-stranded telomeric DNA, changes in the 5' end of the chromosome, and a mild telomere fusion phenotype [117, 139, 141].

3.8. *Non-shelterin telomeric proteins*

Numerous telomeric proteins that are not part of the shelterin complex have been found (Table I - 3).

Table I - 3 Examples of non-shelterin proteins at human telomeres. Direct interactions with shelterin components are indicated where known. Factors recovered in association with shelterin are identified as such [104].

| Protein complex | Nontelomeric function | Effects at telomeres | Interactions |
|------------------|---|---|------------------------------|
| Mre11/Rad50/Nbs1 | recombinational repair DNA damage sensor | T-loop formation/resolution? required for T-loop HR | associated with shelterin |
| ERCC1/XPF | NER, crosslink repair 3' flap endonuclease | deficiency leads to formation of TDMS; implicated in overhang processing after TRF2 loss | associated with shelterin |
| WRN helicase | branch migration G4 DNA resolution | deficiency results in loss of lagging-strand telomeres | TRF2 |
| BLM helicases | branch migration crossover repression | T-loop formation/resolution? | TRF2 |
| DNA-PK | NHEJ | deficiency leads to mild fusion phenotype | associated with shelterin |
| PARP-2 | BER | not known | TRF2 |
| Tankyrases | role in mitosis (tankyrase 1) | positive regulator of telomere length through inhibition of TRF1 | TRF1 |
| Rad51D | unknown (HR?) | deficiency leads to mild fusion phenotype | unknown |

Among those are the TRF1-interacting-**ankyrin**-related (ADP-ribose) polymerases, tankyrase 1 and 2 [142-144]. It is believed that tankyrases are negative regulators of TRF1 [142, 145], as over-expression of tankyrases removes TRF1 from the telomeres. This loss of TRF1 binding, however, can be counteracted by TIN2 [131].

Other important proteins with non-exclusive telomere functions are the WRN and BLM RecQ helicases. Recently it was shown that the WRN protein is involved in the resolution of G-quadruplex structures, which can be found in the lagging strand of the telomeres and need to be removed prior to the DNA replication process. Dysfunction of WRN by mutations in the RecQ-helicase domain leads to sudden sister telomere loss, called STL-phenotype [125]. The role of BLM at the telomeres has not been investigated yet, but interaction of BLM and TRF1 at the ALT-associated PML bodies (APBs) of ALT cells has been shown [146, 147].

RAD51D has also been detected at telomeres [148], most likely due to its role in homology-directed repair of double-stranded breaks (DSBs).

A prominent marker for telomere dysfunction are chromosome end fusions, which take place between the C strand of one telomere and the G strand of another due to covalent end binding, also referred to as **Non Homologous End Joining (NHEJ)**. I will describe the details of this process later (see below).

The MRN complex, composed of Mre11, Rad50 and Nbs1, is recruited to the telomeres through an interaction with TRF2 [149]. While Mre11 and Rad50 are present at the telomeres throughout the cell cycle, Nbs1 is only detectable at telomeres in S phase. While the role of the MRN complex in mammalian cell function is important, its role at the telomeres needs to be further elucidated. However, it appears to act in the processing of unprotected telomeres, since there is an increase in MRN complex localization at unprotected telomeres. So far it has been shown that a mutant allele of Nbs1 induces telomere loss in some settings [150], and Nbs1 also contributes to the telomerase-mediated telomere elongation pathway [151].

3.9. Repression of the telomere-damage response by shelterin

The structural influence of shelterin on the telomere complex allows the hiding of the 3'-overhang in the T-loop structure. Considering that the loss of the 3'-overhang causes a DNA damage response, this would explain shelterin's role in the inhibition of the DNA damage machinery at the sites of telomeres. However,

recent data show the induction of telomere damage foci even in the presence of the 3'-overhang [129], suggesting that shelterin has at least one other mechanism to prevent detection of telomeres by the DNA damage surveillance. It is therefore proposed that the T-loops created by shelterin result in nucleosomal organization, which conceals the chromosome ends from the DNA damage surveillance. In recent studies of ATM, 53BP1, and fission yeast Crb2 it was suggested that a key event in the DNA damage response is a change in the nucleosomal organization at the site of DNA damage [152, 153]. Formation of the T-loop structure, initiated by the shelterin complex, might constitutively hide methylated residues within the nucleosomes, which are necessary for 53BP1 to trigger the DNA damage machinery to the sites of damage. When the telomeres are exposed or if shelterin is inhibited, the telomeres and the nucleosomes are exposed and a 53BP1-dependent DNA damage response is initiated. However, it must be noted that this model of telomere end protection is still evolving and that other factors like the MRN complex and 9-1-1/RFC might also play a more crucial role in telomere damage signaling. Therefore, shelterin counter-tactics to telomere damage signaling need to be further investigated.

3.10. The response to telomere attrition

Telomere attrition in primary human cells results from the programmed shortening of human telomeres and limits their proliferation. When a telomere reaches a critical length, a cell cycle arrest is initiated, which has the hallmarks of a DNA damage response: DNA damage foci are detectable in (newly) senescent cells, the ATM kinase pathway is activated, and p53 enforces a G1/S arrest [154]. It appears that the shortest telomere, not the mean telomere length, triggers the induction of senescence. The effects of short telomeres are similar (or the same) to the cellular response to telomeres that lack shelterin.

Dysfunctional mammalian telomeres are similar to DSBs and therefore their processing is similar: either by NHEJ or homologous recombination (HR). While NHEJ causes telomere fusions, formation of dicentric chromosomes, and the

associated genome instability, HR can delete large segments of telomeric DNA and mediate exchange of sequences between sister telomeres.

3.10.1. NHEJ

A prominent phenotype of telomere dysfunction are chromosome end-to-end fusions. They can occur when telomeres are shortened, when shelterin components are inhibited, and upon loss of other telomere-associated proteins such as TRF2. As briefly mentioned before, these fusions are covalent connections between the C strand of one telomere and the G strand of another (Figure 1 - 5), and may occur before or after DNA replication. The resulting dicentric chromosome can become attached to both spindle poles and lead to a problem for chromosome segregation in anaphase. Consequently, in anaphase cells with dicentric chromosomes, characteristic chromatin bridges are observed. Factors involved in this process are DNA ligase IV and Ku70/80, DNA-PKcs and XRCC4. In general telomere fusions depend on the prior removal of the 3'-overhang and the nucleotide excision repair factors ERCC1/XPF have been implicated in this process [155].

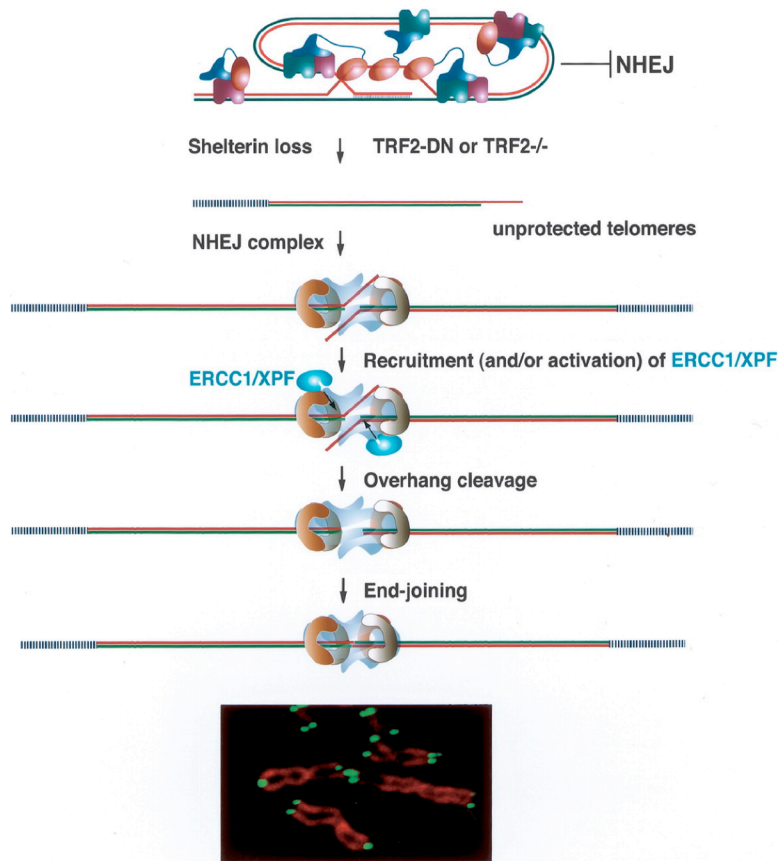


Figure I - 5 Proposed role for shelterin in protecting telomeres from NHEJ and overhang loss. Telomeres are proposed to be resistant to NHEJ because of their T-loop configuration, which will block the NHEJ complex from accessing to the chromosome end. Upon loss of shelterin, T-loops are proposed to be destabilized (or not formed), allowing engagement of the NHEJ pathway. Prior to the ligation of chromosome ends by DNA ligase IV, the DNA-PK complex is proposed to form a synaptic structure that activates and/or recruits ERCC1/XPF. This nuclease is implicated in cleavage of the 3' overhang. End-joining of telomeres results in dicentric chromosomes (example shown at bottom). After DNA replication, fusions can occur between sister and non-sister telomeres. NHEJ can also occur prior to DNA replication, giving rise to chromosome-type fusions in metaphase (not shown) [104].

3.10.2. HR

There are three types of HR that have detrimental outcomes at chromosome ends. The first is homologous recombination between sister telomeres, also called Telomere Sister Chromatid Exchange (T-SCE). It is crucial for a cell that the exchanged telomeres are equal in length to avoid lengthening of one sister

telomere at the expense of the other. In normal mouse and human cells, T-SCE is not very frequent, but ALT cells, which maintain their telomeres by a recombination pathway, have very frequent T-SCE [156-158]. Different levels of repression might be the reason for T-SCE in ALT versus normal cells.

Telomeres are also threatened by a HR reaction referred to as T-loop HR [159]. T-loops are at risk for resolution by Holiday junction (HJ) resolvases because an HJ could be formed if the 5' end of the telomere pairs with the displacement loop (D-loop). Branch migration in the direction of the centromere could generate a double HJ and resolution of the structure by crossover events would delete the whole loop segment, leaving a drastically shortened telomere at the chromosome end (Figure I - 6). Proteins involved in this process are the MRN complex and XRCC3, a Rad51 paralog associated with HJ resolution activity. Studies have shown that a mutant form of TRF2, which lacks the N-terminus, promotes T-loop HR, but further studies are necessary to characterize this process. However, it has been shown that the presence of telomeric circles, as they are found in ALT cells, lead to the further enhancement of this variant of HR [159, 160].

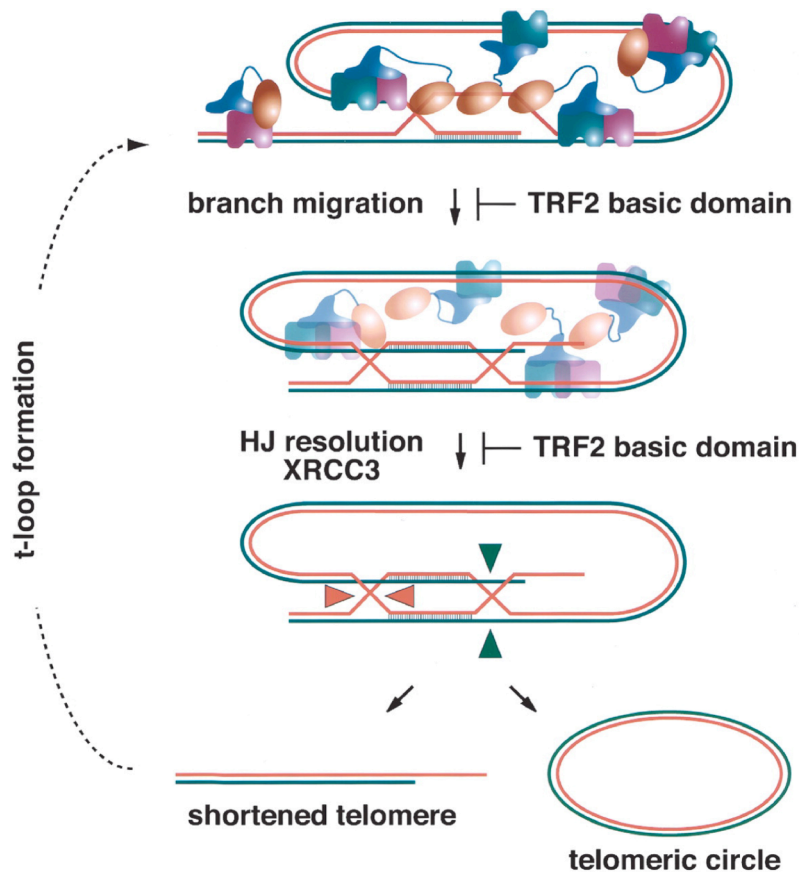


Figure I - 6 Control of T-loop HR by shelterin. Model depicting how late steps in HR can lead to sudden loss of telomeric DNA. Branch migration at the T-loop base can generate one or two HJs. Resolution of the double HJ in the direction shown will generate a shortened telomere and a circular telomeric DNA. T-loop HR is observed when an N-terminal truncation mutant of TRF2, lacking the basic domain, is over-expressed. The circular product of T-loop HR is also observed in ALT cells and at very low levels in unperturbed normal human cells. In ALT cells, the circles could provide a mechanism for telomere maintenance through rolling-circle replication [104].

A third type of HR is the recombination between a telomere and interstitial telomeric DNA. While not common in human cells, mouse cells contain large stretches of telomeric sequences within their chromosomes. Recombination between telomeres and these elements could generate a terminal deletion, extrachromosomal fragments, inversions, and translocations. ERCC1/XPF might suppress this event since mouse cells lacking ERCC1 generate large extrachromosomal elements that contain a single stretch of telomeric DNA, presumably at a chromosome internal site [155].

3.11. The role of TRF2 in telomere protection and ATM inhibition

Recent studies have shown that the shelterin subunit TRF2 has a weak interaction with the ATM kinase [161]. As a part of the shelterin complex, TRF2 is required to prevent mammalian telomeres from activating DNA damage checkpoints. Surprisingly, the results in this study show inhibitory effects on ATM's ability to respond to DNA damage upon TRF2 over-expression. High levels of TRF2 abrogated the cell cycle arrest after ionizing radiation and diminished several other readouts of the DNA damage response, including phosphorylation of Nbs1, stabilization of p53, and upregulation of p53 targets. In response to TRF2 over-expression, the ATM autophosphorylation on S1981, an early step in the activation of this kinase, was inhibited. *In vitro* studies revealed that TRF2 binds to a region of ATM containing S1981, and ATM immunoprecipitates contained TRF2. We propose that TRF2 has the ability to inhibit ATM activation at telomeres. Strikingly, we found ATM localization to the sites of telomeres, mainly in S-phase and late G2 [162]. From this, and from the pure abundance of TRF2 at the telomeres but not elsewhere in the nucleus, we conclude that this mechanism of checkpoint control could specifically block a DNA damage response at telomeres without affecting the surveillance of chromosome internal damage. However, from this model we also predict that over-expression of TRF2 leads to a pure abundance of TRF2 elsewhere in the

nucleus. In a mouse model this could lead to suppression of checkpoints and therefore potentially to tumor formation (Figure I - 7).

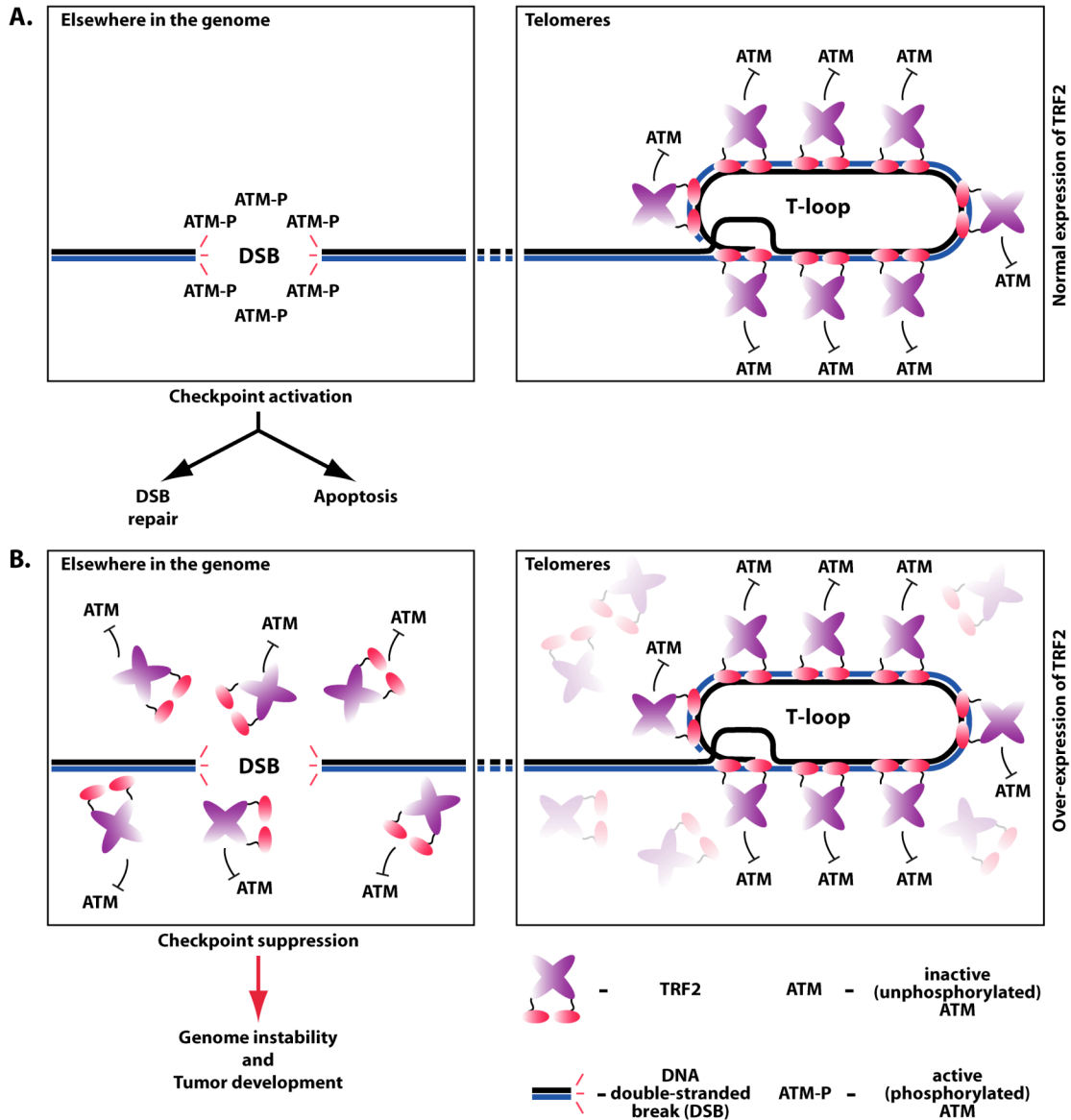


Figure I - 7 TRF2 over-expression in mouse hematopoietic stem cells might cause genome instability and tumor development. (A) Normal levels of TRF2 protein are sufficient to suppress telomeres from signaling as DNA double-stranded breaks (DSB) by suppressing the ATM dependent DNA damage machinery. DSBs elsewhere in the genome are not affected by the inhibitory effect of TRF2 on ATM. Normal checkpoint activation can occur, followed by either DSB repair or apoptosis. (B) Over-expression of TRF2 leads to the abundance of TRF2 throughout the nucleus, which might expend the inhibitory effect of TRF2 to genomic regions other than the telomeres and potentially suppresses checkpoint activation, resulting in genome instability and eventual tumor development.

In this thesis I focused on the over-expression of TRF2 in a mouse model. With respect to previous *in vitro* results, I predicted TRF2's potential to act as an oncogene *in vivo*. First, I will describe the design of the vector system for the TRF2 transgene and the method I used to transduce hematopoietic bone marrow stem cells with my vector constructs. Next, I will show how I characterized the primary recipient mice in regard to the transgene. I will then study the effects of TRF2 over-expression on tumor development by macroscopical observations and how its over-expression is affecting the differentiation pattern of hematopoietic stem cells. Additionally, I will show data regarding over-expression of the TRF2 pattern in observed tumors. Finally, I will look into genome instability of tumors from mice over-expressing TRF2.

4. Methods and Material

4.1. *Cell culture*

Primary cells. Human fibroblasts HeLa 1.2.11 and mouse fibroblast-like 3T3 cells were obtained from ATCC. Cells were grown in 1x DMEM supplemented with 10% (v/v) FBS, 0.1 mM non-essential amino acids, 100 units/ml Penicillin and 0.1 mg/ml Streptomycin.

Cells were passaged by treatment with trypsin and seeded at 5×10^5 cells per 10 cm dish. Cell numbers were determined by counting a 1:20 dilution of the cell suspension using a Coulter Counter. For storage in a -80 °C liquid nitrogen freezer, cells were collected from a 15 cm plate (approximately 7×10^6 cells), resuspended in 1 ml of 2xA freezing media (40 ml FBS, 0.4 ml gentamycin stock solution (stock solution is 50 mg/ml gentamycin (Sigma) and filtered through a 0.2 μ m filter). Subsequently, 1 ml of 2xD freezing media was added (40 ml PVP stock solution (stock solution is 100 mg/ml PVP (Sigma) prepared in HEPES buffered saline), 30 ml DMSO (Sigma) 4 ml HEPES stock solution (stock solution is 1 M HEPES (pH 7.6)), and 126 ml L15 media (Sigma) and filtered through a 0.2 μ m filter) and the cell suspension was aliquoted into two cryogenic vials. The vials were placed in a Cryo 1 C Freezing Container (NALGENE) at -80 °C for at least one day, but not longer than 3 month, and subsequently transferred to liquid nitrogen.

4.2. *Lentiviral vectors*

Standard techniques were used for cloning. TRF2 constructs were generated by PCR from a full-length cDNA clone (clone #1639). The p156RRLsinPPTCAG-EGFP-PRE(masa) vector (a gift from the Verma lab, The Salk Institute) was used to generate the GFP-mTRF2 expression vector. The same version without GFP was used to generate the mTRF2 expression vector. The GFP-control construct,

p156RRLsinPPTmCMV-GFP-PRE, was a gift from Nien Hoong, The Salk Institute.

4.3. *Lentiviral plasmid isolation*

Lentiviral vectors were transformed into *E. coli* TOP10 bacteria cells (Invitrogen) using standard molecular techniques. Cells were grown in 500 ml of LB broth Miller media (EMD) supplemented with 50 µg/ml Ampicillin at 37 °C and 230 rpm. Cell suspensions were centrifuged in 750 ml buckets for 10 minutes at 5000 rpm (Sorvall RT7). The bacteria were resuspended in 40 ml of Solution I (1% (v/v) Glucose, 25 mM Tris (pH 8), 10 mM EDTA in ddH₂O) and placed on ice. 80 ml of Solution II (0.2 M NaOH, 1% (w/v) SDS in ddH₂O) was added to the resuspended cells, mixed by gentle inversion, and incubated on ice for 5 minutes. Next, 60 ml of cold Solution III (3 M Potassium Acetate, 1 M Glacial acetic acid) were added, first mixed gently by inversion and then more vigorously, and incubated for 10 minutes on ice. Suspensions were centrifuged for 30 minutes at 4000 rpm at 4 °C (Beckman J-6B). The supernatant was poured through a funnel lined with layered gauze pads to filter out protein debris. Then 100 ml of cold isopropanol were added to the supernatant, mixed by inversion, and placed on ice for 10 minutes, before centrifuging for 20 minutes at 8000 rpm (J2-21 Beckman), the supernatant was poured off and the pellet was drained upside down on a paper towel, then resuspended in 8.5 ml of 10 mM Tris pH 7.5/1 mM EDTA total volume. 8.8 g CsCl was added and mixed until dissolved, when 300 µl of ethidium bromide stock (10 mg/ml) (Pierce) was added. The mixture was loaded in Vti 90 tubes (Beckman) and centrifuged over night at 60000 rpm at room temperature (Beckman L8-80M Ultracentrifuge). The resulting band was pulled out using a 22-gauge needle and a syringe and transferred to a 15 ml tube. The ethidium bromide was removed by extraction with about 4 ml of isopropanol/CsCl until the DNA was no longer pink. The plasmid DNA was precipitated by adding two original volumes of TE (10 mM Tris pH 8/1 mM EDTA pH 8) and three original volumes of isopropanol. The mixture was vortexed and incubated for 5 minutes at room temperature, then subsequently centrifuged for 10 minutes at 3000 rpm

at room temperature, and the supernatant was then discarded. The plasmid DNA was dissolved in 400 μ l of TE, 5 μ l of RNase A stock (20 mg/ml) added, and incubated for 30 minutes at 37 °C. After Phenol/Chloroform extraction, the plasmid DNA was precipitated by adding 20 μ l of 3 M Sodium acetate and 800 μ l ethanol. The suspension was incubated for 1 minute and centrifuged for 10 minutes at maximum speed in a table centrifuge. After a final ethanol wash, the plasmid DNA was resuspended in 400 μ l TE.

4.4. *Transfection of primary cells*

Cells were transfected using Lipofectamine 2000 (Invitrogen) as described in the distributors manual. Briefly, one day before transfection, cells were plated at 1×10^6 cells in 500 μ l of 1x DMEM supplemented with 10% (v/v) FBS and 0.1 mM non-essential amino acids so cells reach 90 to 95% confluence at the time of transfection. The plasmid DNA was diluted into 50 μ l of Opti-MEM I Reduced Serum Medium without Serum and gently mixed. In parallel, Lipofectamine 2000 was diluted in 50 μ l Opti-MEM I Medium and incubated for 5 minutes at room temperature. Then plasmid/lipofectamine mixtures were combined, gently mixed and incubated for 20 minutes at room temperature. 100 μ l of the solution were aliquoted to the well containing cells and medium and mixed gently. Cells were incubated over night at 37 °C, when the medium was replaced by fresh medium containing antibiotics. Cells were further processed for *Western* analysis and immunofluorescence after 48 hours, as described (4.12 and 4.13).

4.5. *Lentivirus production*

293T cells were plated on one 15 cm plate and grown in 1x DMEM supplemented with 10% (v/v) FBS, 0.1 mM non-essential amino acids, 100 units/ml Penicillin and 0.1 mg/ml Streptomycin and grown to confluence. Cells

were trypsinized and split into twelve 15 cm plates coated with poly-L-lysine (Sigma). 293T cells were transfected when cells reached approximately 70% confluence. The three packing plasmids and lentiviral vector containing the transgene were mixed in a 50 ml tube. For twelve 15 cm dishes the DNA transfection cocktail contained 95 µg of pVSVG, 68 µg of pREV, 176 µg pMDL, and 270 µg transgenic lentiviral vector. The CaCl₂ was mixed well with the plasmid preparation to a final concentration of 0.25 M. Subsequently, an equal volume of 2x BBS solution was added to the calcium-DNA mixture, followed by gentle mixing. The mixture was incubated for 10 minutes at room temperature and a volume of 2.25 ml was added dropwise to each 15 cm plate and cells were incubated over night at 3% CO₂ at 37 °C. The medium was changed 12 to 16 hours post transfection. The plates were further incubated at 10% CO₂ at 37 °C. Virus containing media was harvested at 24 h and 48 h intervals post-transfection. Every sample was immediately filtered through a 0.22 µm cellulose acetate filter and stored at 4 °C. The collected medium was loaded into ultracentrifuge tubes (Beckman) and centrifuged in a SW28 rotor for 2 hours at 19400 rpm (Beckman L8-80M ultracentrifuge) at room temperature. The supernatant was poured off and tubes were kept inverted. Recalcitrant medium drops were aspirated from the tubes. The pellet was resuspended in 1 ml HBSS (8 g/l NaCl, 0.4 g/l KCl, 60 mg/l KH₂PO₄, 47.9 mg/l Na₂HPO₄, 1 g/l Glucose, 0.35 g/l NaHCO₃), and the tube was washed twice with 500 µl each. The collections were pooled and loaded on top of 1.5 ml of phosphate-buffered 20% (w/v) sucrose into small ultracentrifuge tubes (Beckman). Tubes were then centrifuged in the SW55 rotor for 2 hours at 21000 rpm in a L8-80M ultracentrifuge (Beckman) at room temperature. Supernatant was removed and pellet resuspended in two steps of 100 µl each in a final volume of 200 µl in HBSS. The virus suspension was vortexed for 1 to 2 h at low speed at room temperature, quick-spun in microcentrifuge for 2 seconds and the supernatant was aliquoted in 20 µl aliquots and stored at -80 °C. 1 µl of concentrated viral supernatant was mixed with 89 µl 1x PBS (pH 7.4) (8.2 g/l NaCl, 0.2 g/l KCl, 1.7 g/l

$\text{Na}_2\text{HPO}_4 \cdot 7\text{H}_2\text{O}$, 0.2 g/l KH_2PO_4) + 10 μl 5% Triton from the p24 ELISA kit (Perkin-Elmer) and stored at -20°C .

4.6. *Mice*

B6.SJL-Ptprc^a Pep3^b/BoyJ mice (The Jackson Laboratory) were used to isolate bone marrow positive for CD45.1. TgN(beta-act-EGFP) mice [163] (a gift from the Verma lab, The Salk Institute) were used to isolate GFP-positive donor bone marrow. C57BL/6J (The Jackson Laboratory) were chosen as recipient mice.

4.7. *Isolation of bone marrow*

For the generation of the Primary #1 population, bone marrow was isolated from 15 male B6.SJL-Ptprc^a Pep3^b/BoyJ (CD45.1 donor) and 5 male TgN(beta-act-EGFP) (GFP donor). For the generation of the Primary #2 population, bone marrow was isolated from 20 male B6.SJL-Ptprc^a Pep3^b/BoyJ (CD45.1 donor). The mice were sacrificed by cerebral dislocation, and the femur and tibia were placed into 1x PBS/2 % (v/v) BIT9500 (StemCell Technologies). To isolate the bone marrow, the femur and tibia were ground by mortar and pestle. The suspension was filtered through a Cell Strainer (BD Falcon), and then centrifuged for 10 minutes at 700 x g. The pellet was resuspended in 1x PBS and cell numbers were determined by counting a 1:20 dilution of the suspension using a Coulter Counter. Suspensions were diluted to 5×10^7 cells/ml. To enrich hematopoietic stem cells, cell suspensions were separated using the StemStepTM cell separation system (StemCell Technologies) as directed. The cell numbers of the enriched hematopoietic stem cells were determined as described above and resuspended in Myelocult M5300 (StemCell Technologies).

4.8. *Infection of bone marrow*

Sorted bone marrow cells were diluted to approximately 1.2×10^7 to 1.4×10^7 cells/ml in Myelocult M5300 medium and 200 μ l virus were mixed with the cells in both primary experiments, Primary #1 and Primary #2. The suspension was incubated at 37 °C over night and in the following morning the suspension was washed once with 1x HBSS, centrifuged for 5 minutes at 400 x g, and resuspended in 1x HBSS.

4.9. *Transplantation of bone marrow*

Prior to transplantation, recipient C57BL/6J mice were irradiated with 11 Gy and deeply anesthetized. Each mouse received lateral tail vein injections of 300 μ l 1x HBSS containing 100.000 to 200.000 cells. During the first two weeks post transplantation all mice were maintained on Baytril water (Bayer Health Care). All mice were stored in the Biohazard suite at the Salk Institute's Animal Facility throughout the course of the experiment.

4.10. *Genotyping of primary and secondary recipient mice*

Genomic DNA from blood and tissue samples of C57BL/6J mice as well as HeLa 1.2.11 expressing GFP-mTRF2 cells was isolated using the DNeasy tissue kit (Qiagen). DNA was resolved from the column using 50 μ l prewarmed TE. Nested PCR was performed by PCR using the outer PCR primer pair (mTRF2 Outer F1: 5'-GCA GAT TGC TGT TGG AGG AGG-3'; WPRE R1: 5'-GCC ACA ACT CCT CAT AAA GAG ACA G-3'), generating a 626 bp PCR-product, followed by PCR using the inner PCR primer pair (mTRF2 Inner F1: 5'-ATG TCA GCA TCC AAG CCC AGA G-3'; mTRF2 Inner R1: 5'-CCA GTT TCC TTC CCC GTA TTT G-3'), generating a 252 bp PCR-product. For details on PCR-mixture and PCR-program see Table M - 1.

Table M - 1 PCR-mixture and -program for genotyping. (A) PCR-mixture for outer and inner PCR. * = 1 μ l of unpurified PCR-product of the outer PCR was used as a template for the inner PCR. (B) PCR-program for the outer and inner PCR.

| A. Outer PCR | | | Inner PCR | | |
|------------------------|---------|-------------|------------------------|---------|-------------|
| | μ l | Final [c] | | μ l | Final [c] |
| DNA | 2 | - | DNA | 2 | - |
| 10x PCR Buffer | 2.5 | 1x | 10x PCR Buffer | 2.5 | 1x |
| MgCl ₂ | 2.5 | 2.5 mM | MgCl ₂ | 2.5 | 2.5 mM |
| Primer 1 | 0.25 | 0.5 μ M | Primer 1 | 0.25 | 0.5 μ M |
| Primer 2 | 0.25 | 0.5 μ M | Primer 2 | 0.25 | 0.5 μ M |
| <i>Taq</i> -polymerase | 0.2 | 1 U | <i>Taq</i> -polymerase | 0.2 | 1 U |
| dNTP | 0.5 | 0.2 mM | dNTP | 0.5 | 0.2 mM |
| ddH ₂ O | 16.8 | | ddH ₂ O | 17.8 | |
| 25 μ l | | | 25 μ l | | |

| B. Outer PCR | | Inner PCR | |
|--------------|-------|-----------|-------|
| 1' | 95 °C | 1' | 95 °C |
| 30" | 58 °C | 30" | 60 °C |
| 45" | 72 °C | 30" | 72 °C |
| 30" | 95 °C | 30" | 95 °C |
| 5' | 72 °C | 5' | 72 °C |
| Hold 4 °C | | Hold 4 °C | |

Integration of the transgene into the hematopoietic system of primary recipient mice was verified by nested PCR and the PCR-product was separated on a 1.3% (w/v) Agarose gel and visualized by Ethidium Bromide (EtBr) (Pierce) under UV light. The gel was blotted onto a Hybond-N+ nitrocellulose membrane, (Amersham) followed by standard *Southern* analysis procedures. The cDNA of mTRF2, which was initially used as a template for the generation of TRF2 lentivectors, served as a probe for the TRF2 transgene and was radioactively labeled with ³² γ -dCTP. The membrane was stored in a Phosphorimager cassette (Amersham) and the exposed screen was analyzed on a Typhoon 8600 imager (Molecular Dynamics).

Genomic DNA isolated from tumor tissue samples was screened in a one-step PCR using the outer primer pair, generating a 626 bp PCR-product. The PCR-

product was separated on a 1.3% (w/v) Agarose gel and visualized by EtBr under UV-light. No *Southern* analysis was performed with these samples.

4.11. Protein isolation

Primary cells were washed with 1x PBS on plate and trypsinized using 2.5% (v/v) Trypsin/EDTA. Cell numbers were determined by counting a 1:20 dilution of the cell suspension using a Coulter Counter. Subsequently, cells were centrifuged for 5 minutes at 1000 rpm and washed twice in 1x PBS. The cell pellet was resuspended at a dilution of 10000 cells/ μ l in 4x NuPAGE LDS sample buffer (Invitrogen).

Tissue samples of spleen were mashed through a 70 μ m Cell Strainer (BD Falcon) in the presence of 1x PBS/2% (v/v) FCS. Cell numbers were determined by counting a 1:20 dilution of the cell suspension using a Coulter Counter. The cell suspension was then centrifuged for 5 minutes at 1000 rpm and washed twice in 1x PBS. The cell pellet was resuspended at a dilution of 10000 cells/ μ l in 4x NuPAGE LDS sample buffer (Invitrogen).

4.12. Western analysis

Whole cell extracts of primary cells or protein extracts from tissue samples and resuspended in 4x NuPAGE LDS sample buffer (Invitrogen) were separated on 3-8% (w/v) Tris-Acetate gradient gels (Invitrogen) and transferred to nitrocellulose by electroblotting for 80 minutes at 30 V at 4 °C. Membranes were stained with 20 mg/ml Ponceau S in ddH₂O (Sigma) for 2 minutes to verify transfer. Blocking and incubation with primary (incubation for either 4 hours at room temperature or over night at 4 °C) and secondary antibodies (incubation for 45 minutes at room temperature) was performed in 5% (w/v) milk and 0.1% (v/v) Tween in 1x PBS. Primary antibodies were as follows: rabbit-anti-mTRF2 #6889 (1/1000, Karlseder lab), mouse-anti- γ -Tubulin GTU-88 (1/10000, Sigma), rabbit-

anti-ATM Protein Kinase pS1981 (1/500, Rockland), rabbit-anti-p53 pS15 (1/1000, Santa Cruz), mouse-anti-GFP (1/200, Chemicon International). After incubation with secondary antibodies (1/5000, Amersham), all blots were developed using the ECL kit (Amersham).

4.13. Immunofluorescence on cultured cells, bone marrow and spleen

Mouse fibroblast-like 3T3 and human fibroblast HeLa 1.2.11 cells were grown in a 10 cm plate on microscope cover slips (Fisherbrand). Bone marrow and spleen suspension from C57BL/6J mice were attached to microscope slides by loading 200 μ l of cell suspension into cytofunnels (Thermo Electron Corporation) and centrifugation in a Shandon Cytospin 4 Cytocentrifuge (Thermo Scientific) for 10 minutes at 800 rpm. Coverslips and microscope slides were rinsed in 1x PBS, fixed in phosphate-buffered 4% (v/v) formaldehyde for 10 minutes at room temperature, washed twice in 1x PBS for 5 minutes each, and blocked and permeabilized with 0.1% (v/v) Triton-X 100, 5% normal goat serum (Vector) and 1% (w/v) BSA in 1x PBS for at least 30 minutes. All antibody incubation steps were carried out in a darkened humidified chamber at room temperature. Antibodies were diluted in 0.1% (v/v) Triton-X 100, 5% normal goat serum, (Vector) and 1% (w/v) BSA in 1x PBS. The first antibody incubation was for 2 hours, followed by three wash steps with 1x PBS for 5 minutes each. Primary antibodies were as follows: rabbit-anti-mTRF1 #6888 (1/500, Karlseder lab), rabbit-anti-mTRF2 #6889 (1/500, Karlseder lab), mouse-anti-TRF2 (1/500, upstate biotechnology). The secondary antibody incubation was for 45 minutes, followed by three wash steps with 1x PBS. Secondary antibodies were as follows: donkey-anti-rabbit-FITC (1/200, Jackson), donkey-anti-mouse-FITC (1/200, Jackson), donkey-anti-rabbit-TRITC (1/200, Jackson). DAPI (4', 6'-diamidino-2-phenylindole) was added to the final wash steps for a final dilution of 1/10000. Microscope slides and cover slips were then embedded upside-down in ProLong Gold (Molecular Probes) and sealed with nail polish. Pictures were

taken on an Axioplan2 Zeiss microscope with a Hamamatsu digital camera supported by OpenLab software.

4.14. Immunofluorescence on microtome sections

Tissue sections of mice were isolated and fixed in phosphate-buffered 4% (v/v) formaldehyde for one day, then transferred to 30% (w/v) phosphate-buffered sucrose. The tissues were prepared as free-floating freezing microtome sections (40 μ m) and stored at in tissue cryo-protection solution (TCS) at -20 °C until time of immunofluorescence preparation. Tissues were removed from TCS and washed in TBS pH 7.6 (6.1 g/l Trizma base, 9 g/l NaCl) for three times and then blocked for 1 hour (3% (v/v) FCS in TBS with 0.25% (v/v) Triton-X 100). Tissues incubated with the first antibody, rabbit-anti-ATM Protein Kinase pS1981 (1/500, Rockland), were incubated over night at 4 °C. Next morning, tissues were rinsed in TBS two times, 15 minutes each, and rinsed in 3% (v/v) FCS in TBS with 0.25% (v/v) Triton-X 100 for 15 minutes. The tissues were incubated with the second antibody, goat-anti-rabbit-TRITC (1/200, Jackson), in 3% (v/v) FCS in TBS with 0.25% (v/v) Triton-X 100 for 1 to 2 hours, followed by three wash steps with TBS. To counterstain, tissues were incubated in a 1/30000 dilution of DAPI in TBS for 5 minutes. Tissues were mounted on a coverslip using Dabco/PVA, dried over night at 4 °C in the dark, and sealed with nail polish. Pictures were taken on a Leica TCS SP2 AOBS and analyzed by LCS Lite software.

4.15. Flow cytometry

Flow cytometric analysis was used to determine differentiation patterns in sorted GFP-negative and GFP-positive bone marrow, and to determine transgene expression in developed tumors from transplanted C57BL/6J mice. Flow cytometry was also applied for the analysis of the Annexin V apoptosis assay. To detect CD45.1 donor bone marrow, aliquots of bone marrow cells and

thymocytes were stained with anti-mouse CD45.1 antibody (A20) conjugated to R-Phycoerythrin (R-PE). If mice were transplanted with GFP donor bone marrow, a GFP signal was used to evaluate the presence of donor bone marrow. Cell suspensions were also stained with 7-Amino-Actinomycin D (7-AAD, BD Biosciences) to determine the cells viability. Lineage analysis was performed by double staining using anti-mouse CD45.1 R-PE antibody with each of the following antibodies conjugated to either allophycocyanine (APC) for GR-1 (Ly-6G), CD3 ϵ (145-2C11), CD4 (RM4-5.B), CD11b (M1/70), CD19 (1D3), CD34 (RAM34), or a goat-anti-mouse secondary antibody conjugated to AF-350 to detect Mac-1 (WT.5) and CD8 (53-6.7). All primary antibodies were purchased from BD Biosciences, and the secondary antibody was purchased from Molecular Probes. Flow cytometric analysis was performed on a LSR I 3-laser 6-color analytical flow cytometer (Becton-Dickinson) and data were analyzed using the CellQuest software (Becton-Dickinson).

4.16. Cell sorting for colony forming assay (CFA) and liquid assay

Bone marrow cells harvested from a CD45.1 donor bone marrow transplanted mouse were separated into GFP-positive and GFP-negative pools using the FACS Vantage SE DiVa (Becton-Dickinson).

For the CFA, 24000 cells were resuspended in 12 ml MethoCult GF3434 (StemCell Technologies) and divided into six 35 mm miniplates. 2000 cells were seeded per plate and incubated for three weeks at 37 °C. Colonies were counted and characterized using light microscopy and the presence of the GFP signal was evaluated by fluorescence microscopy.

For the liquid culture 2000 cells were plated in the cavity of a 24-well plate in M5300 medium (StemCell Technologies) supplemented with the cytokines IL-3 and IL-6 (StemCell Technologies) and SCF (StemCell Technologies) at 100 ng/ μ l each. Differentiation patterns were analyzed by flow cytometry after two weeks of incubation at 37 °C.

4.17. Annexin V apoptosis assay

Mice were irradiated at 5 Gy and thymus and spleen were isolated after 4 hours. The thymus was mashed through a 70 μ m cell strainer (BD Falcon) in the presence of 1x PBS/2% (v/v) FCS. The thymocyte suspension was stored on ice until further processed. The spleen was isolated and flash frozen in liquid nitrogen until further prepared for confocal microscopy. Thymocyte numbers were determined by counting a 1:20 dilution of the suspension using a Coulter Counter. Roughly 300000 thymocytes were filled into a 15 ml Falcon tube and their volume was adjusted to 5 ml with 1x PBS. The suspension was centrifuged for 5 minutes at 4000 rpm at room temperature, the supernatant was removed and the pellet was washed once in 5 ml 1x PBS, centrifuged for 5 minutes at 4000 rpm, and the pellet was resuspended in 300 μ l Annexin V binding buffer (10 mM HEPES pH 7.4, 150 mM NaCl, 5 mM KCl, 1 mM MgCl₂, 1.8 mM CaCl₂). The Annexin V AF-647 antibody (Molecular Probes) was added to the suspension at a dilution of 1/100 and mixed. The mixture was incubated on ice for 15 minutes and then analyzed by flow cytometry.

4.18. Pathological observations

Tissue samples of mice were fixed in 4% (v/v) p-formaldehyde for one day, subsequently transferred to phosphate-buffered 30% (w/v) sucrose and stored at 4 °C in the dark. Pathological studies were carried out at the Department of Pathology, UC Davis.

4.19. Peptide nucleic acid (PNA) fluorescence in-situ hybridization (FISH) on metaphase spreads

FISH was performed essentially as described [164] with minor modifications. Intact spleen was flushed with 1x PBS/2% (v/v) FCS using a syringe attached

with a 25-gauge needle and suspended splenocytes subsequently were centrifuged at 1000 rpm for 5 minutes. Splenocytes were then resuspended in 200 μ l 1x PBS/2% (v/v) FCS and transferred into one well of a 24-Well plate. Splenocytes were supplemented with 3 ml 1x DMEM with 10% (v/v) FCS, 0.1 mM non-essential amino acids, 100 units/ml Penicillin and 0.1 mg/ml Streptomycin, and 0.1 μ g/ml colcemid. The splenocyte suspension was incubated at 37 °C for 90 minutes, transferred to a 15 ml conical falcon tube, and the volume was brought to 15 ml with 1x PBS. This sample was again centrifuged at 1000 rpm for 5 minutes. The supernatant was completely removed and splenocytes were resuspended in 5 ml 0.075 M KCl, prewarmed to 37 °C. For exactly 7 minutes the cells were incubated at 37 °C, with occasional inversion to mix. The suspension was once more centrifuged at 1000 rpm for 5 minutes and the supernatant was decanted, leaving roughly 200 μ l of KCl on top of cells. The splenocytes were resuspended in the remaining KCl by gently tapping the tube. While vortexing at full speed, drop-by-drop 500 μ l of methanol:glacial acetic acid (3:1) were added, followed by an additional 500 μ l. Added more quickly. Finally, the suspension was filled to 10 ml with methanol:glacial acetic acid (3:1) and stored at 4 °C over night.

Fixed splenocytes were spun at 1000 rpm for 5 minutes to remove most of the supernatant and the splenocytes were resuspended in the remaining volume of approximately 500 μ l by gently tapping the tube. The slides were incubated in methanol:glacial acetic acid (3:1) and transferred to cold ddH₂O prior to metaphase spread preparation. Splenocytes were dropped on water-wetted slides from about 1 m distance, let dry a couple of seconds, and washed with fresh fixative with Pasteur pipette from the edge of the microscope slide. The slides were then placed on a humidified heatblock at 80 °C for 3 minutes. Slides were stored over night at room temperature.

Metaphase spreads were fixed in phosphate-buffered 4% (v/v) formaldehyde for 2 minutes, washed in 1x PBS three times for 5 minutes each and then treated with pepsin (2 mg/ml) (Sigma) in acidified water (pH 2) at 37 °C for 10 minutes. The fixed cells were washed twice in 1x PBS for 2 minutes, fixed again in

phosphate-buffered 4% (v/v) formaldehyde, washed three times in 1x PBS for 5 minutes each, and then dehydrated in an ethanol series (5 minutes in 70% (v/v) ethanol, 5 minutes in 95% (v/v) ethanol, and five minutes in 100% (v/v) ethanol) and air-dried. A small amount (50 – 100 μ l of hybridization mix (10 mM Tris (pH 7.2), 70% (v/v) deionized formamide, 0.5% (v/v) blocking solution (Boehringer Mannheim), 0.5 μ g **Peptide-Nucleic Acid** (PNA) probe per ml (FITC-CCCTAACCCCTAACCCCTAA, synthesized by Applied Biosystems) was placed on the slide. A glass coverslip was placed on top of the slide with hybridization mix. The cellular DNA was denatured by placing the slide at 80 °C for 3 minutes on a heatblock, and the probe was allowed to hybridize for 2 hours at room temperature in a darkened humidified chamber. Subsequently, the slide was washed two times, 15 minutes each in 10 mM Tris (pH 7.2), 70% (v/v) deionized formamide, 0.1% (w/v) BSA, and washed three times 5 minutes each in 0.1 M Tris-HCl (pH 7.4), 0.15 M NaCl, 0.08% (v/v) Tween. To the final washing step DAPI was added to a final dilution of 1/10000. Finally, the slides were dehydrated in an ethanol series as described above, air-dried, and the slides were then embedded in ProLong Gold (Molecular Probes), covered by microscope cover slides and sealed with nail polish. Pictures were taken on Axioplan2 Zeiss microscope with a Hamamatsu digital camera supported by OpenLab software.

5. Results

5.1. Experimental overview of the over-expression of recombinant mTRF2 in C57BL/6J mice

Over the course of the project I performed a series of experiments to investigate the possible oncogenic activity of TRF2 *in vivo*. At this point I would like to give an overview (Figure 1). It shows how primary and secondary mouse colonies were generated, which type of donor bone marrow was used for the transduction and transplantation, and how I planned to follow up tumor development in transplanted mice.

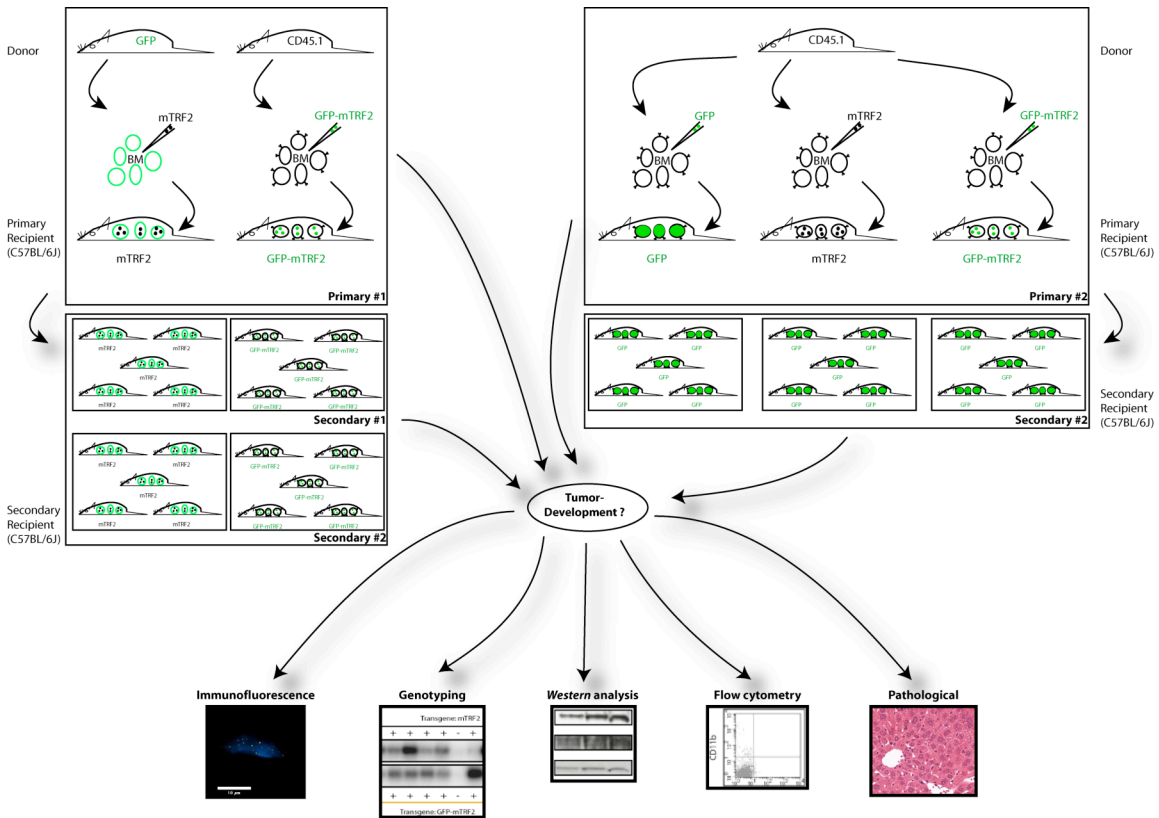


Figure 1 Experimental setup for the over-expression of recombinant mTRF2 in the hematopoietic system of C57BL/6J mice. Primary recipients for transgenic mTRF2, GFP-mTRF2 and GFP were generated in two independent experiments, termed Primary #1 and Primary #2. To increase chances of tumor-development, bone marrow from selected primary recipients was transplanted into secondary recipient mice, termed Secondary #1 and Secondary #2. If tumor-development occurred in either population, selected specimens were further investigated applying Immunofluorescence, Genotyping, Western analysis, Flow cytometry, and/or pathological analysis.

5.2. Functional over-expression of recombinant mTRF2 and GFP-mTRF2 in vitro

Two vector constructs were designed for the over-expression of recombinant mouse TRF2 (mTRF2) in the hematopoietic system of C57BL/6J mice (4.2). To verify the functional expression of both recombinant proteins, mTRF2 and GFP-mTRF2, I transfected 3T3 cells with both constructs. The localization of recombinant TRF2 to telomeres is considered a sufficient indicator for functional expression.

Western analysis confirmed over-expression of both recombinant proteins, which were successfully detected at the expected size of 66 kDa for mTRF2 and 94 kDa for GFP-mTRF2 (Figure 2).

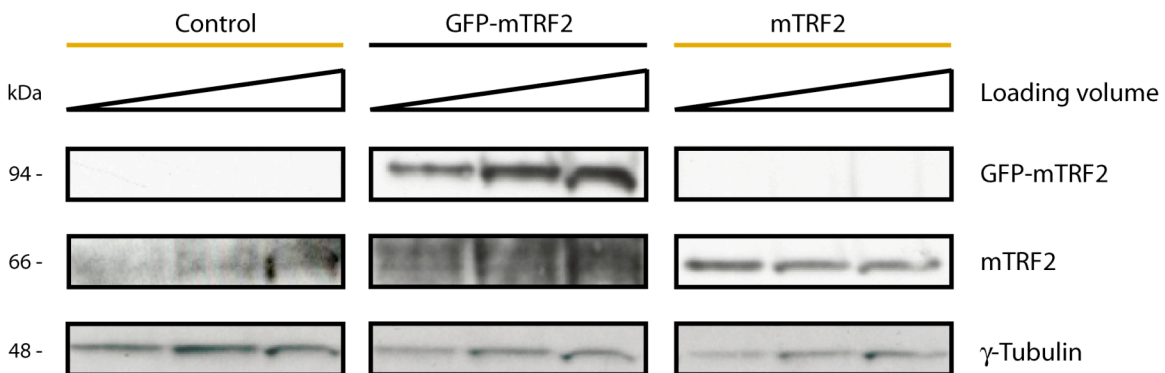


Figure 2 Recombinant mTRF2 and GFP-mTRF2 was over-expressed in 3T3 cells by transfection. Endogenous TRF2, recombinant mTRF2, and recombinant GFP-mTRF2 were detected using an antibody specific for TRF2. γ -Tubulin was used as a loading control.

Functional expression of both recombinant proteins was shown by immunofluorescence (Figure 3). The telomere repeat binding factor, TRF1, was a positive control for telomere localization. In control 3T3 cells, endogenous TRF1 and TRF2 colocalize and show distinct foci within the nucleus. After their transient transfection into 3T3 cells, telomeric localization for both recombinant proteins was detected, evidenced by their colocalization with endogenous TRF1 at the telomeres. Thus, both recombinant proteins are functionally over-expressed *in vitro*.

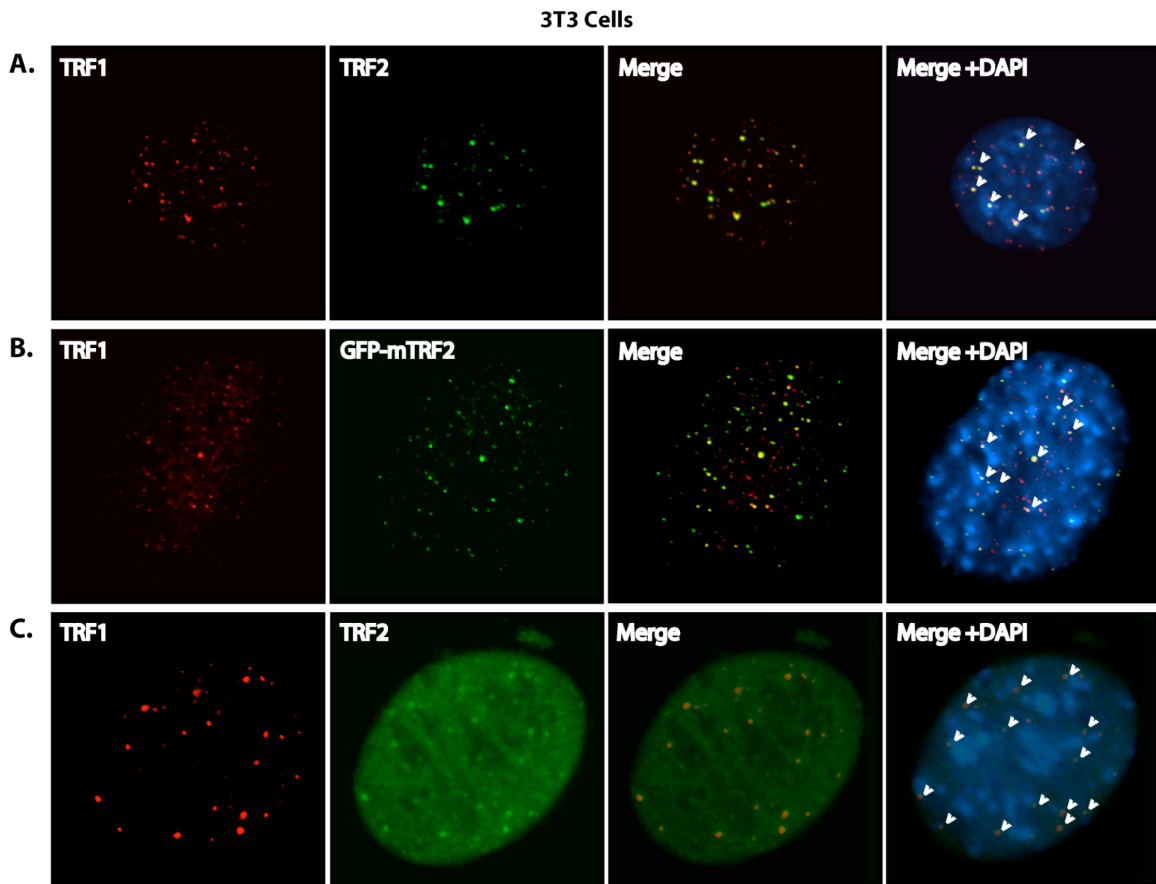


Figure 3 Functional expression of transgenic mTRF2 in 3T3 cells displayed by immunofluorescence. (A) Untransfected 3T3 control cells stained for endogenous TRF1 and TRF2. (B) Over-expressed GFP-mTRF2 and (C) mTRF2 do colocalize with endogenous TRF1. Chromatin was counterstained with DAPI. White arrows indicate colocalization of TRF1 with (A) endogenous and (B+C) over-expressed (GFP-)mTRF2. Immunofluorescence, 63x1.25.

5.3. *Production and quantitative verification of lentivirus batches*

The lentiviral backbone of the two constructs was used to produce virus batches. Each viral titer was verified by a p24 ELISA assay, which detects the presence of viral particles. For the mTRF2 construct I measured a virus titer of 3×10^9 particles/ml, for GFP-mTRF2 8.5×10^9 particles/ml. Both virus batches were then used to infect bone marrow and to generate the “Primary #1” colony. In an effort to improve the viral titer and to increase the viral infection efficiency, I attempted to optimize the virus production and produced another virus batch. I included in this second virus production a virus based on a GFP-control construct, in addition to the two TRF2 constructs. I again quantified all three viruses by a p24 ELISA. Although I attempted to improve the virus titer, the second virus production was in fact less efficient than the first production based on the p24 ELISA results. For the mTRF2 construct I measured a virus titer of 8.2×10^7 particles/ml, for GFP-mTRF2 6.4×10^8 particles/ml and for GFP-control 3.8×10^9 particles/ml. Despite having a low virus titer, all three batches were subsequently used for the generation of the “Primary #2” colony.

5.4. Transduction and transplantation of bone marrow into primary C57BL/6J recipient mice

In the course of the project I generated two primary C57BL/6J recipient mouse colonies (Figure 4). In the first round I transplanted a total of 32 C57BL/6J recipient mice (Primary #1). 13 mice received GFP donor bone marrow transduced with mTRF2 and 19 mice received CD45.1 donor bone marrow transduced with GFP-mTRF2. In the second round I used the optimized virus batches of recombinant mTRF2, GFP-mTRF2 and GFP-control to infect CD45.1 donor bone marrow. The infected bone marrow was then transplanted in a second round of primary transplantations into a total of 53 C57BL/6J recipient mice (Primary #2). 19 mice received CD45.1 donor bone marrow transduced with mTRF2, 17 mice received CD45.1 donor bone marrow transduced with GFP-mTRF2, and as a control I transduced CD45.1 donor bone marrow with a GFP-control lentivirus and transplanted it into 17 C57BL/6J recipient mice. Both primary colonies were subsequently monitored for tumor development over time.

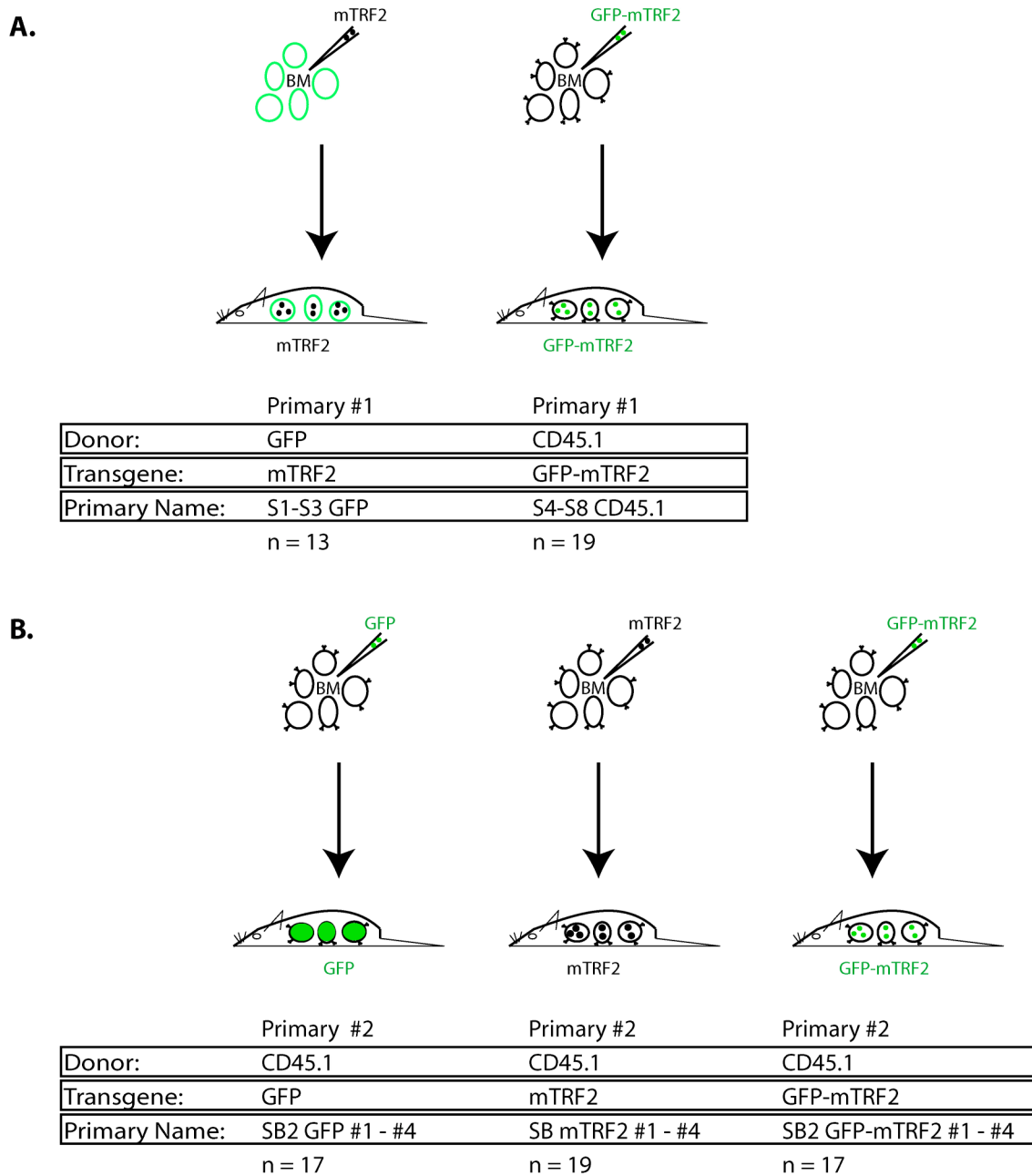


Figure 4 Generation of primary recipient mice by lentiviral transduction of transgenic TRF2 into GFP and CD45.1 donor bone marrow. (A) Primary #1 colonies were generated by the transduction of GFP donor bone marrow with the mTRF2 transgene and CD45.1 donor bone marrow with the GFP-mTRF2 transgene. (B) For the Primary #2 colony only CD45.1 donor bone marrow was used and transduced with a GFP-control, the mTRF2 and the GFP-mTRF2 transgene. Recipient mice were always C57BL/6J.

5.5. Functional over-expression of the *mTRF2* transgene in CD45.1 donor bone marrow

After showing functional over-expression of recombinant mTRF2 *in vitro*, I was interested to see if this functionality was also present in transduced CD45.1 donor bone marrow. Therefore, I infected CD45.1 bone marrow with the produced lentivirus for GFP-mTRF2 and mTRF2. After 10 days in culture I could detect over-expression of both transgenes in the bone marrow (Figure 5).

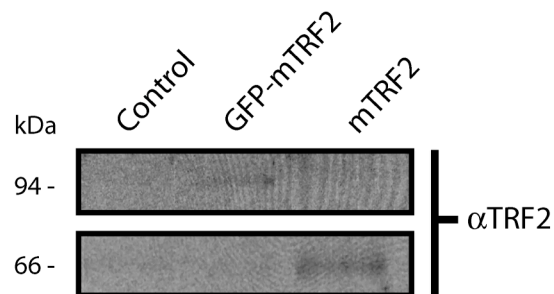


Figure 5 Over-expression of recombinant (GFP-)mTRF2 in bone marrow cells isolated from CD45.1 donor mice. Endogenous and recombinant (GFP-)TRF2 was detected by a TRF2 specific antibody.

Functional expression of GFP-mTRF2 in bone marrow could also be shown by immunofluorescence. As a positive control for telomere localization I stained again for endogenous TRF1. As seen in 3T3 cells, recombinant GFP-mTRF2 colocalized with endogenous TRF1 (Figure 6). Thus, recombinant mTRF2 was functionally expressed in CD45.1 donor bone marrow.

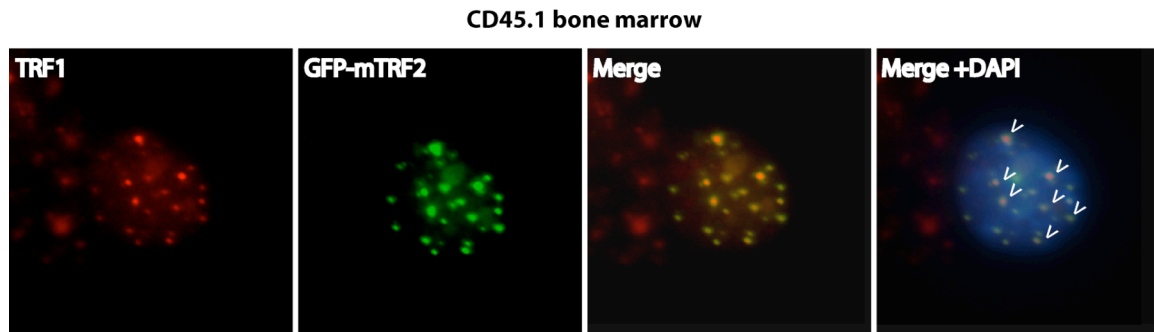


Figure 6 Functional expression of recombinant GFP-mTRF2 in CD45.1 donor bone marrow cells. GFP-mTRF2 was visualized by the GFP-tag and TRF1 was detected by a TRF1 specific antibody. Chromatin was counterstained with DAPI. White arrows indicate colocalization of endogenous TRF1 with recombinant GFP-mTRF2. Immunofluorescence, 63x1.25.

5.6. Detection of virus integration into the hematopoietic system of C57BL/6J primary recipient mice by nested PCR and Southern analysis

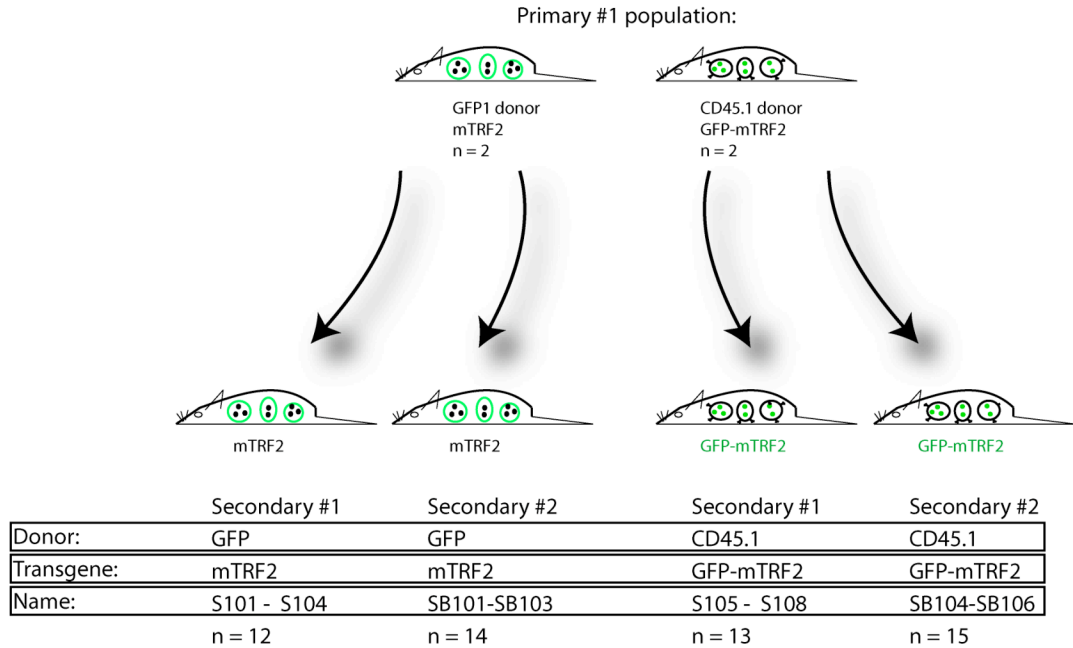
Successful integration of transgenic TRF2 into the hematopoietic system of recipient mice was confirmed by nested PCR followed by *Southern* analysis. I isolated genomic DNA from blood of all primary transplanted mice. A specifically designed primer pair (Figure 7) was used to detect the integration of transgenic mTRF2 and GFP-mTRF2 by nested PCR. The amplified PCR product was then analyzed by *Southern* analysis to verify its sequence specificity (Figure 8). Based on the *Southern* analysis, 26 out of 32 mice (Primary #1) and 15 out of 36 mice (Primary #2), respectively, showed the integration of either transgenic mTRF2 or GFP-mTRF2 into their hematopoietic system. As expected, in mice that received bone marrow transduced with a GFP-control transgene, transgenic mTRF2 was not detectable.

Taken together, these results show the successful integration of transgenic mTRF2 and GFP-mTRF2 into the hematopoietic system of primary C57BL/6J recipient mice.

5.7. Transplantation of bone marrow from primary recipients into secondary C57BL/6J recipient mice

To further promote tumor progression in recipient mice, I transplanted bone marrow from primary recipient mice that was successfully transduced with transgenic TRF2 (Figure 9). To do this, I isolated primary bone marrow from the Primary #1 colony and transplanted it into irradiated C57BL/6J secondary recipients. A total of seven secondary recipient populations were generated: two populations received bone marrow transduced with mTRF2, another two populations received bone marrow transduced with GFP-mTRF2, and the negative control received bone marrow transduced with a GFP-control transgene. Depending on the time of transplantation, I subdivided all secondary recipient populations into Secondary #1 and Secondary #2. As with the primary colonies, I monitored the secondary populations for tumor development.

A.



B.

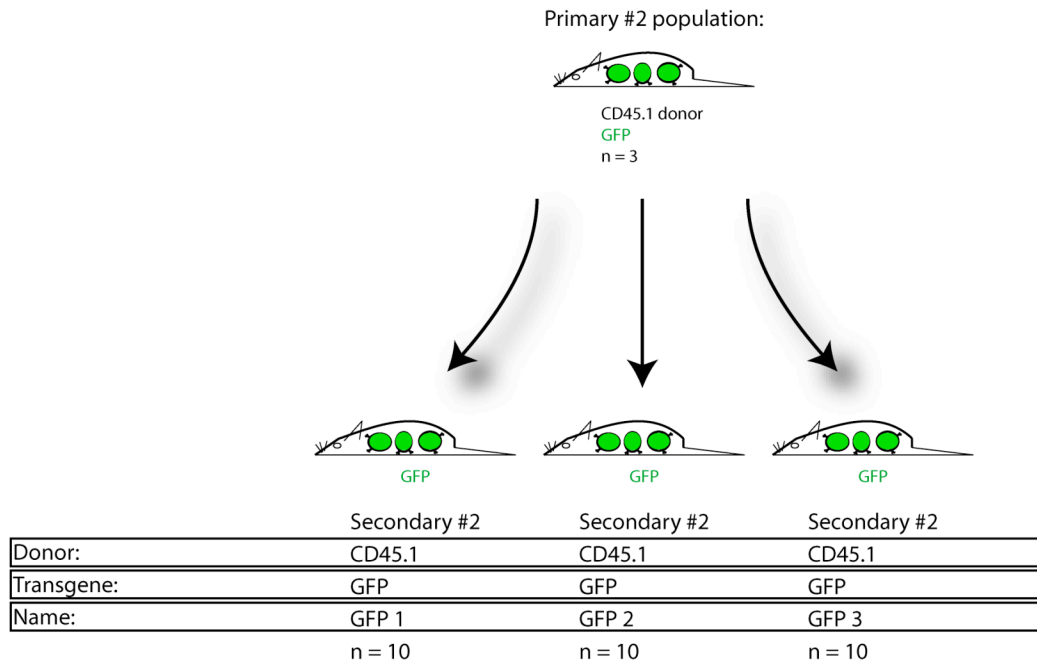


Figure 9 Transplantation of bone marrow from primary recipient mice into secondary recipient mice. (A) A total of four secondary populations for mTRF2 and GFP-mTRF2 were generated. Each secondary population received bone marrow from one individual Primary #1 donor, either CD45.1 donor bone marrow over-expressing GFP-mTRF2 or GFP donor bone marrow over-expressing mTRF2. (B) For the GFP-control transgene a total of three secondary populations, each from one individual Primary #2 donor, expressing the GFP-control protein in CD45.1 donor bone marrow, were generated. All recipient mice were C57BL/6J.

5.8. Functional over-expression of transgenic mTRF2 in the hematopoietic system of C57BL/6J mice

Once I was able to show that transgenic TRF2 can be functionally over-expressed *in vitro*, I investigated functional over-expression of the transgene in recipient mice *in vivo*. As shown by immunofluorescence studies in Figure 10, I could detect expression of the TRF2 transgene in bone marrow of a secondary recipient mouse. Again, I used endogenous TRF1 as a marker for telomeres. I observed colocalization of TRF1 and recombinant TRF2, in bone marrow and spleen, which confirmed that transgenic TRF2 is functionally expressed in C57BL/6J recipient mice.

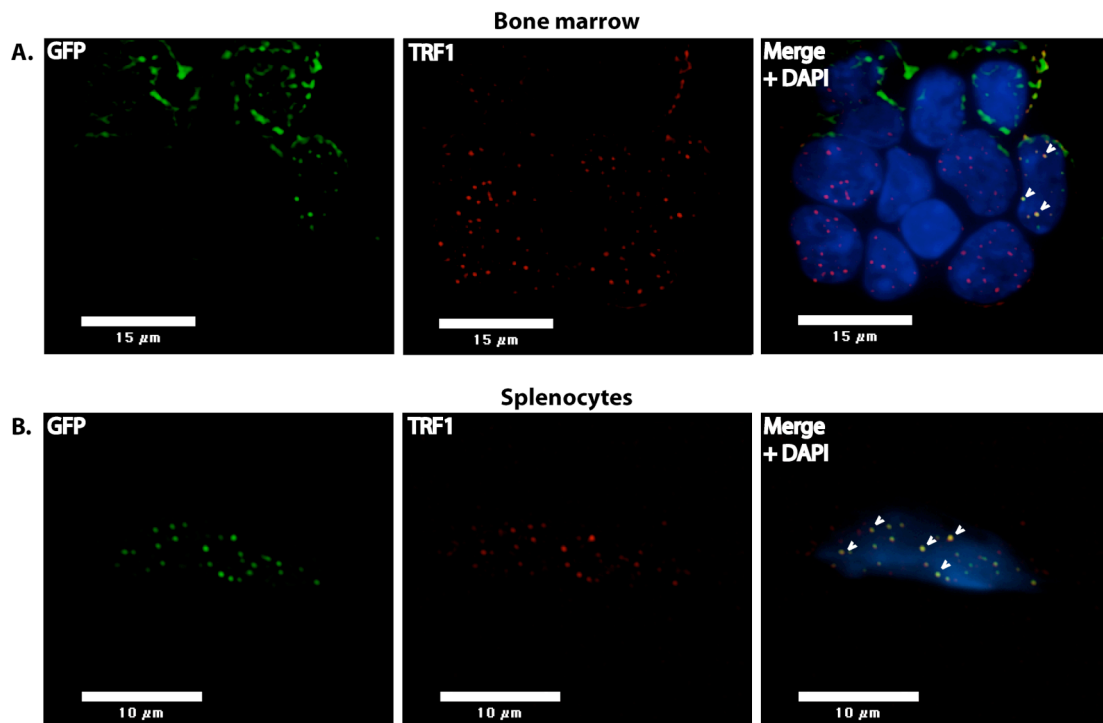


Figure 10 Transgenic GFP-mTRF2 is functionally expressed in the hematopoietic system of recipient C57BL/6J mice. In (A) bone marrow and (B) spleen GFP-mTRF2 colocalizes with endogenous TRF1. GFP-mTRF2 was visualized by the GFP-tag, TRF1 was detected by a TRF1 specific antibody. Chromatin was counterstained with DAPI. White arrows indicate colocalization of endogenous TRF1 with recombinant GFP-mTRF2. Immunofluorescence, 63x1.25.

5.9. Tumor occurrence in TRF2 over-expressing C57BL/6J recipient mice

Tumor-development in all primary and secondary recipient C57BL/6J mice was investigated and documented throughout the course of the experiment. To be considered as a potential TRF2 related tumor, the individual mouse had to fulfill a set of defined criteria (Figure 11):

I monitored a total of 152 mice, 30 mice were transduced with a GFP-control transgene and 122 mice were transduced with the TRF2 transgene. As the first criteria, only mice were considered that received bone marrow transduced with the TRF2 transgene.

Then I screened all primary mice that received bone marrow potentially transduced with the TRF2 transgene to confirm integration. Secondary mTRF2 and GFP-mTRF2 mice were considered to be positive since they received bone marrow from a successfully transduced and verified primary mouse. After genotyping by nested PCR I considered 95 mice out of the 122 mice for TRF2 related tumor development.

Since I assumed that TRF2 is interfering with the apoptosis cascade by inhibiting the ATM pathway, I considered previous results on ATM $-/-$ and p53 $-/-$ knock-out mouse models as a standard for the expected time to observe tumor development. ATM deficient mice develop thymic lymphomas at approximately two to four month of age [165] and p53 deficient mice show spontaneous development of a variety of neoplasms by six months of age [166]. I assumed a similar time frame for TRF2 and predicted initiation of tumor development at approximately 26 weeks after transplantation. It might be possible that my mouse model does not completely inactivate the apoptosis pathway and rather resembles a p53 $+/-$ phenotype. To take this into account, I extended the time frame to 52 weeks. A total of nine out of the 95 mice died at an age of 52 weeks or earlier.

At last an individual mouse had to show macroscopical signs of tumor development to be considered. Eight out of the remaining nine mice were showing those signs, mainly a drastically enlarged thymus, spleen, liver, and kidneys. It is important to note that although an organ might look normal macroscopically, it may still possess tumor pathology.

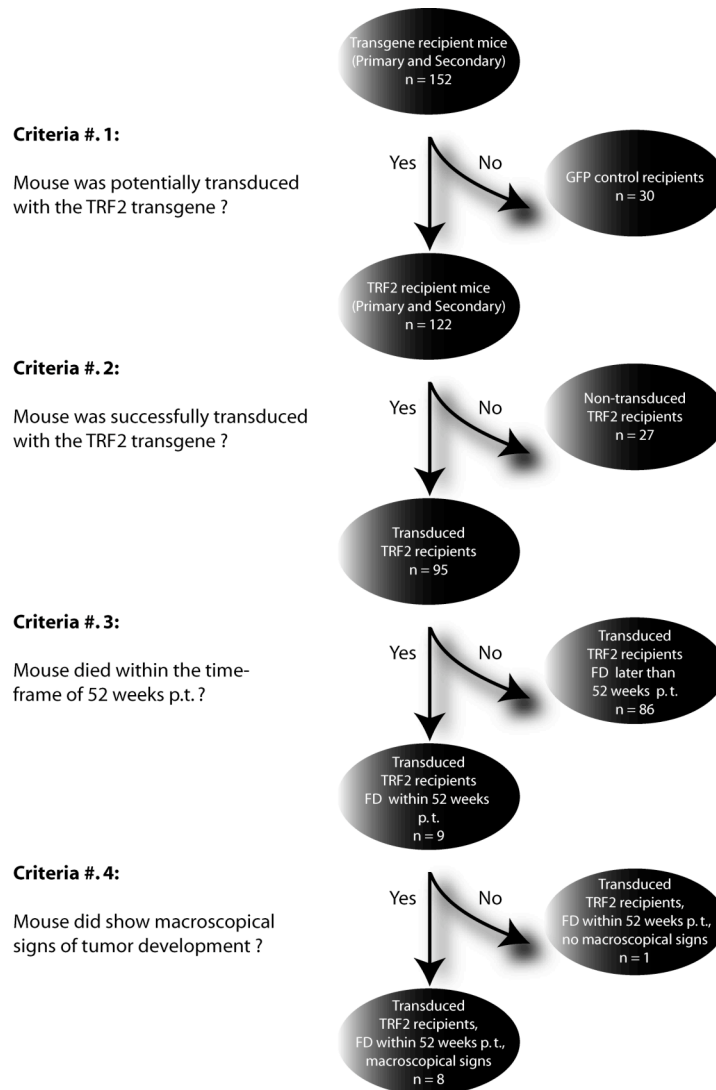


Figure 11 Applied criteria for the definition of TRF2 related tumor development. Four criteria were applied to determine if an occurring tumor might be related to the expression of transgenic TRF2. Only a total of eight tumors were eventually considered. One tumor was derived from a primary recipient and seven tumors from secondary recipients. p.t. - post transplantation; FD - found dead.

Taken together, I macroscopically observed potential TRF2 related tumor development in eight mice. One mouse was a primary recipient; the other seven mice were secondary recipient mice (Table 1).

Table 1 Summary of potential TRF2 related tumors. (A) Background information of mice that potentially developed a TRF2 related tumor. (B) Macroscopical observations of organs from considered mice. FD - found dead.

| Name | Donor | Trans-plantation | Trans-gene | Age FD (weeks) |
|--------------|--------|------------------|------------|----------------|
| A. S1-GFP R2 | GFP | Primary #1 | mTRF2 | 52 |
| S101 R1L1 | GFP | Secondary #1 | mTRF2 | 32 |
| S104 R1L1 | GFP | Secondary #1 | mTRF2 | 36 |
| SB102 R1L1 | GFP | Secondary #1 | mTRF2 | 33 |
| S106 R1L1 | CD45.1 | Secondary #2 | GFP-mTRF2 | 36 |
| S107 R2 | CD45.1 | Secondary #1 | GFP-mTRF2 | 52 |
| S108 (-) | CD45.1 | Secondary #1 | GFP-mTRF2 | 46 |
| SB105 L1 | CD45.1 | Secondary #2 | GFP-mTRF2 | 42 |

| Name | Spleen | Liver | Thymus | Kidney |
|--------------|-----------------|-----------------|-----------------|-----------------|
| B. S1-GFP R2 | Enlarged | Normal | Normal | Normal |
| S101 R1L1 | Enlarged | Enlarged | Enlarged | Normal |
| S104 R1L1 | Enlarged | Enlarged | Enlarged | Enlarged |
| SB102 R1L1 | Enlarged | Normal | Enlarged | Normal |
| S106 R1L1 | Normal | Normal | Enlarged | Enlarged |
| S107 R2 | Enlarged | Normal | Enlarged | Enlarged |
| S108 (-) | Enlarged | Normal | Enlarged | Normal |
| SB105 L1 | Enlarged | Normal | Enlarged | Normal |

5.10. Mouse Colony-Forming cell assay

The potential of hematopoietic stem cells to produce heterogeneous populations of actively dividing hematopoietic progenitors, which proliferate and differentiate into mature blood cells, can also be observed *in vitro*. Such an assay allows quantifying multi-potential progenitors and lineage-restricted progenitors of the erythroid, granulocytic, monocyte-macrophage, and megakaryocyte-myelopoietic pathways, as well as a subset of mouse pre-B lymphoid cells. When cultured in a suitable semi-solid matrix, individual progenitors, called colony-forming cells (CFCs), proliferate to form discrete cell clusters or colonies.

To further investigate if TRF2 over-expression in hematopoietic stem cells can promote abnormal growth and differentiation patterns, I applied such a colony-forming assay. For this particular experiment I isolated bone marrow from a primary recipient mouse, which received donor bone marrow successfully transduced with the GFP-mTRF2 transgene. To promote the growth of bone marrow erythroid progenitors (BFU-E and CFU-E), granulocyte-macrophage progenitors (CFU-GM), and pluripotent granulocyte-macrophage, erythroid and megakaryocyte progenitors (CFU-GEMM), I selected a media enriched with stem cell factors (SCF) and selected cytokines (IL-3 and IL-6).

To overcome a potential low transduction rate, I performed flow cytometry to enrich the cell population for donor derived bone marrow cells that show a GFP-signal from the GFP-tagged TRF2 recombinant protein (GFP-positive). In parallel, I also selected for bone marrow cells that were negative for GFP and therefore non-transduced (internal negative control). As an additional external negative control, I isolated bone marrow from a non-transplanted C57BL/6J mouse.

For this experiment I decided to split the cells into a methylcellulose-based assay to investigate cell growth, as well as differentiation patterns, by fluorescent microscopy (5.10.1) and also into a liquid-based assay, which would permit subsequent flow cytometry analysis (5.10.2).

5.10.1. CFC Assay in MethoCult Media

After three weeks in culture the CFCs in MethoCult media were analyzed using fluorescent microscopy. Although colonies formed in all three assays, the number of colonies in the GFP-positive assay was not different from the internal, GFP-negative and the external, C57BL/6J negative control. Surprisingly, colonies from GFP-mTRF2 expressing cells, which were initially sorted for their GFP-signal, did not show any GFP-signal when analyzed by fluorescence microscopy.

5.10.2. Liquid-based CFC Assay in M5300 Media

Cells cultured in M5300 media for over two weeks were subsequently analyzed by flow cytometry (Figure 12).

After two weeks in culture 19.9% cells in the GFP-positive assay did show a GFP-signal (A and B, top). Strikingly, 19.3% of cells positive for GFP were also positive for CD45.1 with a total rate of 85.9% CD45.1 positive cells in this assay. In contrast, cells from the C57BL/6J control and the GFP-negative assay only showed background levels for GFP (1.5% and 1.8%) and CD45.1 (4.6% and 5.8%) (A and B, top). Thus, cells in the GFP-positive assay were successfully sorted for GFP-mTRF2 expression and a subset of cells maintained this expression over two weeks in culture.

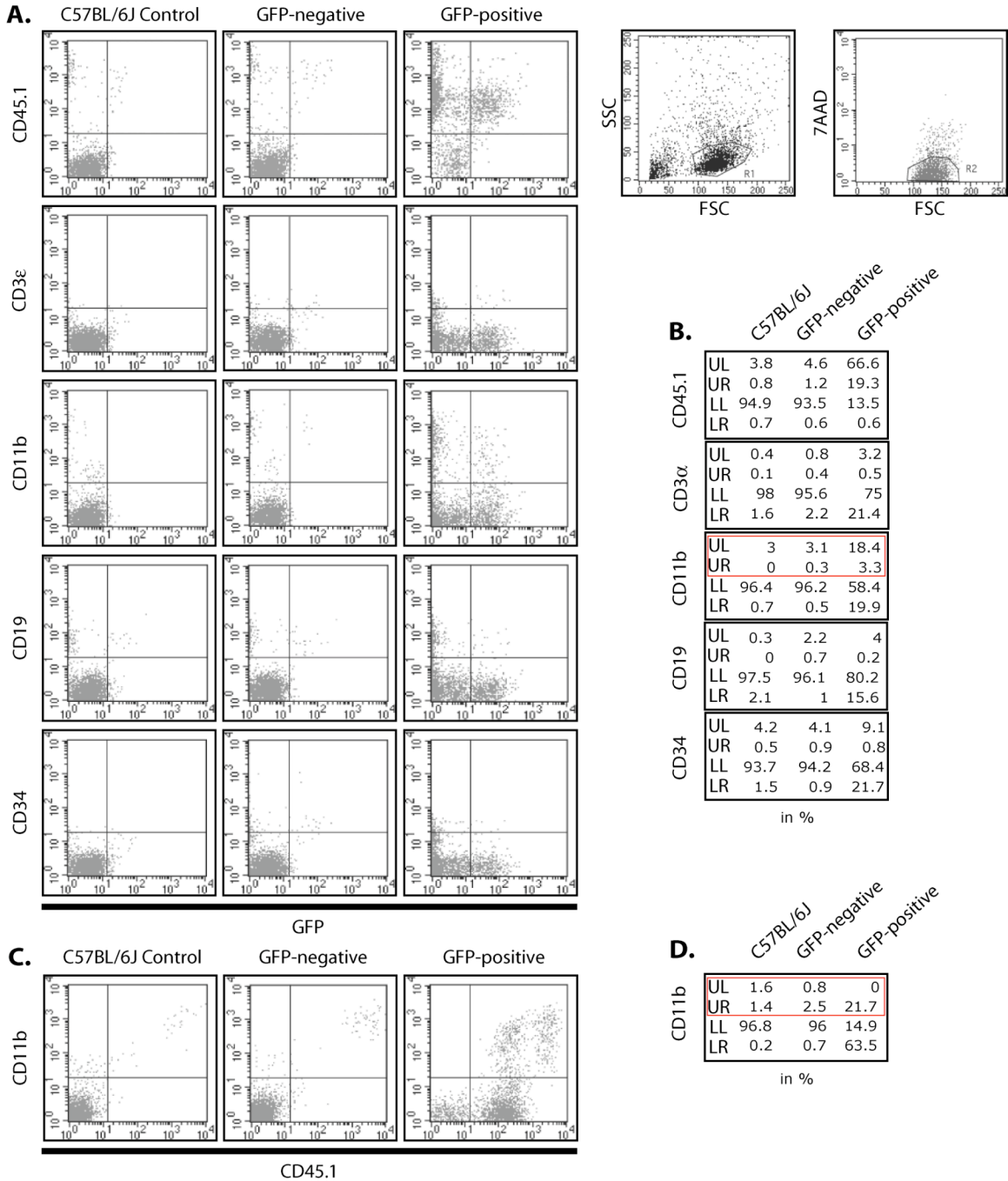


Figure 12 Differentiation analysis on sorted bone marrow cells with respect to their over-expression of GFP-mTRF2. (A) GFP-mTRF2 expressing bone marrow was analyzed after two weeks in liquid culture by flow cytometry using a set of differentiation markers. As a negative control, bone marrow from the same mouse negative for GFP-mTRF2 and bone marrow from a C57BL/6J mouse were analyzed. (B) %-values in (A). (C) Same as (A), but sorting for CD11b positive cells in respect to the CD45.1 status. (D) %-values in (C). Red frames indicate differences in CD11b differentiation in the three compared populations (see 5.10.2 for details).

I then analyzed the levels of differentiation in each of the three assays with respect to their GFP-signal (A). I applied four different surface markers: CD3 ϵ , CD11b, CD19 and CD34. Except for CD11b, I only measured marginal differences in the differentiation pattern in the presence of GFP-mTRF2 over-expression (B). For CD11b, however, I scored a total of 19.7% of cells positive for this surface marker, compared to 3% in the C57BL/6J control assay and 3.4% in the GFP-negative assay. Surprisingly, the majority of cells positive for CD11b in the GFP-positive assay did not show a GFP-signal. To further investigate the origin of this CD11b positive population, I measured the levels of CD11b in respect to CD45.1 surface marker (C). Interestingly, all cells positive for CD11b had its origin in the CD45.1 donor bone marrow since they were positive for this surface marker (D). Taken together, these data suggest that cells sorted for a GFP-signal (from the GFP-mTRF2 expression) show a different differentiation pattern than GFP-negative control cells do.

5.11. Induction of apoptosis in mice over-expressing TRF2

To see how cells from mice over-expressing TRF2 in their hematopoietic system respond to DNA damage and if these cells are impaired in their ability to activate the ATM-dependent apoptosis pathway, I measured levels of apoptosis by flow cytometry (5.11.1) and confocal microscopy (5.11.2).

5.11.1. Detection of irradiation induced apoptosis by Annexin V

Annexin V is a marker for the early detection of apoptotic cells, which can be followed by flow cytometry. In normal cells the phospholipid phosphatidylserine (PS) is located on the inner leaflet of the plasma membrane. During the early stages of apoptosis, PS is translocated to the outer layer and is exposed on the external surface of the cell. This early event in apoptosis can be detected by using a sensitive method that detects PS exposure. Annexin V is a Ca^{2+} -dependent phospholipid binding protein. Although it can bind to a variety of phospholipids, it has highest affinity for phosphatidylserine (PS) [167], so when apoptosis initiates, Annexin V binding to the cell surface increases. To measure levels of apoptosis, I irradiated primary mice, which were positive for the integration of the mTRF2 transgene. As a positive control I chose either a C57BL/6J mouse or a primary GFP-control mouse. Mice were tested before and after irradiation and levels of apoptosis in thymocytes were measured by flow cytometry (Figure 13). Non-irradiated thymocytes from mice transduced with the mTRF2 transgene were showing 2.1% of apoptotic cells compared to 54.2% of apoptotic cells post irradiation. In contrast, thymocytes from a C57BL/6J control mouse were showing 2.6% apoptotic cells prior irradiation and 49% post irradiation (A). Next I repeated the experiment in mice over-expressing the GFP-mTRF2 transgene compared to GFP-control mice. Non-irradiated thymocytes from mice transduced with the GFP-mTRF2 transgene were showing 1.1% of apoptotic cells compared to 46.3% of apoptotic cells post irradiation. In contrast, thymocytes from a GFP-control mouse were showing 5.1% apoptotic cells prior irradiation and 49.7% post irradiation (B).

In my experiments thymocyte suspensions from mice over-expressing TRF2 do not show lower levels of apoptosis post irradiation.

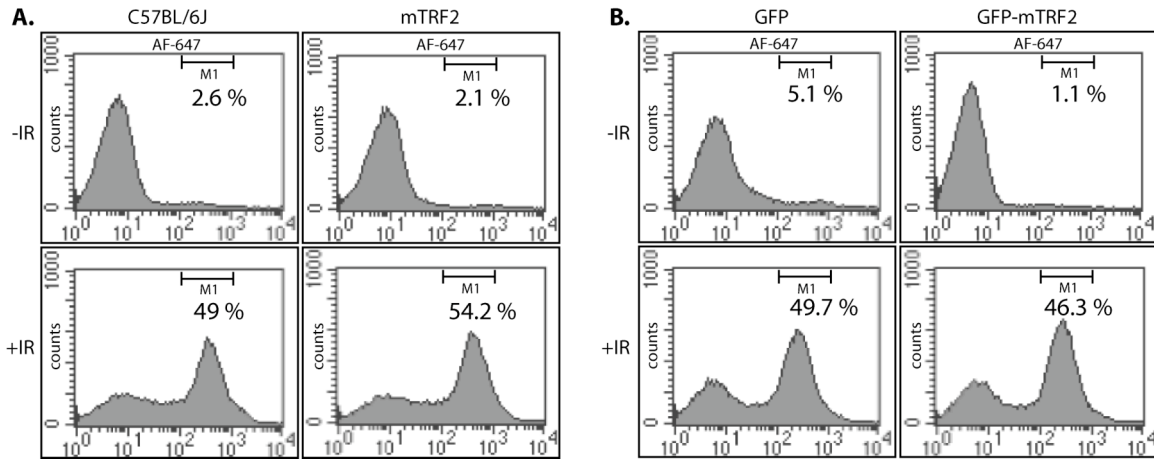


Figure 13 Irradiation induced apoptosis in mice over-expressing mTRF2 and GFP-mTRF2 measured by the percentage of Annexin V positive thymocytes using flow cytometry. (A) Percentage of apoptotic thymocytes in mice over-expressing mTRF2 compared to thymocytes from C57BL/6J control mice and (B) percentage of apoptotic thymocytes in mice over-expressing GFP-mTRF2 compared to thymocytes from GFP over-expressing mice, prior and post irradiation (IR) with 5 Gy.

5.11.2. Detection of irradiation-induced apoptosis in individual cells over-expressing TRF2 by confocal microscopy

I stated above that whole thymocyte suspensions from mice over-expressing TRF2 do not show decreased levels of apoptosis compared to control mice, post irradiation. I wished to determine if this was only due to the low transduction rate with the TRF2 transgene, and individual cells over-expressing TRF2 might in fact be able to withstand irradiation-induced apoptosis.

Therefore, I performed an immunodetection for the activated form of ATM with respect to the expression of GFP-mTRF2, on spleen tissue before and after irradiation (Figure 14).

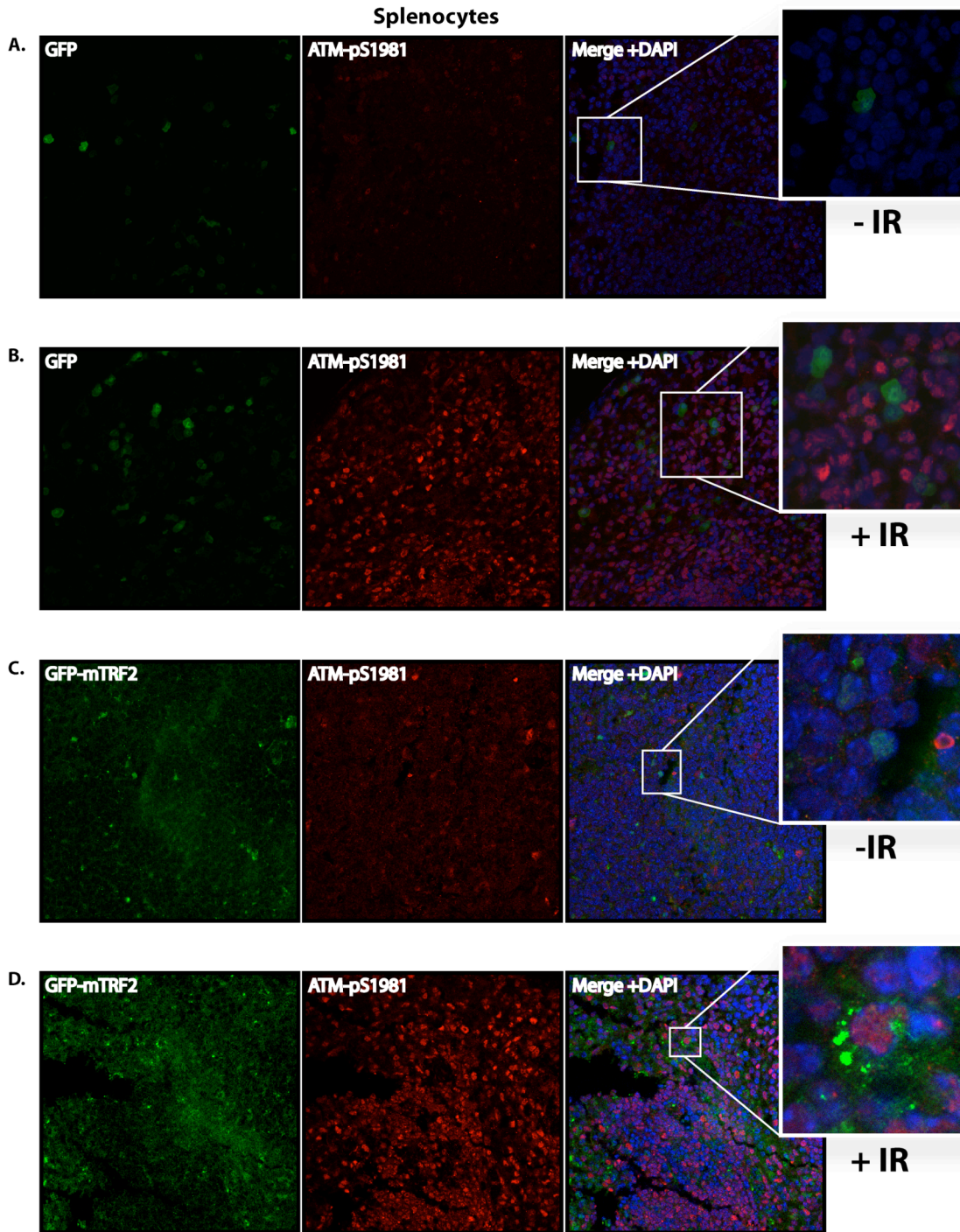


Figure 14 Irradiation induced ATM activation in spleen from mice over-expressing **GFP** or **GFP-mTRF2**. (A and B) ATM activation in mice over-expressing GFP compared to (C and D) ATM activation in mice over-expressing GFP-mTRF2, prior and post irradiation (IR) with 5 Gy. Phosphorylated ATM was detected using an antibody against the Serine-1981 phosphorylation at ATM (ATM-pS1981). DNA was counterstained with DAPI. White squares show a magnified area of the tissue. Confocal image, 63x.

In spleen from a GFP-control mouse, irradiation activated ATM was not detectable prior to irradiation (A). As expected, ATM became activated by irradiation and was detectable in the majority of splenocytes (B). This result correlates with previous results from the Annexin V assay. Surprisingly, while a nuclear GFP-mTRF2 signal was detectable in a small number of splenocytes prior to irradiation (C), this nuclear pattern disappeared completely post irradiation. Instead I detected a rather non-specific GFP-signal coming from the cytoplasm of a small number of cells, which also show ATM activation (D).

Together these observations confirm the results from the Annexin V assay and suggest that the over-expression of TRF2 in mice does not abrogate the activation of ATM upon irradiation.

5.12. Western analysis of tumorigenic tissue for transgenic TRF2

I observed tumor development in a number of secondary mice, which received bone marrow transduced with transgenic TRF2, and screened them for the over-expression of TRF2 by *Western* analysis. While I investigated numerous tissues from tumorigenic mice, I did not observe TRF2 over-expression.

Figure 15 shows a characteristic result for my *Western* analysis. Due to certain criteria (5.9) I considered some of the tumorigenic tissues as good candidates for being affected by a TRF2 related tumor. In parallel to the *Western* analysis I applied immunofluorescence on bone marrow and splenocytes from this individual mouse and found only a subset of cells that over-expressed GFP-mTRF2 (Figure 10).

Taken together, my *Western* and immunofluorescence analysis did not show any evidence of TRF2 over-expression in the observed tumor tissues.

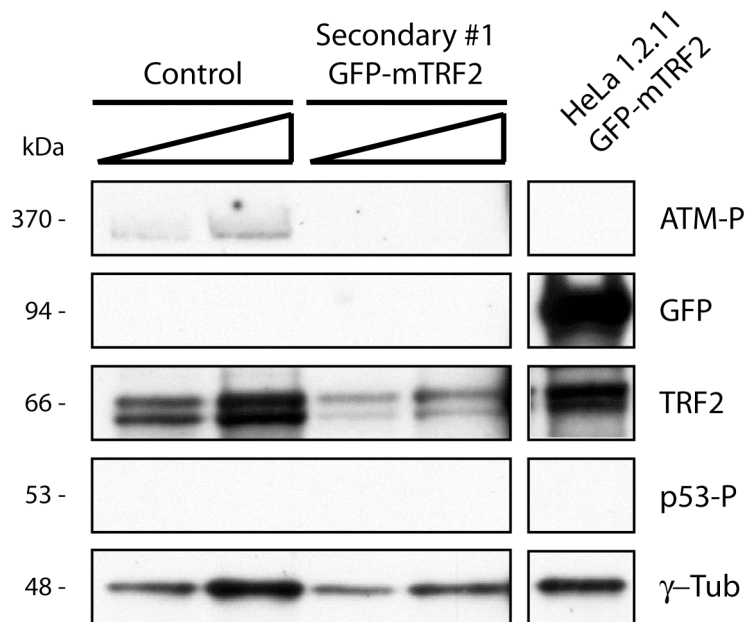


Figure 15 *Western analysis of spleen from a secondary recipient mouse, which expressed GFP-mTRF2 and died from a CD4/CD8-double-positive T-cell lymphoma.* Protein samples were probed with an antibody against GFP, p53-pS15 (p53-P), ATM-pS1981 (ATM-P) and TRF2. γ -Tubulin (γ -Tub) was included as a loading control. As a negative control, a protein sample from a C57BL/6J control spleen was loaded. As a positive control, protein extract from HeLa 1.2.11 cells expressing GFP-mTRF2 was loaded.

5.13. Genotyping for transgenic TRF2 integration in tumorigenic tissue samples

My previous results suggested that tumor development in mice transduced with TRF2 was independent from the over-expression of the transgene. However, I considered the possibility that TRF2 over-expression might be important for initiating tumor development, but dispensable, or even antagonistic, for further tumor growth and therefore may be silenced. In this case, the transgene should still be detectable within the genome of tumorigenic tissue. I genotyped a large number of collected tissue samples from primary and secondary recipient mice to screen for the TRF2 transgene (Figure 16 and Table 2). I also included tissue samples from primary and secondary GFP-control mice as internal negative controls. As a positive control I included genomic DNA of 3T3 cells transduced

with GFP-mTRF2 at a rate of 70%, 22% and 2%. This allowed for semi-quantitative calculations on the transduction rate of the genomic samples.

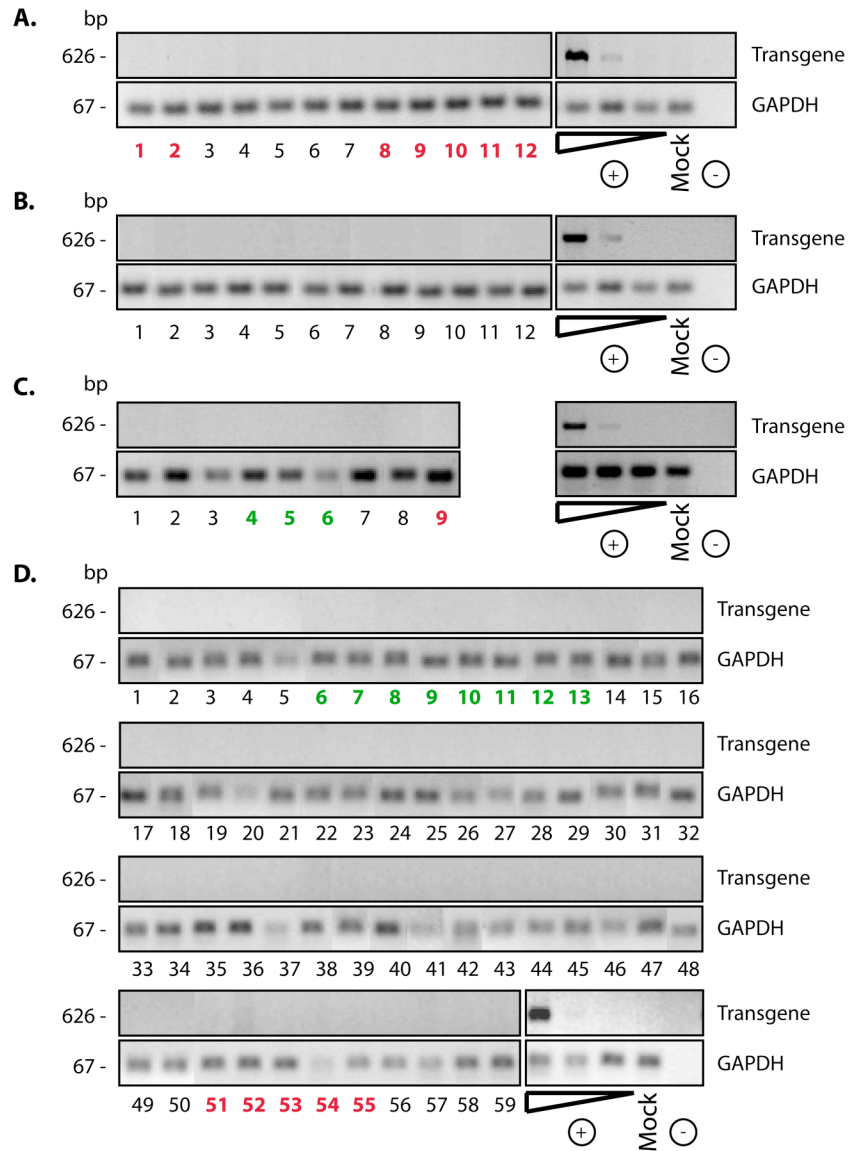


Figure 16 Genotyping for the integration of transgenic TRF2 in tissue samples from mice transduced with GFP, GFP-mTRF2 or mTRF2. GAPDH was selected as a positive PCR control. As a semi-quantitative transduction indicator (+), 3T3 cells were transduced with GFP-mTRF2 at a rate of 70%, 22% and 2%. 'Mock' indicates genomic DNA from a C57BL/6J negative control mouse. (-) indicates a ddH₂O negative control. Genomic DNA from GFP-control mice is labeled in green color, genomic DNA from potential TRF2 related tumors is labeled in red color. See Tab. 2 for a detailed legend.

Table 2 Origin of the genomic DNA used in genotyping assay in Figure 16. Genomic DNA from GFP-control mice is marked by a green background color, genomic DNA from potential TRF2 related tumors is marked by a red background color. LN - lymph node.

| Lane | Trans-plantation | Donor | Trans-gene | Tissue |
|-------|------------------|--------|------------|--------|
| A. 1 | Primary #1 | GFP | mTRF2 | BM |
| A. 2 | | " | " | Spleen |
| A. 3 | Primary #1 | GFP | mTRF2 | BM |
| A. 4 | | " | " | Spleen |
| A. 5 | Primary #1 | GFP | mTRF2 | BM |
| A. 6 | Primary #1 | CD45.1 | GFP-mTRF2 | BM |
| A. 7 | Primary #2 | CD45.1 | GFP-mTRF2 | BM |
| A. 8 | Secondary #1 | GFP | mTRF2 | BM |
| A. 9 | | " | " | Spleen |
| A. 10 | | " | " | Thymus |
| A. 11 | Secondary #1 | CD45.1 | GFP-mTRF2 | BM |
| A. 12 | | " | " | Thymus |

| Lane | Trans-plantation | Donor | Trans-gene | Tissue |
|-------|------------------|--------|------------|--------|
| B. 1 | Primary #1 | GFP | mTRF2 | BM |
| B. 2 | Primary #1 | GFP | mTRF2 | BM |
| B. 3 | Primary #1 | GFP | mTRF2 | BM |
| B. 4 | Primary #1 | GFP | mTRF2 | BM |
| B. 5 | Primary #1 | GFP | mTRF2 | BM |
| B. 6 | Primary #1 | GFP | mTRF2 | BM |
| B. 7 | Primary #1 | CD45.1 | GFP-mTRF2 | BM |
| B. 8 | Primary #1 | CD45.1 | GFP-mTRF2 | BM |
| B. 9 | Primary #1 | CD45.1 | GFP-mTRF2 | BM |
| B. 10 | Primary #1 | CD45.1 | GFP-mTRF2 | BM |
| B. 11 | Primary #1 | CD45.1 | GFP-mTRF2 | BM |
| B. 12 | Primary #2 | CD45.1 | GFP-mTRF2 | BM |

| Lane | Trans-plantation | Donor | Trans-gene | Tissue |
|------|------------------|--------|------------|--------|
| C. 1 | Primary #1 | CD45.1 | GFP-mTRF2 | BM |
| C. 2 | Primary #1 | CD45.1 | GFP-mTRF2 | BM |
| C. 3 | Primary #1 | CD45.1 | GFP-mTRF2 | BM |
| C. 4 | Primary #2 | CD45.1 | GFP | BM |
| C. 5 | | " | " | Spleen |
| C. 6 | | " | " | Thymus |
| C. 7 | Primary #2 | CD45.1 | GFP-mTRF2 | BM |
| C. 8 | Primary #2 | CD45.1 | GFP-mTRF2 | BM |
| C. 9 | Secondary #1 | CD45.1 | GFP-mTRF2 | Thymus |

| Lane | Trans-plantation | Donor | Trans-gene | Tissue |
|-------|------------------|--------|------------|--------|
| D. 1 | Primary #1 | CD45.1 | GFP-mTRF2 | BM |
| D. 2 | Primary #1 | CD45.1 | GFP-mTRF2 | BM |
| D. 3 | | " | " | Liver |
| D. 4 | | " | " | Spleen |
| D. 5 | | " | " | LN |
| D. 6 | Primary #2 | CD45.1 | GFP | BM |
| D. 7 | Primary #2 | CD45.1 | GFP | BM |
| D. 8 | Primary #2 | CD45.1 | GFP | BM |
| D. 9 | Primary #2 | CD45.1 | GFP | BM |
| D. 10 | | " | " | Spleen |
| D. 11 | Primary #2 | CD45.1 | GFP | BM |
| D. 12 | Primary #2 | CD45.1 | GFP | BM |
| D. 13 | Primary #2 | CD45.1 | GFP | BM |
| D. 14 | Primary #2 | CD45.1 | mTRF2 | BM |
| D. 15 | Primary #2 | CD45.1 | mTRF2 | BM |
| D. 16 | Primary #2 | CD45.1 | mTRF2 | Spleen |
| D. 17 | Primary #2 | CD45.1 | mTRF2 | BM |
| D. 18 | Primary #2 | CD45.1 | mTRF2 | BM |
| D. 19 | Primary #2 | CD45.1 | mTRF2 | BM |
| D. 20 | | " | " | Thymus |
| D. 21 | | " | " | Liver |
| D. 22 | Primary #2 | CD45.1 | mTRF2 | BM |
| D. 23 | Primary #2 | CD45.1 | mTRF2 | BM |
| D. 24 | Primary #2 | CD45.1 | mTRF2 | BM |
| D. 25 | | " | " | Spleen |
| D. 26 | Primary #2 | CD45.1 | mTRF2 | BM |
| D. 27 | Primary #2 | CD45.1 | mTRF2 | BM |
| D. 28 | Primary #2 | CD45.1 | mTRF2 | BM |
| D. 29 | | " | " | Spleen |
| D. 30 | Primary #2 | CD45.1 | mTRF2 | BM |
| D. 31 | Primary #2 | CD45.1 | mTRF2 | BM |
| D. 32 | Primary #2 | CD45.1 | mTRF2 | BM |
| D. 33 | Primary #2 | CD45.1 | mTRF2 | BM |
| D. 34 | Primary #2 | CD45.1 | GFP-mTRF2 | BM |
| D. 35 | | " | " | Spleen |
| D. 36 | | " | " | Liver |
| D. 37 | | " | " | Lung |
| D. 38 | | " | " | Kidney |
| D. 39 | Primary #2 | CD45.1 | GFP-mTRF2 | BM |
| D. 40 | Primary #2 | CD45.1 | GFP-mTRF2 | BM |
| D. 41 | Primary #2 | CD45.1 | GFP-mTRF2 | BM |
| D. 42 | Primary #2 | CD45.1 | GFP-mTRF2 | BM |
| D. 43 | | " | " | Spleen |
| D. 44 | Primary #2 | CD45.1 | GFP-mTRF2 | BM |
| D. 45 | | " | " | Spleen |
| D. 46 | Secondary #1 | GFP | mTRF2 | BM |
| D. 47 | | " | " | Thymus |
| D. 48 | Secondary #1 | GFP | mTRF2 | BM |
| D. 49 | Secondary #1 | GFP | mTRF2 | BM |
| D. 50 | Secondary #1 | CD45.1 | GFP-mTRF2 | BM |
| D. 51 | Secondary #1 | GFP | mTRF2 | BM |
| D. 52 | | " | " | Spleen |
| D. 53 | | " | " | Kidney |
| D. 54 | | " | " | Thymus |
| D. 55 | | " | " | Liver |
| D. 56 | Secondary #2 | CD45.1 | GFP-mTRF2 | BM |
| D. 57 | | " | " | Thymus |
| D. 58 | | " | " | Liver |
| D. 59 | | " | " | Spleen |

The genotyping results suggested that none of the screened genomic DNA contained traces of transgenic TRF2, and the observed tumors were not caused by the TRF2 transgene.

5.14. Pathological observations on potential TRF2 related tumor tissue

Tissue sections of all potential TRF2 related tumors (5.9, Table 1) were also characterized by pathological analysis (Figure 17).

I found that seven out of the eight mice showed a large cell, blastic T-cell lymphoma, involving liver, spleen and thymus. Spleen, liver and thymus were infiltrated and replaced by a diffuse monotonous neoplastic infiltrate composed of cells with large oval nuclei, with a delicate chromatin pattern, and scant cytoplasm. The cells had a brisk mitotic rate but characteristically had foci of apoptotic cells. The renal glomeruli displayed a thickening of the basement membrane and some were hyalinized (A).

Another mouse (S1-GFP R2) showed signs of myeloid leukemia; the spleen was enlarged and replaced by immature myeloid cells and showed almost no lymphoid areas. The liver had several small clusters of myeloid cells. The kidney had extensive thickening of the glomerular basement membrane with many hyalinized glomeruli. There were infiltrates of plasma cells in the hilus and in cluster within the cortex (B).

I found tumor development in mice that were transduced with the TRF2 transgene and which developed these tumors within a timeframe of 52 weeks of age. The pathological observations furthermore suggested tumor development in organs that appeared macroscopically normal (compare Table 1 B versus Figure 17 A and B). I cannot rule out that my macroscopical observations were insufficient to detect every potential TRF2 related tumor that occurred in the course of this project.

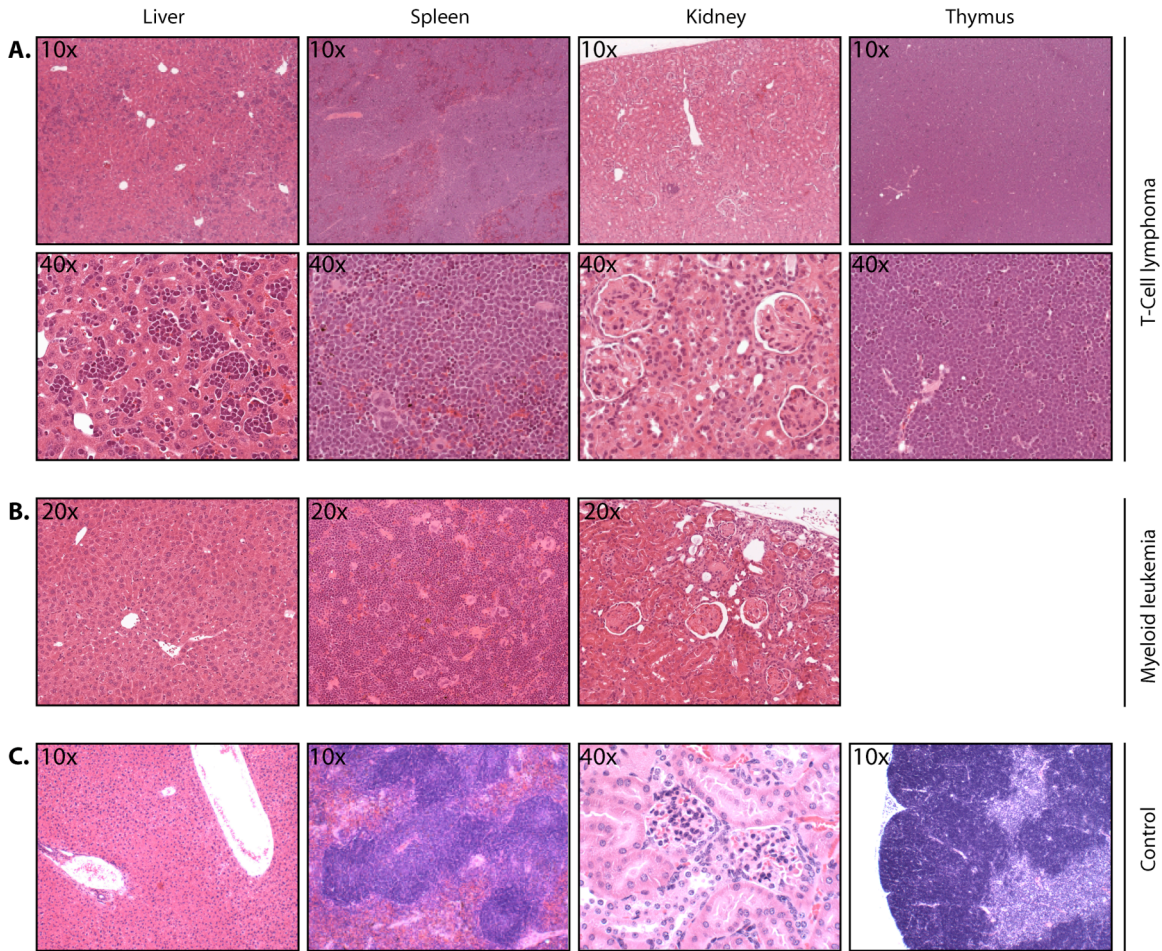


Figure 17 H&E - staining of tumor tissue. (A) Tissue samples from a secondary recipient mouse, which developed a large cell, blastic T-cell lymphoma, involving liver, spleen and thymus. Spleen, liver and thymus were infiltrated and replaced by a diffuse monotonous neoplastic infiltrate composed of cells with large oval nuclei with a delicate chromatin pattern and spare cytoplasm. The cells had a brisk mitotic rate but characteristically had foci of apoptotic cells. The renal glomeruli had thickening of the basement membrane and some were hyalinized. (B) Tissue samples from a primary recipient mouse, which developed myeloid leukemia in the course of the experiment. The spleen was enlarged and replaced by immature myeloid cells and was showing almost no lymphoid areas. The liver had several small clusters of myeloid cells. The kidney had extensive thickening of the glomerular basement membrane with many hyalinized glomeruli. There were infiltrates of plasma cells in the hilus and in cluster within the cortex. Both mice were successfully transduced with the TRF2 transgene. Staining was applied on sections of liver, thymus, spleen and kidney. The lower panels (C) show sections of control tissue from a healthy C57BL/6J mouse.

5.15. Characterization of T-cell lymphoma by flow cytometry

To further characterize the T-cell lymphoma that developed in a larger group of mice transduced with the TRF2 transgene, I analyzed thymocytes that displayed pathological evidence of a T-cell lymphoma by flow cytometry (Figure 18). The figure shows a typical result for flow cytometric analysis.

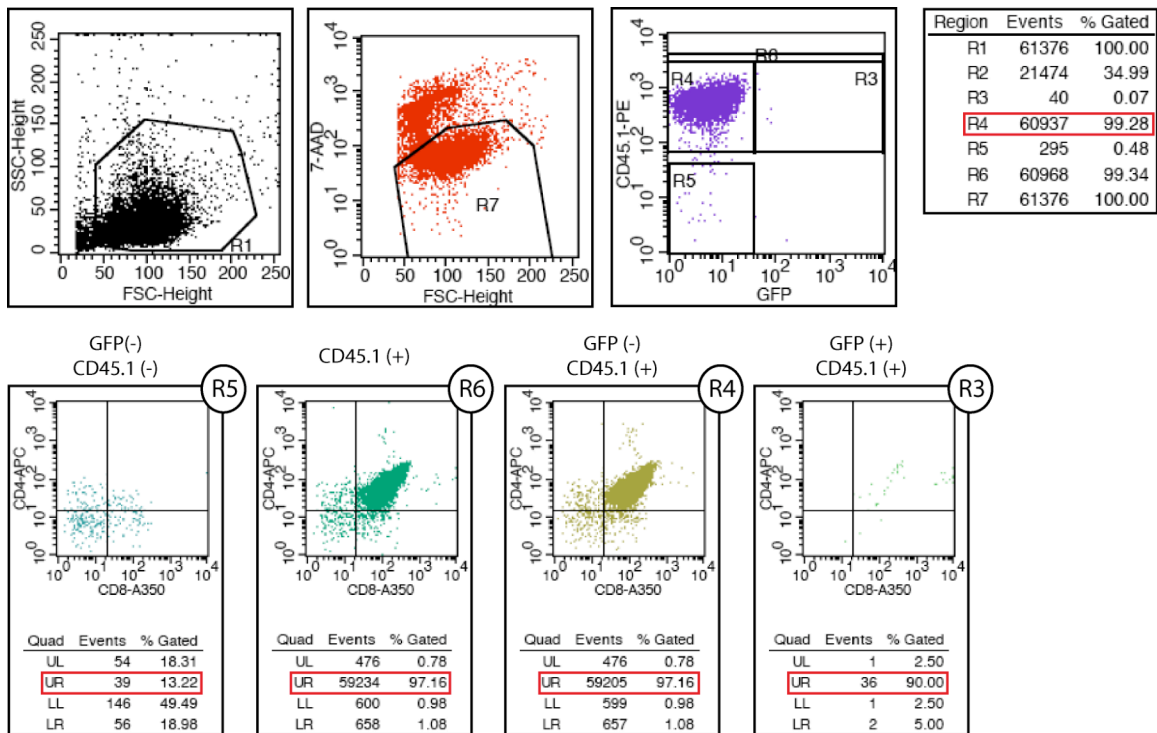


Figure 18 Flow cytometric analysis of thymoma material. The enlarged thymus of a secondary recipient mouse expressing GFP-mTRF2 was prepared for FACS analysis. As tumor markers CD4 and CD8 were used. The red frames indicate percentages (%) of CD4/CD8-double-positive populations. The analysis suggests the presence of a donor derived CD4/CD8-double-positive T-cell lymphoma, which is negative for GFP-mTRF2.

I confirmed the presence of a CD4/CD8-double-positive T-cell lymphoma. A total of 97.2% of cells positive for CD45.1 were double-positive for CD4 and CD8. However, only 0.1% of all thymocytes in the assay were positive for GFP.

Thymocytes negative for CD45.1 were low in numbers and did not show any specific CD4/CD8 pattern. Thus, the observed CD4/CD8-double-positive T-cell lymphoma originated from the CD45.1 donor population but appeared not to be caused by the immediate over-expression of GFP-mTRF2.

5.16. Analysis of pathological samples and metaphase spreads for genome instability

In the course of the project I observed tumor development in a number of mice. Despite being initially transduced with the TRF2 transgene, these tumors did not show evidence of current expression of the transgene. While an insufficient transduction rate with the transgene and TRF2 unrelated tumor development is one possibility, genome instability, as it is a hallmark of many tumors, might also lead to the loss of the TRF2 transgene. Therefore, I screened pathological samples of the T-cell lymphomas for anaphase bridges (Figure 19).

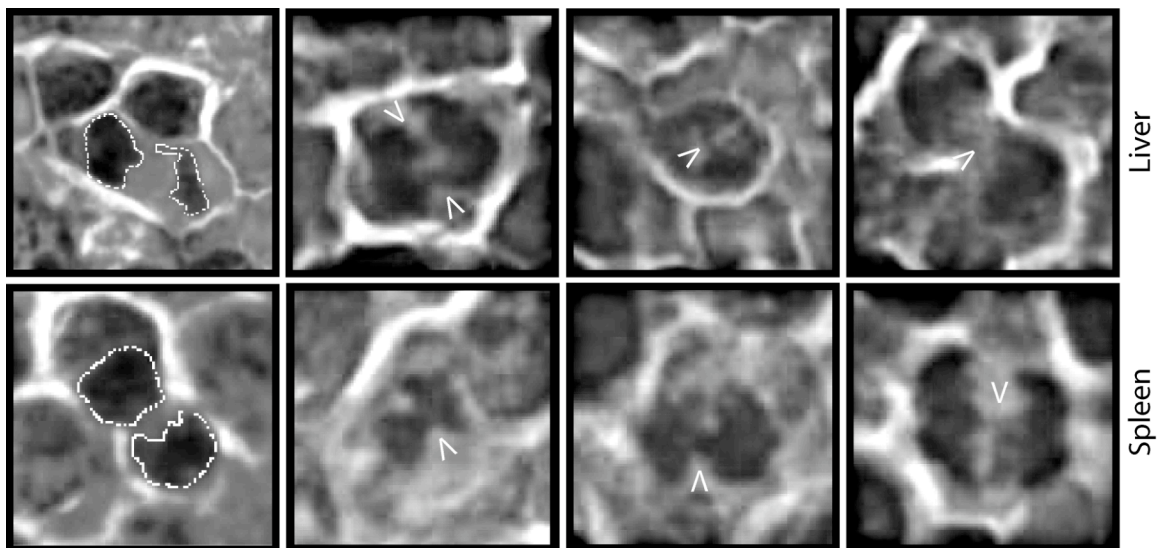


Figure 19 Anaphase bridges in H&E - stained liver and spleen sections from a secondary recipient mouse carrying a CD4/CD8-double-positive T-cell lymphoma. The arrows point to the chromatin bridges between the separating chromosomes. A dashed line outlines normal anaphases displayed in the pictures to the very left.

Anaphase bridges are caused by the uncontrolled non-homologous end fusions of double-stranded breaks. This leads to new, randomly distributed breaks during mitosis when the fused chromosomes are pulled apart. As a result, further genome instability occurs, which eventually leads to the loss of genomic DNA.

The occurrence of anaphase bridges in the investigated spleen and liver cells indicate genome instability. In addition to the presence of anaphase bridges I also found genome instability in metaphase spreads from the same tumors (Figure 20). The metaphase spreads displayed multiple telomere signals at telomeres as well as signs of polyploidy, both characteristics of genome instability.

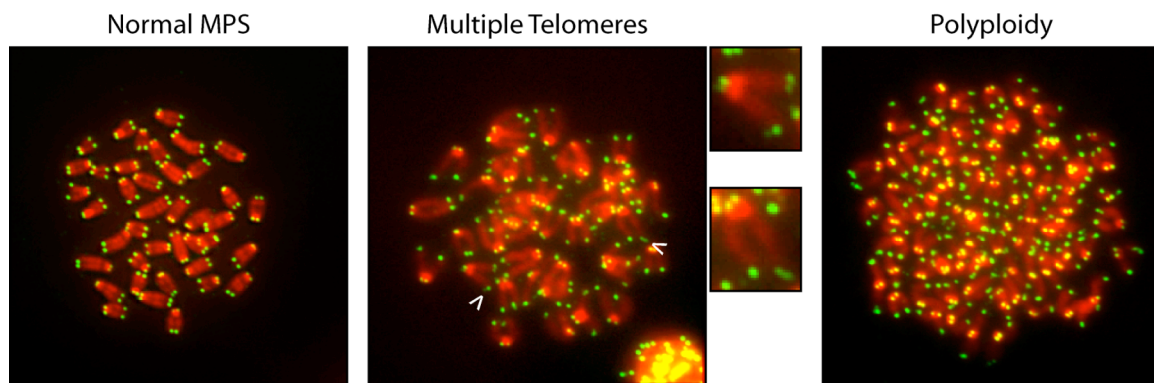


Figure 20 Genome instability was observed in metaphase spreads (MPS) prepared from splenocytes of a secondary recipient mouse carrying a CD4/CD8-double-positive T-cell lymphoma. The telomeres were stained with a telomere specific probe conjugated to FITC (green). Chromatin was counterstained with DAPI. The arrows point to chromosome ends with multiple telomeres (see enlarged pictures). Immunofluorescence, 63x1.25.

6. Discussion

The telomeric repeat binding factor TRF2 is an important component of shelterin and it plays a central role in the protection of telomeres from the DNA damage machinery. The MRN subunit Mre11 is part of the DNA damage sensors of the ATM pathway [168-170] and as such it also associates with telomeres. TRF2 appears to play a central role in preventing telomeres from activating ATM. The kinase ATM [171] acts as an important transducer of the DNA damage signal and requires autophosphorylation on S1981 to be activated. Phosphorylation of S1981 leads to concomitant dissociation into monomers, which is presumed to be the active form of the kinase [152]. Double-stranded breaks and other genome stress lead to a rapid conversion of the ATM pool into active ATM-pS1981 monomers and, in turn, to the phosphorylation of regulators of the G1/S, intra-S, and G2/M cell cycle transitions [152]. Activation of ATM also takes place in response to telomere damage and, as shown recently, during the telomere replication process in late G2 [172]. In both cases the unprotected telomeres associate with phosphorylated ATM [173]. Furthermore, ATM targets become phosphorylated in aging cells with shortened telomeres [154]. There is also evidence for a role of ATM in the telomere damage pathway, which showed the diminished ability of ataxia telangiectasia (A-T) cells to mount a DNA damage response after telomere uncapping [173, 174]. However, several lines of evidence suggest that a second PIKK (phosphatidylinositol 3-kinase-like kinase), such as ATR or DNA-PKcs, can transduce the telomere damage signal in the absence of ATM [173, 175].

As I described in the introduction, it is presumed that TRF2 is an important part of the shelterin complex and protects the telomeres from uncontrolled processing through the DNA damage machinery, most likely by hiding the 3'-overhang via strand-invasion into the duplex part of the telomeres. However, while hiding the 3'-overhang in the T-loop structure, the T-loop displays structural features resembling DNA lesions, including single strand to double strand transitions, 3'

and 5' ends, and single-stranded DNA. Therefore, human telomeres may need additional mechanisms to circumvent checkpoint activation.

The *in vitro* data that initiated this thesis work is based on experiments suggesting that the removal of TRF2 from the telomeres results in the localization of the activated, phosphorylated form of ATM to unprotected chromosome ends [173] and induces ATM-dependent apoptosis [174]. More recently it has been suggested that TRF2 protects telomeres through a direct interaction with ATM and blocks its activation.

TRF2 binds ATM in a region surrounding S1981 and prevents its phosphorylation and inhibits the monomerization and activation of ATM. As a result, TRF2 abrogates the downstream outcomes of the ATM dependent DNA damage response, including phosphorylation of various ATM downstream targets and cell cycle arrest [161]. Therefore, high concentrations of TRF2 at sites of telomeres protect telomeres from processing by the DNA damage machinery. Since TRF2 appears to be abundant only at the sites of telomeres, this protection mechanism seems to be limited to telomeres. This could change if TRF2 is upregulated throughout the nucleus, e.g. by over-expression, in which case high levels of TRF2 could inhibit ATM and the DNA damage machinery also at other sites of the genome where double-stranded breaks need to be processed. As a result, these breaks could not be sufficiently processed and genome instability would occur. Thus, TRF2 would be a potent suppressor of the DNA damage machinery. In turn, in many tumor cells the ability to regulate checkpoints and to sufficiently process DNA damage is compromised. This is mainly due to mutations in genes in the ATM/p53 pathway, but also other checkpoint regulating tumor-suppressor proteins. It has been shown that patients suffering from A-T are estimated to have a 100-fold increased risk of cancer compared to the general population. Lymphoid cancers predominate in childhood, and epithelial cancers, including breast cancer, are seen in adults [176]. Considering that the inhibition of ATM by mutations has such a severe impact and results in a drastic development of tumors, it is intriguing to elucidate if the inhibition of ATM by over-expression of TRF2 can cause a similar tumorigenic phenotype.

ATM $-/-$ mice displayed growth retardation, neurologic dysfunction, male and female infertility secondary to the absence of mature gametes, defects in T-lymphocyte maturation, and extreme sensitivity to irradiation. The majority of animals developed malignant thymic lymphomas between two and four months of age. Several chromosomal anomalies were detected in these tumors. Fibroblasts from these mice grew slowly and exhibited abnormal radiation-induced G1 checkpoint function. ATM-disrupted mice resemble the ataxia telangiectasia phenotype in humans [165]. In addition, mutations in the p53 tumor-suppressor gene, an ATM downstream target protein, are frequently observed genetic lesions in human cancers. p53 $-/-$ mice appear normal but are prone to spontaneous development of a variety of neoplasms by six months of age [166].

I designed a mouse model in the course of this thesis work to investigate TRF2's potential to act as an oncogene *in vivo* when over-expressed in the hematopoietic system. Based on the *in vitro* results and on previous mouse models for ATM and p53 deletions, I expected that the over-expression of TRF2 will have an inhibitory effect on ATM throughout the nucleus and prevent the correct processing of randomly occurring DNA double-stranded breaks, which eventually leads to tumor formation.

I started the project by designing two transgenic TRF2 constructs, which would allow the over-expression of TRF2 in the hematopoietic system of C57BL/6J mice. I cloned mTRF2 and GFP-mTRF2 into a lentiviral vector system and tested their functionality by transfection into murine 3T3 cells. My immunofluorescence data suggested functional expression of both transgenes *in vitro*. I further confirmed over-expression of both transgenes by *Western* analysis. Thus, I designed and verified two functional TRF2 expression systems, allowing the over-expression of TRF2 in murine cells *in vitro*.

I then used the lentiviral backbone of the designed vector system to produce virus batches carrying both transgenes. The lentivirus was produced in 293T cells and the quality of each virus batch was validated in a p24 ELISA assay. For

the first virus batch, which I eventually used for the generation of the Primary #1 mouse colony, I measured p24 values of 3×10^9 particles/ml for the mTRF2 lentivirus and 8.5×10^9 particles/ml for the GFP-mTRF2 lentivirus. I considered both viral titers as adequate to sufficiently transduce hematopoietic stem cells from donor bone marrow.

Next, I transduced donor bone marrow from CD45.1 and GFP donor mice with the corresponding lentivirus. By immunofluorescence and *Western* analysis I detected functional over-expression of both transgenes in murine bone marrow. I subsequently transplanted transduced bone marrow into irradiated C57BL/6J recipient mice, termed Primary #1, and monitored them for tumor development over time.

To show engraftment of the transplanted bone marrow and the successful integration of the transgene into the hematopoietic system, I genotyped recipient mice four months after their transplantation. Although I detected the transgene in the majority of all recipient mice, the detection failed when I used just the outer primer pair of the nested PCR. This suggested a very low integration rate, possibly due to a lower viral titer than the p24 ELISA assay initially suggested. Although I believe that over-expression of TRF2 in hematopoietic cells in principal could promote tumor development despite a low transduction rate, it is desirable to see high transduction efficiency for a number of reasons. First, high transduction efficiency increases the chance of potential TRF2 related tumor development because more hematopoietic stem cells are expressing the transgene. Second, larger numbers of TRF2 over-expressing cells would allow the detection of early processes during tumor development in a small subset of cells by methods like flow cytometry or colony forming assays.

I therefore decided to generate a second colony of recipient mice, termed Primary #2. The lentivirus production protocol was optimized to yield a high viral titer. By a p24 ELISA assay I measured values of 8.2×10^7 particles/ml for mTRF2 and 6.4×10^8 particles/ml for GFP-mTRF2 for the new virus batches. In addition I included the production of a GFP-control lentivirus and measured for this virus a p24 ELISA value of 3.8×10^9 particles/ml. Although the p24 ELISA values in this

second production process were roughly tenfold lower than in the first lentivirus production process, I believe that this was influenced by the difference in the number of dead particles in the virus batches.

For the generation of the Primary #2 colony I infected CD45.1 donor bone marrow and transplanted it into irradiated C57BL/6J recipient mice. Four months post transplantation, I genotyped the Primary #2 colony. Surprisingly, the number of mice positive for either transgenic mTRF2 or GFP-mTRF2 was lower than in the Primary #1 colony. Since I used the same nested PCR method to detect the presence of the transgene in both colonies, I concluded a less effective transduction of the donor bone marrow in the case of the Primary #2 colony. This would suggest that I did not effectively optimize the viral production.

I realized at this point that a major challenge for this project was low transduction efficiency. Surprisingly, although I attempted to optimize the viral production, the optimization process had the opposite effect and led to lower transduction efficiency. To overcome the challenge of low transduction rates and to further promote tumor growth, I expanded bone marrow from primary recipient mice positive for transgenic TRF2 into secondary recipient mice.

In the course of the project I followed a total of 122 mice potentially over-expressing transgenic TRF2. While I observed tumor development in some of them, I applied a number of criteria to judge if the tumor could be related to TRF2 over-expression. To be considered as a potential TRF2 related tumor, the individual mouse had to be positive for the TRF2 transgene. This was initially confirmed by the genotyping assay. The previous *in vitro* studies also suggested that over-expressed TRF2 interferes with the ATM pathways, thereby blocking downstream targets like p53 from being activated. It was observed that p53 *-/-* mice showed tumor development at approximately six months of age [166]. Considering the age of all mice at the time of transplantation (eight weeks) and the fact that the impact of the transgene might be weaker due to the low transduction efficiency, I considered only mice that were 52 weeks of age or younger when they showed signs of sickness. The final requirement for TRF2-related tumorigenesis had to be the macroscopical observation of tumor

development in these mice. Taken together, I observed potential TRF2 related tumor development in eight out of 122 mice. Among these eight mice was one primary recipient mouse; all other mice were secondary recipients. Interestingly, I discovered later into the project that the primary recipient mouse suffered from myeloid leukemia, while the seven secondary recipient mice suffered most likely from a large T-cell lymphoma. I confirmed for two out of the seven secondary mice a T-cell lymphoma based on pathological data and flow cytometry. A T-cell lymphoma is macroscopically characterized by an enlarged thymus. I observed tumor enlargement in all secondary recipient mice, which, by my criteria, may have developed a TRF2 related tumor. This finding suggested that T-cell lymphoma also developed in those secondary mice that were not pathologically analyzed. In contrast, I did not observe tumor development in any of the GFP-control mice within 52 weeks of age. Thus, I detected an increase in T-cell tumor development in secondary recipient mice carrying transgenic TRF2.

For my next approach to link over-expression of transgenic TRF2 with tumor development, I analyzed protein extracts from all potential TRF2 related tumor samples for the presence of the transgene by *Western* analysis. Surprisingly, I could not detect higher levels of TRF2 in any of the investigated tissues. I also screened for levels of activated ATM. Although I detected decreased levels of activated ATM in tumor samples, suggesting an inhibited ATM pathway, I did not see this result in all tumor samples. In parallel, when I analyzed tumorigenic tissue by fluorescence microscopy, expression of transgenic TRF2 was detectable only in a subset of cells. Therefore, my *Western* and immunofluorescence analysis did not provide further evidence for the correlation of tumor development, TRF2 over-expression and ATM inhibition. Consequently, when I analyzed tumorigenic tissue of a mouse transduced with the GFP-mTRF2 transgene by flow cytometry I did not only confirm the presence of a CD4/CD8-double-positive T-cell lymphoma, I also found that the majority of the lymphoma cells were negative for a GFP signal. This suggests again that transgenic TRF2 is not the cause for the T-cell lymphoma development.

Because I detected an increase in tumor development independent of the actual expression of the potential transgene, I considered a temporal, early stage tumorigenic effect of the TRF2 transgene. I assumed that TRF2 over-expression would promote early stage tumor formation, but would then be no longer needed for further tumor growth or even have an antagonistic effect. TRF2 would therefore act through a “Hit & Run” mechanism. If TRF2 over-expression would be antagonistic to promote further tumor growth, gene silencing could facilitate the inhibition of further TRF2 over-expression. In this case, the transgenic TRF2 expression would be inhibited on the protein level, but the presence of the transgene would be still detectable. Therefore, I analyzed a large number of genomic DNAs by genotyping for the presence of transgenic TRF2. I could not detect the presence of the TRF2 transgene in any of the samples, including genomic DNA isolated from T-cell lymphoma developing mice. This result suggests that the TRF2 transgene is not present in the developed T-cell lymphoma. I propose two possibilities: either the transgene was never expressed in the individual mice and tumor development occurred without TRF2 over-expression, or the TRF2 transgene was disrupted and could not be detected by genotyping.

Disruption of genomic information can be caused by genome instability, which is often a hallmark of cancer. Genome instability is characterized by chromosome-fusions. In anaphase this appears as chromatin bridges and eventually leads to chromosome breaks, inevitably leading to genome disruption and loss of genomic information. To determine the presence of genome instability in the T-cell lymphomas, I screened the pathological specimens for anaphase bridges. Indeed, the investigated T-cell lymphomas were characterized by brisk mitotic rates and did show numerous anaphase bridges. Although I cannot rule out that tumor development occurred independently from the TRF2 transgene, this result may suggest that the transgene was deleted by genome instability.

Instead of linking tumor development to a transgene post tumor occurrence, I also wondered if I could show TRF2's oncogenic potential in healthy tissue, by performing a colony-forming assay (CFA). Therefore, I isolated bone marrow

from an individual GFP-mTRF2 over-expressing mouse, sorted the cells into GFP-negative and GFP-positive, and grew them in a CFA and also in a liquid assay. Although I did detect more colony growth in the GFP-positive compared to the GFP-negative CFA over time, the numbers were not significantly different. However, when I analyzed the liquid assay by flow cytometry, I detected an increase in the population of CD11b cells within the assay sorted for GFP-positive cells compared to GFP-negative cells. Although I initially sorted for GFP-positive cells, the increase in CD11b positive cells emerged from the CD45.1 population, but it no longer showed a GFP-signal. I conclude from this result that the initial expression of GFP-mTRF2 in bone marrow cells appears to influence the differentiation pattern over time. However, I cannot explain why the GFP-signal was lost. I am also aware that I investigated only one individual mouse and further quantitative analysis is needed to support my results.

I knew from the previous studies on TRF2 that it has the potential to inhibit ATM *in vitro*. If a cell enters apoptosis, this is frequently connected to ATM, which is a key player in the apoptosis pathway. Apoptosis can be induced by irradiation and this induction should fail in an organism where the apoptosis pathway is abrogated due to a lack of ATM activity. Therefore, I predicted that mice over-expressing TRF2 in their hematopoietic system should show signs of apoptosis inhibition. To measure apoptosis *in situ* I used flow cytometry to measure levels of the early apoptosis marker Annexin V in thymocytes before and after irradiation and compared the results to GFP-control mice. However, TRF2 over-expressing mice did not show any difference in the levels of apoptosis after irradiation compared to GFP-control mice.

Taking the previous results of this study into consideration, a number of reasons could account for the outcome of this experiment. TRF2 might be unable to inhibit ATM *in vivo* and *in vitro* results may not be transferable to a mouse model. More likely, the low transduction rate by transgene-containing virus led to only a subset of cells over-expressing TRF2 and these cells would show an abrogated apoptosis pathway. To investigate further, I checked individual cells over-expressing TRF2 for the presence of ATM-pS1981 after irradiation using

confocal microscopy. While I found cells over-expressing TRF2 before irradiation, these cells were lost after irradiation. In addition, cells negative for transgenic TRF2 showed normal activation of ATM, confirming the Annexin V results. I do not have an explanation for the loss of transgenic TRF2 over-expression, but one could speculate that TRF2 over-expressing cells are very sensible to irradiation. Summarizing the results of this thesis work so far, I observed a small increase in tumor development in mice that were transduced with transgenic TRF2 compared to control mice, although I could not show the actual over-expression of the transgene in an established tumor by fluorescent microscopy or flow cytometry. These findings suggest that TRF2 is not a strong oncogene. First, I successfully transduced the hematopoietic system of recipient mice with transgenic TRF2 and detected functional expression of recombinant TRF2 in the mouse model. The observed TRF2 over-expression, however, was only detectable in a small subset of cells, which probably diminished the potential tumor phenotype, but did not abrogate it. In fact, I did see a slight increase in the development of CD4/CD8-double-positive T-cell lymphomas in secondary recipient mice. It is important to mention that I see these tumors in independent secondary colonies and I can therefore rule out clonal tumors. The transplantation of TRF2 over-expressing bone marrow from one primary recipient into multiple secondary recipients should have increased the chance of a TRF2 related tumor development. The observation that a small increase in CD4/CD8-double-positive T-cell lymphomas was detected and that I did not see tumor development in the control mice, initially proposed that transgenic TRF2 leads to the tumor development. However, since transgenic TRF2 was not presently expressed in the observed tumors, and even more surprisingly, no genomic evidence of the transgene was detectable, a deletion of the transgene might have occurred post tumor initiation. Again, this could suggest that TRF2 has an antagonistic effect on the very same tumor it initiated. Once it initiated tumor development, it might hinder further tumor growth. The genome instability I observed in the developed tumor cells could result in the loss of the TRF2 transgene.

A loss of the transgenic TRF2 signal was also observed upon irradiation and subsequent confocal analysis, which suggests that cells over-expressing TRF2 are highly unstable. Irradiation induces double-stranded breaks and in a healthy cell, the ATM pathway usually responds to these types of damage. However, assuming TRF2 abrogates the ATM pathway, double-stranded breaks will not be processed and will lead to genome instability and eventually cause the loss of the TRF2 transgene. However, this is only a theoretical possibility and unlikely to happen in actual cells and there are more reasonable explanations why TRF2 was not detectable in the tumor tissue.

In these studies I also observed a potential impact of the TRF2 transgene on the differentiation pattern. I could see by flow cytometry that bone marrow cells sorted for the expression of recombinant TRF2 differentiated differently over time than untransduced cells from the very same bone marrow, in particular I saw an increase in the CD11b positive cell population. However, it is inaccurate to call this differentiation pattern significant since it was only observed in bone marrow derived from one individual mouse.

When I measured the CD4/CD8-double-positive T-cell lymphomas by flow cytometry, I observed that the tumors were not expressing the TRF2 transgene. This might suggest spontaneous development of T-cell lymphomas, although irradiation could be ruled out as the reason, because the tumors were donor derived and donor cells were not irradiated.

Finally, I did not see a specific correlation for the activation of ATM in the observed tumors. *Western* analysis detected ATM activation in tumorigenic tissue, but not in all investigated T-cell lymphomas. Due to the lack of over-expression of recombinant TRF2 in these lymphomas it is difficult to make a connection between ATM inhibition and TRF2 over-expression.

To determine if TRF2 can act as an oncogene in the mouse hematopoietic system, I used lentiviral technology to deliver the transgene. This method allows the study of a transgene explicitly during the hematopoiesis. However, if I were to repeat the study, I would partially change the setup of my technical approach. I

consider the sufficient transduction of the hematopoietic system with the TRF2 transgene as the integral part of my studies. As mentioned before, I did experience a very low transduction rate of the hematopoietic system for the TRF2 transgene. A high transduction rate of the donor bone marrow would be in a repetition of the study a primary target. To overcome potentially low transduction rates I would, in addition to optimizing the viral titer, enrich TRF2-positive cells by flow cytometry either before transplantation or after transplantation. Subsequently I would transplant the enriched TRF2-positive cells into recipient mice. This method would guarantee a higher transduction rate and would make it easier to answer some of my questions, e.g. is the TRF2 transgene lost due to genome instability? However, the technical approach should be sufficient to determine if the TRF2 transgene is a strong oncogene. In this case, a single tumorigenic TRF2 over-expressing cell would automatically expand to a clonal tumor.

In parallel to my work, another group provided results arguing that TRF2 is a potent oncogene when over-expressed in C57BL/6J mice [177, 178]. This group knocked-in transgenic TRF2 under the control of a bovine keratin K5 promoter and the generated mice were therefore termed K5TRF2. This promoter targets TRF2 to basal cells and stem cells of the epidermis. As a result these mice have a severe light-sensitivity such as premature skin deterioration, hyperpigmentation and increased incidence of skin tumors. Furthermore these mice are more susceptible to UV-induced skin carcinogenesis, similar to mice deficient in components of the NER pathway. The researchers in this study claimed that the transgenic TRF2 mice showed an increased susceptibility to develop skin tumors and suggested a role of TRF2 in skin tumorigenesis. They furthermore proposed that the XPF nuclease, a component of the NER pathway and also localized to telomeres, is largely responsible for the telomere degradation associated with TRF2 over-expression. According to these results the researchers suggested that the interaction between TRF2 and XPF increases XPF activity at telomeres,

leading to XPF-dependent telomere loss. In turn, TRF2 may deregulate NER at non-telomeric DNA lesions resulting in increased sensitivity to UV-damage. In a later study from the same group, the researchers presented data suggesting that TRF2's role as an oncogene is exaggerated in the absence of telomerase. To show that, they used mice expressing TRF2 under the control of a K5 promoter, but in this study the observed mice were negative for the catalytic subunit of telomerase in mice, TERC (K5TRF2/TERC^{-/-} mice). In their studies telomerase deficiency dramatically accelerates TRF2-induced epithelial carcinogenesis in telomerase deficient mice expressing TRF2. Their data also showed a dramatically accelerated TRF2-induced epithelial carcinogenesis in the absence of telomerase, coinciding with increased chromosomal instability and DNA damage. They also observed an increase in telomere recombination, suggesting that TRF2 favors the activation of alternative telomere maintenance mechanisms. Finally, the researchers claimed in their model that the DNA damage response was not compromised. Levels of activation of ATM, Chk2, and p53 accumulation were normal in the observed K5TRF2/TERC^{-/-} tumors.

Other groups have previously reported increased levels of TRF2 mRNA in human multistep hepatocarcinogenesis as well as in gastric carcinomas [179, 180]. Interestingly, these groups observed an inverse correlation of levels of TRF2, and other telomere proteins like TRF1 and TIN2 [180], and telomere length. They suggested that increased protein levels of TRF2 and other telomeric proteins prevent the access of telomerase and inhibit telomere elongation. As a result, telomere crisis is induced and promotes tumor development.

In principle, my approach is not comparable with the one described above. Instead of over-expressing the TRF2 transgene in basal cells and stem cells of the epidermis, I targeted the hematopoietic system of mice. In the alternative strategy, the effect of TRF2 over-expression in the skin depends on the presence of XPF, and is largely enhanced by UV-induced damage. Considering the proposed *in vitro* results for TRF2 over-expression [161], I assumed that increased levels of TRF2 alter the DNA damage machinery, due to the inhibition

of ATM, and promote the accumulation of unrepaired DNA double-stranded breaks, which eventually leads to the development of tumors within the hematopoietic system. Although I see an increase in the development of CD4/CD8-double-positive T-cell lymphomas, the actual over-expression of TRF2 is not detectable in these tumors.

FISH results also did not show the loss of telomere signals. Although FISH is not a quantitative tool to measure telomere length, the complete loss of signal of any given telomere can be detected by this method. I did, however, detect the presence of genome instability by the presence of anaphase bridges, double-telomeric signals at a number of telomere ends, and by polyploidy, all of which are hallmarks of cancer. With regard to previous results and considering that I over-expressed TRF2 in a telomerase positive background, I suggest that the increase of genome instability in mice over-expressing TRF2 in basal cells and stem cells of the epidermis in the absence of telomerase is mainly a hallmark of cancer, but not due to the over-expression of TRF2 *per se*. However, I cannot rule out the additive effect of TRF2 and XPF with UV-damage leads to additional genome instability. My hematopoietic TRF2 model is not suitable for studies investigating the impact of UV-light.

Neither tumors derived from K5TRF2/TERC^{-/-} mice or the tumors observed in my experiments showed tempered activation of components of the DNA damage machinery. Activation of ATM and p53 was observed in these tumors, although not always. This suggests that the tumorigenic effect of TRF2 does not inhibit ATM by a direct interaction.

The impact of telomerase deficiency on tumor development in mice has been discussed elsewhere [181]. It has been found that mice lacking telomerase in an ATM-deficient background have a lower rate of tumorigenic translocations and tumor formation. Initial studies on the impact of over-expressed TRF2 [182] in primary human fibroblasts with a compromised apoptosis pathway also revealed that TRF2 lowers the occurrence of telomere fusions and overall genome instability. These two studies suggest that over-expression of TRF2 stabilizes short telomeres and inhibits genome instability rather than promote tumor

formation. That, however, could change if over-expressed TRF2 has an enhanced effect together with UV-damage and other telomere factors, like XPF. In this case, TRF2 is actually protecting the telomeres from a damage response by inhibiting the access of the DNA damage machinery. As another effect it promotes the activity of factors like XPF. Since telomere fusions require the prior removal of the 3'-overhang, a probable function of XPF, increased XPF activity might lead to more telomere fusions. Again, taking all known results into account, TRF2 over-expression should rather stabilize short telomeres and decrease the number of telomere fusions and overall genome instability. Or, if it is a potent oncogene, its effect should be indirect by compromising the proper function of the DNA damage machinery via ATM inhibition.

Based on my results I suggest that TRF2 is not, if at all, a strong oncogene. I did observe over-expression of TRF2 in the hematopoietic system but I did not find tumor development in combination with an acute over-expression of TRF2 within the tumor. Although I did observe genome instability, I do consider this as an indication of cancer rather than an effect of TRF2 over-expression. Therefore I am also positive that TRF2 did not get lost after tumor initiation due to genome instability. As mentioned previously, genome instability in cells is not promoted by over-expressing TRF2 [182]. I also think that it is difficult to draw a connection between upregulation of TRF2 mRNA levels in tumor tissue and actual protein levels of TRF2. It is important to measure the actual presence of TRF2 protein at the telomeres, as this is the prominent area where the protein carries out its main function. I also suggest that the effect of TRF2 over-expression, as observed in K5TRF2 mice, is caused by the pure abundance of TRF2 at the telomeres. It has been shown that the shelterin complex is composed of six different proteins. Any imbalance on the protein level, as caused by over-expression, within this complex might disturb the proper function of shelterin. But depending on the choice of the promoter used to over-express a transgene, strong over-expression might artificially disrupt the shelterin complex. In the case of K5TRF2 mice it could be that the artificial increase of TRF2 is compromising the function of the other shelterin subunits, thereby disrupting the telomere complex and causing

dysfunctional telomeres. Of course, it is possible that this might define the oncogenic potential of TRF2, meaning if TRF2 is highly over-expressed, it will disrupt the shelterin complex, cause telomere dysfunction, genome instability, and tumor formation. However, it has only been shown that TRF2 mRNA levels are upregulated, in addition to TRF1 and POT1 mRNA levels [180], but to which extent the actual TRF2 protein contributes to that is not known. In my experiments, strong over-expression of TRF2 did not cause a significant increase in the development of tumors and I did not observe over-expression of TRF2 in the investigated CD4/CD8-double-positive T-cell lymphomas. Therefore, I suggest that TRF2 is not a dominant oncogene in the mouse hematopoietic system.

7. References

1. Watson, J.D., *Origin of concatemeric T7 DNA*. Nat New Biol, 1972. 239(94): p. 197-201.
2. Olovnikov, A.M., *A theory of marginotomy*. J. Theoretical Biology, 1973. 41: p. 181-190.
3. Klobutcher, L.A., et al., *All gene-sized DNA molecules in four species of hypotrichs have the same terminal sequence and an unusual 3' terminus*. Proc Natl Acad Sci U S A, 1981. 78(5): p. 3015-9.
4. Pluta, A.F., B.P. Kaine, and B.B. Spear, *The terminal organization of macronuclear DNA in Oxytricha fallax*. Nucleic Acids Res, 1982. 10(24): p. 8145-54.
5. Henderson, E.R. and E.H. Blackburn, *An overhanging 3' terminus is a conserved feature of telomeres*. Mol Cell Biol, 1989. 9(1): p. 345-8.
6. Wellinger, R.J., A.J. Wolf, and V.A. Zakian, *Origin activation and formation of single-strand TGI-3 tails occur sequentially in late S phase on a yeast linear plasmid*. Mol Cell Biol, 1993. 13(7): p. 4057-65.
7. Wellinger, R.J., A.J. Wolf, and V.A. Zakian, *Saccharomyces telomeres acquire single-strand TGI-3 tails late in S phase*. Cell, 1993. 72(1): p. 51-60.
8. Makarov, V.L., Y. Hirose, and J.P. Langmore, *Long G tails at both ends of human chromosomes suggest a C strand degradation mechanism for telomere shortening*. Cell, 1997. 88(5): p. 657-66.
9. Munoz-Jordan, J.L., et al., *t-loops at trypanosome telomeres*. Embo J, 2001. 20(3): p. 579-88.
10. Jacob, N.K., R. Skopp, and C.M. Price, *G-overhang dynamics at Tetrahymena telomeres*. Embo J, 2001. 20(15): p. 4299-308.
11. Haber, J.E., *Partners and pathways repairing a double-strand break*. Trends Genet, 2000. 16(6): p. 259-64.
12. Hoeijmakers, J.H., *Genome maintenance mechanisms for preventing cancer*. Nature, 2001. 411(6835): p. 366-74.
13. Muller, H.J., *The remaking of chromosomes*. The Collecting Net, Woods Hole, 1938. 8: p. 182-195.
14. Blackburn, E.H. and J.G. Gall, *A tandemly repeated sequence at the termini of the extrachromosomal ribosomal RNA genes in Tetrahymena*. J Mol Biol, 1978. 120(1): p. 33-53.
15. Blackburn, E.H., *Telomeres and their synthesis*. Science, 1990. 249(4968): p. 489-90.
16. McEachern, M.J. and E.H. Blackburn, *A conserved sequence motif within the exceptionally diverse telomeric sequences of budding yeasts*. Proc Natl Acad Sci U S A, 1994. 91(8): p. 3453-7.
17. Shampay, J., J.W. Szostak, and E.H. Blackburn, *DNA sequences of telomeres maintained in yeast*. Nature, 1984. 310(5973): p. 154-7.
18. Sugawara, N., Szostak, J.W., *Telomeres of Schizosaccharomyces pombe*. Yeast (Suppl.) 1, 1986(S373).

19. Biessmann, H., et al., *Addition of telomere-associated HeT DNA sequences "heals" broken chromosome ends in Drosophila*. Cell, 1990. 61(4): p. 663-73.
20. Levis, R.W., et al., *Transposons in place of telomeric repeats at a Drosophila telomere*. Cell, 1993. 75(6): p. 1083-93.
21. Sheen, F.M. and R.W. Levis, *Transposition of the LINE-like retrotransposon TART to Drosophila chromosome termini*. Proc Natl Acad Sci U S A, 1994. 91(26): p. 12510-4.
22. Blackburn, E.H. and P.B. Challoner, *Identification of a telomeric DNA sequence in Trypanosoma brucei*. Cell, 1984. 36(2): p. 447-57.
23. van der Ploeg, L.H.T., A.Y.C. Liu, and P. Borst, *Structure of the growing telomeres of trypanosomes*. Cell, 1984. 36: p. 459-468.
24. Hiraoka, Y., E. Henderson, and E.H. Blackburn, *Not so peculiar: fission yeast telomere repeats*. Trends Biochem Sci, 1998. 23(4): p. 126.
25. Cangiano, G., La Volpe, A., *Repetitive DNA sequences located in the terminal portion of the Canorhabditis elegans chromosomes*. Nucleic Acid Research, 1993. 21: p. 1133-1139.
26. Okazaki, S., et al., *Identification of a pentanucleotide telomeric sequence, (TTAGG)_n, in the silkworm Bombyx mori and in other insects*. Mol Cell Biol, 1993. 13(3): p. 1424-32.
27. Richards, E.J. and F.M. Ausubel, *Isolation of a higher eukaryotic telomere from Arabidopsis thaliana*. Cell, 1988. 53(1): p. 127-36.
28. Moyzis, R.K., et al., *A highly conserved repetitive DNA sequence, (TTAGGG)_n, present at the telomeres of human chromosomes*. Proc Natl Acad Sci U S A, 1988. 85(18): p. 6622-6.
29. Allshire, R.C., et al., *Telomeric repeat from T. thermophila cross hybridizes with human telomeres*. Nature, 1988. 332(6165): p. 656-9.
30. Saltman, D., et al., *Telomeric structure in cells with chromosome end associations*. Chromosoma, 1993. 102(2): p. 121-8.
31. Kipling, D. and H.J. Cooke, *Hypervariable ultra-long telomeres in mice*. Nature, 1990. 347(6291): p. 400-2.
32. Lingner, J., et al., *Reverse transcriptase motifs in the catalytic subunit of telomerase*. Science, 1997. 276(5312): p. 561-7.
33. Shippen-Lentz, D. and E.H. Blackburn, *Functional evidence for an RNA template in telomerase*. Science, 1990. 247(4942): p. 546-52.
34. Yu, G.L., et al., *In vivo alteration of telomere sequences and senescence caused by mutated Tetrahymena telomerase RNAs*. Nature, 1990. 344(6262): p. 126-32.
35. Price, C.M., *Synthesis of the telomeric C-strand. A review*. Biochemistry (Mosc), 1997. 62(11): p. 1216-23.
36. Dionne, I. and R.J. Wellinger, *Cell cycle-regulated generation of single-stranded G-rich DNA in the absence of telomerase*. Proc Natl Acad Sci U S A, 1996. 93(24): p. 13902-7.
37. Hemann, M.T. and C.W. Greider, *G-strand overhangs on telomeres in telomerase-deficient mouse cells*. Nucleic Acids Res, 1999. 27(20): p. 3964-9.
38. Nikaido, R., et al., *Presence of telomeric G-strand tails in the telomerase catalytic subunit TERT knockout mice*. Genes Cells, 1999. 4(10): p. 563-72.

39. Greider, C.W. and E.H. Blackburn, *The telomere terminal transferase of Tetrahymena is a ribonucleoprotein enzyme with two kinds of primer specificity*. Cell, 1987. 51(6): p. 887-98.
40. Lingner, J., et al., *Three Ever Shorter Telomere (EST) genes are dispensable for in vitro yeast telomerase activity*. Proc Natl Acad Sci U S A, 1997. 94(21): p. 11190-5.
41. Shampay, J. and E.H. Blackburn, *Tetrahymena micronuclear sequences that function as telomeres in yeast*. Nucleic Acids Res, 1989. 17(8): p. 3247-60.
42. Morin, G.B., *The human telomere terminal transferase enzyme is a ribonucleoprotein that synthesizes TTAGGG repeats*. Cell, 1989. 59(3): p. 521-9.
43. Harrington, L.A. and C.W. Greider, *Telomerase primer specificity and chromosome healing*. Nature, 1991. 353(6343): p. 451-4.
44. Morin, G.B., *Recognition of a chromosome truncation site associated with alpha-thalassaemia by human telomerase*. Nature, 1991. 353(6343): p. 454-6.
45. Prowse, K.R., A.A. Avilion, and C.W. Greider, *Identification of a nonprocessive telomerase activity from mouse cells*. Proc Natl Acad Sci U S A, 1993. 90(4): p. 1493-7.
46. Wilkie, A.O., et al., *A truncated human chromosome 16 associated with alpha thalassaemia is stabilized by addition of telomeric repeat (TTAGGG)_n*. Nature, 1990. 346(6287): p. 868-71.
47. Lamb, J., et al., *De novo truncation of chromosome 16p and healing with (TTAGGG)_n in the alpha-thalassemia/mental retardation syndrome (ATR-16)*. Am J Hum Genet, 1993. 52(4): p. 668-76.
48. Melek, M. and D.E. Shippen, *Chromosome healing: spontaneous and programmed de novo telomere formation by telomerase*. Bioessays, 1996. 18(4): p. 301-8.
49. Avilion, A.A., et al., *Human telomerase RNA and telomerase activity in immortal cell lines and tumor tissues*. Cancer Res, 1996. 56(3): p. 645-50.
50. Prowse, K.R. and C.W. Greider, *Developmental and tissue-specific regulation of mouse telomerase and telomere length*. Proc Natl Acad Sci U S A, 1995. 92(11): p. 4818-22.
51. Blasco, M.A., et al., *Functional characterization and developmental regulation of mouse telomerase RNA*. Science, 1995. 269(5228): p. 1267-70.
52. Greenberg, R.A., et al., *Expression of mouse telomerase reverse transcriptase during development, differentiation and proliferation*. Oncogene, 1998. 16(13): p. 1723-30.
53. Martin-Rivera, L., et al., *Expression of mouse telomerase catalytic subunit in embryos and adult tissues*. Proc Natl Acad Sci U S A, 1998. 95(18): p. 10471-6.
54. Liu, Y., et al., *The telomerase reverse transcriptase is limiting and necessary for telomerase function in vivo*. Curr Biol, 2000. 10(22): p. 1459-62.
55. Kim, N.W., et al., *Specific association of human telomerase activity with immortal cells and cancer [see comments]*. Science, 1994. 266(5193): p. 2011-5.
56. Wright, W.E., et al., *Telomerase activity in human germline and embryonic tissues and cells*. Dev Genet, 1996. 18(2): p. 173-9.

57. Broccoli, D., J.W. Young, and T. de Lange, *Telomerase activity in normal and malignant hematopoietic cells*. Proc Natl Acad Sci U S A, 1995. 92(20): p. 9082-6.
58. Counter, C.M., et al., *Telomerase activity in normal leukocytes and in hematologic malignancies*. Blood, 1995. 85(9): p. 2315-20.
59. Kilian, A., et al., *Isolation of a candidate human telomerase catalytic subunit gene, which reveals complex splicing patterns in different cell types*. Hum Mol Genet, 1997. 6(12): p. 2011-9.
60. Meyerson, M., et al., *hEST2, the putative human telomerase catalytic subunit gene, is up-regulated in tumor cells and during immortalization*. Cell, 1997. 90(4): p. 785-95.
61. Nakamura, T.M., et al., *Telomerase catalytic subunit homologs from fission yeast and human [see comments]*. Science, 1997. 277(5328): p. 955-9.
62. Bodnar, A.G., et al., *Extension of life-span by introduction of telomerase into normal human cells*. Science, 1998. 279(5349): p. 349-52.
63. Vaziri, H. and S. Benchimol, *Reconstitution of telomerase activity in normal human cells leads to elongation of telomeres and extended replicative life span*. Curr Biol, 1998. 8(5): p. 279-82.
64. Shay, J.W. and S. Bacchetti, *A survey of telomerase activity in human cancer*. Eur J Cancer, 1997. 33(5): p. 787-91.
65. Cong, Y.S., W.E. Wright, and J.W. Shay, *Human telomerase and its regulation*. Microbiol Mol Biol Rev, 2002. 66(3): p. 407-25.
66. Collins, K., R. Kobayashi, and C.W. Greider, *Purification of Tetrahymena telomerase and cloning of genes encoding the two protein components of the enzyme*. Cell, 1995. 81(5): p. 677-86.
67. Mason, D.X., C. Autexier, and C.W. Greider, *Tetrahymena proteins p80 and p95 are not core telomerase components*. Proc Natl Acad Sci U S A, 2001.
68. Miller, M.C. and K. Collins, *The Tetrahymena p80/p95 complex is required for proper telomere length maintenance and micronuclear genome stability*. Mol Cell, 2000. 6(4): p. 827-37.
69. Harrington, L., et al., *A mammalian telomerase-associated protein*. Science, 1997. 275(5302): p. 973-7.
70. Nakayama, J., et al., *TLP1: a gene encoding a protein component of mammalian telomerase is a novel member of WD repeats family*. Cell, 1997. 88(6): p. 875-84.
71. Beattie, T.L., et al., *Polymerization defects within human telomerase are distinct from telomerase RNA and TEP1 binding*. Mol Biol Cell, 2000. 11(10): p. 3329-40.
72. Holt, S.E., et al., *Functional requirement of p23 and Hsp90 in telomerase complexes*. Genes Dev, 1999. 13(7): p. 817-26.
73. Forsythe, H.L., et al., *Stable association of hsp90 and p23, but Not hsp70, with active human telomerase*. J Biol Chem, 2001. 276(19): p. 15571-4.
74. Seimiya, H., et al., *Involvement of 14-3-3 proteins in nuclear localization of telomerase*. Embo J, 2000. 19(11): p. 2652-61.
75. Dez, C., et al., *Stable expression in yeast of the mature form of human telomerase RNA depends on its association with the box H/ACA small nucleolar RNP proteins Cbf5p, Nhp2p and Nop10p*. Nucleic Acids Res, 2001. 29(3): p. 598-603.

76. Dragon, F., V. Pogacic, and W. Filipowicz, *In vitro assembly of human H/ACA small nucleolar RNPs reveals unique features of U17 and telomerase RNAs*. Mol Cell Biol, 2000. 20(9): p. 3037-48.
77. Mitchell, J.R., E. Wood, and K. Collins, *A telomerase component is defective in the human disease dyskeratosis congenita*. Nature, 1999. 402(6761): p. 551-5.
78. Pogacic, V., F. Dragon, and W. Filipowicz, *Human H/ACA small nucleolar RNPs and telomerase share evolutionarily conserved proteins NHP2 and NOP10*. Mol Cell Biol, 2000. 20(23): p. 9028-40.
79. Chen, J.L., M.A. Blasco, and C.W. Greider, *Secondary structure of vertebrate telomerase RNA*. Cell, 2000. 100(5): p. 503-14.
80. Mitchell, J.R., J. Cheng, and K. Collins, *A box H/ACA small nucleolar RNA-like domain at the human telomerase RNA 3' end*. Mol Cell Biol, 1999. 19(1): p. 567-76.
81. LaBranche, H., et al., *Telomere elongation by hnRNP A1 and a derivative that interacts with telomeric repeats and telomerase [see comments]*. Nat Genet, 1998. 19(2): p. 199-202.
82. Fiset, S. and B. Chabot, *hnRNP A1 may interact simultaneously with telomeric DNA and the human telomerase RNA in vitro*. Nucleic Acids Res, 2001. 29(11): p. 2268-75.
83. Ford, L.P., et al., *Heterogeneous nuclear ribonucleoproteins C1 and C2 associate with the RNA component of human telomerase*. Mol Cell Biol, 2000. 20(23): p. 9084-91.
84. Olson, M.O., M. Dundr, and A. Szebeni, *The nucleolus: an old factory with unexpected capabilities*. Trends Cell Biol, 2000. 10(5): p. 189-96.
85. Ford, L.P., J.W. Shay, and W.E. Wright, *The La antigen associates with the human telomerase ribonucleoprotein and influences telomere length in vivo*. Rna, 2001. 7(8): p. 1068-75.
86. Le, S., R. Sternglanz, and C.W. Greider, *Identification of two RNA-binding proteins associated with human telomerase RNA*. Mol Biol Cell, 2000. 11(3): p. 999-1010.
87. Bryan, T.M., et al., *Evidence for an alternative mechanism for maintaining telomere length in human tumors and tumor-derived cell lines [see comments]*. Nat Med, 1997. 3(11): p. 1271-4.
88. Dunham, M.A., et al., *Telomere maintenance by recombination in human cells*. Nat Genet, 2000. 26: p. 447-450.
89. Henson, J.D., et al., *Alternative lengthening of telomeres in mammalian cells*. Oncogene, 2002. 21(4): p. 598-610.
90. Perrem, K., et al., *Coexistence of alternative lengthening of telomeres and telomerase in hTERT-transfected GM847 cells*. Mol Cell Biol, 2001. 21(12): p. 3862-75.
91. Cerone, M.A., J.A. Londono-Vallejo, and S. Bacchetti, *Telomere maintenance by telomerase and by recombination can coexist in human cells*. Hum Mol Genet, 2001. 10(18): p. 1945-52.
92. Grobelny, J.V., M. Kulp-McEliece, and D. Broccoli, *Effects of reconstitution of telomerase activity on telomere maintenance by the alternative lengthening of telomeres (ALT) pathway*. Hum Mol Genet, 2001. 10(18): p. 1953-61.

93. Stewart, S.A., et al., *Telomerase contributes to tumorigenesis by a telomere length-independent mechanism*. Proc Natl Acad Sci U S A, 2002.
94. Reddel, R.R., *Alternative lengthening of telomeres, telomerase, and cancer*. Cancer Lett, 2003. 194(2): p. 155-62.
95. Saretzki, G., et al., *Ribozyme-mediated telomerase inhibition induces immediate cell loss but not telomere shortening in ovarian cancer cells*. Cancer Gene Ther, 2001. 8(10): p. 827-34.
96. Hahn, W.C., et al., *Inhibition of telomerase limits the growth of human cancer cells*. Nat Med, 1999. 5(10): p. 1164-70.
97. Zhang, X., et al., *Telomere shortening and apoptosis in telomerase-inhibited human tumor cells*. Genes Dev, 1999. 13(18): p. 2388-99.
98. Colgin, L.M., et al., *The hTERTalpha splice variant is a dominant negative inhibitor of telomerase activity*. Neoplasia, 2000. 2(5): p. 426-32.
99. Ludwig, A., et al., *Ribozyme cleavage of telomerase mRNA sensitizes breast epithelial cells to inhibitors of topoisomerase*. Cancer Res, 2001. 61(7): p. 3053-61.
100. Nakabayashi, K., et al., *Decrease in amplified telomeric sequences and induction of senescence markers by introduction of human chromosome 7 or its segments in SUSM-1*. Exp Cell Res, 1997. 235(2): p. 345-53.
101. Perrem, K., et al., *Repression of an alternative mechanism for lengthening of telomeres in somatic cell hybrids*. Oncogene, 1999. 18(22): p. 3383-90.
102. Sfeir, A.J., et al., *Telomere-end processing the terminal nucleotides of human chromosomes*. Mol Cell, 2005. 18(1): p. 131-8.
103. Griffith, J.D., et al., *Mammalian telomeres end in a large duplex loop*. Cell, 1999. 97(4): p. 503-14.
104. de Lange, T., *Shelterin: the protein complex that shapes and safeguards human telomeres*. Genes Dev, 2005. 19(18): p. 2100-10.
105. Zhong, Z., et al., *A mammalian factor that binds telomeric TTAGGG repeats in vitro*. Mol Cell Biol, 1992. 12(11): p. 4834-43.
106. Chong, L., et al., *A human telomeric protein*. Science, 1995. 270(5242): p. 1663-7.
107. Bilaud, T., et al., *Telomeric localization of TRF2, a novel human telobox protein*. Nat Genet, 1997. 17(2): p. 236-9.
108. Broccoli, D., et al., *Human telomeres contain two distinct Myb-related proteins, TRF1 and TRF2*. Nat Genet, 1997. 17(2): p. 231-5.
109. Kim, S.H., P. Kaminker, and J. Campisi, *TIN2, a new regulator of telomere length in human cells*. Nat Genet, 1999. 23(4): p. 405-12.
110. Li, B., S. Oestreich, and T. de Lange, *Identification of human Rap1: implications for telomere evolution*. Cell, 2000. 101(5): p. 471-83.
111. Houghtaling, B.R., et al., *A dynamic molecular link between the telomere length regulator TRF1 and the chromosome end protector TRF2*. Curr Biol, 2004. 14(18): p. 1621-31.
112. Liu, D., et al., *PTOP interacts with POT1 and regulates its localization to telomeres*. Nat Cell Biol, 2004. 6(7): p. 673-80.
113. Ye, J.Z., et al., *POT1-interacting protein PIP1: a telomere length regulator that recruits POT1 to the TIN2/TRF1 complex*. Genes Dev, 2004. 18(14): p. 1649-54.

114. Baumann, P. and T.R. Cech, *Pot1, the putative telomere end-binding protein in fission yeast and humans*. Science, 2001. 292(5519): p. 1171-5.
115. Ye, J.Z., et al., *TIN2 binds TRF1 and TRF2 simultaneously and stabilizes the TRF2 complex on telomeres*. J Biol Chem, 2004. 279(45): p. 47264-71.
116. Mattern, K.A., et al., *Dynamics of protein binding to telomeres in living cells: implications for telomere structure and function*. Mol Cell Biol, 2004. 24(12): p. 5587-94.
117. Yang, Q., Y.L. Zheng, and C.C. Harris, *POT1 and TRF2 cooperate to maintain telomeric integrity*. Mol Cell Biol, 2005. 25(3): p. 1070-80.
118. Griffith, J., A. Bianchi, and T. de Lange, *TRF1 promotes parallel pairing of telomeric tracts in vitro*. J Mol Biol, 1998. 278(1): p. 79-88.
119. Bianchi, A., et al., *TRF1 is a dimer and bends telomeric DNA*. Embo J, 1997. 16(7): p. 1785-94.
120. Broccoli, D., et al., *Comparison of the human and mouse genes encoding the telomeric protein, TRF1: chromosomal localization, expression and conserved protein domains*. Hum Mol Genet, 1997. 6(1): p. 69-76.
121. Fairall, L., et al., *Structure of the TRFH dimerization domain of the human telomeric proteins TRF1 and TRF2*. Mol Cell, 2001. 8(2): p. 351-61.
122. Shen, M., et al., *Characterization and cell cycle regulation of the related human telomeric proteins Pin2 and TRF1 suggest a role in mitosis*. Proc Natl Acad Sci U S A, 1997. 94(25): p. 13618-23.
123. van Steensel, B. and T. de Lange, *Control of telomere length by the human telomeric protein TRF1*. Nature, 1997. 385(6618): p. 740-3.
124. Scherthan, H., et al., *Mammalian meiotic telomeres: protein composition and redistribution in relation to nuclear pores*. Mol Biol Cell, 2000. 11(12): p. 4189-203.
125. Crabbe, L., et al., *Defective telomere lagging strand synthesis in cells lacking WRN helicase activity*. Science, 2004. 306(5703): p. 1951-3.
126. Bianchi, A., et al., *TRF1 binds a bipartite telomeric site with extreme spatial flexibility*. Embo J, 1999. 18(20): p. 5735-44.
127. Karlseder, J., et al., *Targeted deletion reveals an essential function for the telomere length regulator Trf1*. Mol Cell Biol, 2003. 23(18): p. 6533-41.
128. Stansel, R.M., T. de Lange, and J.D. Griffith, *T-loop assembly in vitro involves binding of TRF2 near the 3' telomeric overhang*. EMBO J., 2001. 20: p. E5532-5540.
129. Celli, G.B. and T. de Lange, *DNA processing is not required for ATM-mediated telomere damage response after TRF2 deletion*. Nat Cell Biol, 2005.
130. Kim, S.H., et al., *TIN2 mediates functions of TRF2 at human telomeres*. J Biol Chem, 2004. 279(42): p. 43799-804.
131. Ye, J.Z. and T. de Lange, *TIN2 is a tankyrase 1 PARP modulator in the TRF1 telomere length control complex*. Nat Genet, 2004. 36(6): p. 618-23.
132. Chikashige, Y. and Y. Hiraoka, *Telomere binding of the Rap1 protein is required for meiosis in fission yeast*. Curr Biol, 2001. 11(20): p. 1618-23.
133. Kanoh, J. and F. Ishikawa, *spRap1 and spRif1, recruited to telomeres by Taz1, are essential for telomere function in fission yeast*. Curr Biol, 2001. 11(20): p. 1624-30.

134. Li, B. and T. de Lange, *Rap1 affects the length and heterogeneity of human telomeres*. Mol Biol Cell, 2003. 14(12): p. 5060-8.
135. Wang, F., et al., *The POT1-TPP1 telomere complex is a telomerase processivity factor*. Nature, 2007. 445(7127): p. 506-10.
136. Xin, H., et al., *TPP1 is a homologue of ciliate TEBP-beta and interacts with POT1 to recruit telomerase*. Nature, 2007. 445(7127): p. 559-62.
137. Lei, M., E.R. Podell, and T.R. Cech, *Structure of human POT1 bound to telomeric single-stranded DNA provides a model for chromosome end-protection*. Nat Struct Mol Biol, 2004. 11(12): p. 1223-9.
138. Loayza, D., et al., *DNA binding features of human POT1: a nonamer 5'-TAGGGTTAG-3' minimal binding site, sequence specificity, and internal binding to multimeric sites*. J Biol Chem, 2004. 279(13): p. 13241-8.
139. Hockemeyer, D., et al., *POT1 protects telomeres from a transient DNA damage response and determines how human chromosomes end*. Embo J, 2005. 24(14): p. 2667-78.
140. Hockemeyer, D., et al., *Recent expansion of the telomeric complex in rodents: Two distinct POT1 proteins protect mouse telomeres*. Cell, 2006. 126(1): p. 63-77.
141. Veldman, T., K.T. Etheridge, and C.M. Counter, *Loss of hPot1 function leads to telomere instability and a cut-like phenotype*. Curr Biol, 2004. 14(24): p. 2264-70.
142. Smith, S., et al., *Tankyrase, a poly(ADP-ribose) polymerase at human telomeres*. Science, 1998. 282(5393): p. 1484-7.
143. Kaminker, P.G., et al., *TANK2, a new TRF1-associated PARP, causes rapid induction of cell death upon overexpression*. J Biol Chem, 2001. 13: p. 13.
144. Sbodio, J.I., H.F. Lodish, and N.W. Chi, *Tankyrase-2 oligomerizes with tankyrase-1 and binds to both TRF1 (telomere-repeat-binding factor 1) and IRAP (insulin-responsive aminopeptidase)*. Biochem J, 2002. 361(Pt 3): p. 451-9.
145. Smith, S. and T. de Lange, *Tankyrase promotes telomere elongation in human cells*. Curr Biol, 2000. 10(20): p. 1299-302.
146. Yankiwski, V., et al., *Nuclear structure in normal and Bloom syndrome cells*. Proc Natl Acad Sci U S A, 2000. 97(10): p. 5214-9.
147. Stavropoulos, D.J., et al., *The Bloom syndrome helicase BLM interacts with TRF2 in ALT cells and promotes telomeric DNA synthesis*. Hum Mol Genet, 2002. 11(25): p. 3135-44.
148. Tarsounas, M., et al., *Telomere maintenance requires the RAD51D recombination/repair protein*. Cell, 2004. 117(3): p. 337-47.
149. Zhu, X.D., et al., *Cell-cycle-regulated association of RAD50/MRE11/NBS1 with TRF2 and human telomeres*. Nat Genet, 2000. 25(3): p. 347-52.
150. Bai, Y. and J.P. Murnane, *Telomere instability in a human tumor cell line expressing a dominant-negative WRN protein*. Hum Genet, 2003. 113(4): p. 337-47.
151. Ranganathan, V., et al., *Rescue of a telomere length defect of Nijmegen breakage syndrome cells requires NBS and telomerase catalytic subunit*. Curr Biol, 2001. 11(12): p. 962-6.

152. Bakkenist, C.J. and M.B. Kastan, *DNA damage activates ATM through intermolecular autophosphorylation and dimer dissociation*. Nature, 2003. 421(6922): p. 499-506.
153. Huyen, Y., et al., *Methylated lysine 79 of histone H3 targets 53BP1 to DNA double-strand breaks*. Nature, 2004. 432(7015): p. 406-11.
154. d'Adda di Fagagna, F., et al., *A DNA damage checkpoint response in telomere-initiated senescence*. Nature, 2003. 426(6963): p. 194-8.
155. Zhu, X.D., et al., *ERCC1/XPF removes the 3' overhang from uncapped telomeres and represses formation of telomeric DNA-containing double minute chromosomes*. Mol Cell, 2003. 12(6): p. 1489-98.
156. Bailey, S.M., M.A. Brennenman, and E.H. Goodwin, *Frequent recombination in telomeric DNA may extend the proliferative life of telomerase-negative cells*. Nucleic Acids Res, 2004. 32(12): p. 3743-51.
157. Bechter, O.E., J.W. Shay, and W.E. Wright, *The frequency of homologous recombination in human ALT cells*. Cell Cycle, 2004. 3(5): p. 547-9.
158. Londono-Vallejo, J.A., *Telomere length heterogeneity and chromosome instability*. Cancer Lett, 2004. 212(2): p. 135-44.
159. Wang, R.C., A. Smogorzewska, and T. de Lange, *Homologous recombination generates T-loop-sized deletions at human telomeres*. Cell, 2004. 119(3): p. 355-68.
160. Cesare, A.J. and J.D. Griffith, *Telomeric DNA in ALT Cells Is Characterized by Free Telomeric Circles and Heterogeneous t-Loops*. Mol Cell Biol, 2004. 24(22): p. 9948-57.
161. Karlseder, J., et al., *The telomeric protein TRF2 binds the ATM kinase and can inhibit the ATM-dependent DNA damage response*. PLoS Biol, 2004. 2(8): p. E240.
162. Verdun, R.E., et al., *Functional Human Telomeres Are Recognized as DNA Damage in G2 of the Cell Cycle*. Mol Cell, 2005. 20(4): p. 551-561.
163. Okabe, M., et al., *'Green mice' as a source of ubiquitous green cells*. FEBS Lett, 1997. 407(3): p. 313-9.
164. Lansdorp, P.M., et al., *Heterogeneity in telomere length of human chromosomes*. Hum Mol Genet, 1996. 5(5): p. 685-91.
165. Barlow, C., et al., *Atm-deficient mice: a paradigm of ataxia telangiectasia*. Cell, 1996. 86(1): p. 159-71.
166. Donehower, L.A., et al., *Mice deficient for p53 are developmentally normal but susceptible to spontaneous tumours*. Nature, 1992. 356(6366): p. 215-21.
167. Raynal, P. and H.B. Pollard, *Annexins: the problem of assessing the biological role for a gene family of multifunctional calcium- and phospholipid-binding proteins*. Biochim Biophys Acta, 1994. 1197(1): p. 63-93.
168. Carson, C.T., et al., *The Mre11 complex is required for ATM activation and the G2/M checkpoint*. Embo J, 2003. 22(24): p. 6610-20.
169. Petrini, J.H. and T.H. Stracker, *The cellular response to DNA double-strand breaks: defining the sensors and mediators*. Trends Cell Biol, 2003. 13(9): p. 458-62.
170. Uziel, T., et al., *Requirement of the MRN complex for ATM activation by DNA damage*. Embo J, 2003. 22(20): p. 5612-21.

171. Shiloh, Y., *ATM and related protein kinases: safeguarding genome integrity*. Nat Rev Cancer, 2003. 3(3): p. 155-68.
172. Verdun, R.E. and J. Karlseder, *The DNA damage machinery and homologous recombination pathway act consecutively to protect human telomeres*. Cell, 2006. 127(4): p. 709-20.
173. Takai, H., A. Smogorzewska, and T. de Lange, *DNA damage foci at dysfunctional telomeres*. Curr Biol, 2003. 13(17): p. 1549-56.
174. Karlseder, J., et al., *p53- and ATM-dependent apoptosis induced by telomeres lacking TRF2*. Science, 1999. 283(5406): p. 1321-5.
175. Wong, K.K., et al., *Telomere dysfunction and Atm deficiency compromises organ homeostasis and accelerates ageing*. Nature, 2003. 421(6923): p. 643-8.
176. Morrell, D., E. Cromartie, and M. Swift, *Mortality and cancer incidence in 263 patients with ataxia-telangiectasia*. J Natl Cancer Inst, 1986. 77(1): p. 89-92.
177. Munoz, P., et al., *XPF nuclease-dependent telomere loss and increased DNA damage in mice overexpressing TRF2 result in premature aging and cancer*. Nat Genet, 2005. 37(10): p. 1063-71.
178. Blanco, R., et al., *Telomerase abrogation dramatically accelerates TRF2-induced epithelial carcinogenesis*. Genes Dev, 2007. 21(2): p. 206-20.
179. Matsutani, N., et al., *Expression of telomeric repeat binding factor 1 and 2 and TRF1-interacting nuclear protein 2 in human gastric carcinomas*. Int J Oncol, 2001. 19(3): p. 507-12.
180. Oh, B.K., et al., *Up-regulation of telomere-binding proteins, TRF1, TRF2, and TIN2 is related to telomere shortening during human multistep hepatocarcinogenesis*. Am J Pathol, 2005. 166(1): p. 73-80.
181. Qi, L., et al., *Telomere fusion to chromosome breaks reduces oncogenic translocations and tumour formation*. Nat Cell Biol, 2005. 7(7): p. 706-11.
182. Karlseder, J., A. Smogorzewska, and T. de Lange, *Senescence induced by altered telomere state, not telomere loss*. Science, 2002. 295(5564): p. 2446-9.

Wissenschaftlicher Werdegang

- 09/2003 – 05/2007 The Salk Institute for Biological Studies, La Jolla
- “Oncogenic analysis of TRF2 in the murine hematopoietic system”
- Promotion zum Dr. rer. nat.
- (in Kooperation mit der Gottfried Wilhelm Leibniz Universität Hannover)*
- 01/2002 – 10/2002 Institut für Chemo- und Biosensorik, Münster
- “Entwicklung eines optischen DNA-Sensors zum simultanen Nachweis des *invA*-Gens von *Salmonella* spp. und des *ctxA*-Gens von *Vibrio cholerae*”
- Diplomarbeit
- 10/1997 – 10/2002 Westfälische Wilhelms Universität Münster
- Studium der Biologie, Ernennung zum Dipl.-Biologen